QUANTIFICATION AND CHARACTERIZATION OF MOBILE COLLOIDS: THEIR POTENTIAL ROLE IN CARBON CYCLING UNDER VARYING REDOX CONDITIONS

by

Jing Yan

A dissertation submitted to the Faculty of the University of Delaware in partial fulfillment of the requirements for the degree of Doctor of Philosophy in Plant and Soil Sciences

Fall 2016

QUANTIFICATION AND CHARACTERIZATION OF MOBILE COLLOIDS: THEIR POTENTIAL ROLE IN CARBON CYCLING UNDER VARYING REDOX CONDITIONS

by

Jing Yan

Approved: _____
D. Janine Sherrier, Ph.D.
Chair of the Department of Plant and Soil Sciences

Approved: _____
Mark Rieger, Ph.D.
Dean of the College of Agriculture and Natural Resources

Approved: _____
Ann L. Ardis, Ph.D.
Senior Vice Provost for Graduate and Professional Education

I certify that I have read this dissertation and that in my opinion it meets the academic and professional standard required by the University as a dissertation for the degree of Doctor of Philosophy.

Signed: _____

Yan Jin, Ph.D.
Professor in charge of dissertation

I certify that I have read this dissertation and that in my opinion it meets the academic and professional standard required by the University as a dissertation for the degree of Doctor of Philosophy.

Signed: _____

Deb Jaisi, Ph.D.
Member of dissertation committee

I certify that I have read this dissertation and that in my opinion it meets the academic and professional standard required by the University as a dissertation for the degree of Doctor of Philosophy.

Signed: _____

Holly Michael, Ph.D.
Member of dissertation committee

I certify that I have read this dissertation and that in my opinion it meets the academic and professional standard required by the University as a dissertation for the degree of Doctor of Philosophy.

Signed: _____

Bruce Vasilas, Ph.D.
Member of dissertation committee

ACKNOWLEDGMENTS

Completing my Ph.D. degree is probably the most challenging activity that I have done in my life till now. I often joked that it might be even harder than my first steps as a baby. It has been a great privilege to spend these years in the Department of Plant and Soil Sciences at the University of Delaware. I would like to thank my mentors, colleagues, and friends who shared the best and worst moments of this journey.

Foremost, I would like to express my sincere gratitude to my advisor, Dr. Yan Jin, for her continuous support, thoughtful guidance, warm encouragement, and insightful discussions throughout my whole Ph.D. education. She patiently provided the vision, encouragement and advice necessary for me to complete my studies and dissertation. I feel very lucky and grateful for this opportunity to work with her, and I believe this experience not only provide me academic skills, but also shape my thinking in my future life.

Besides my advisor, I would like to thank the rest of my dissertation committee: Dr. Deb Jaisi, Dr. Holly Michael, and Dr. Bruce Vasilas, for their encouragement, insightful comments, challenging questions and constructive feedback.

My sincere thanks also go to the staff at Soil Testing Lab, Civil and Environmental Engineering Laboratories, Bioimaging Center of Delaware Biotechnology Institute, Material Characterization Lab at Harker's ISE Lab at the University of Delaware, including Karren Gartley, Catherine Olsen, Debbie Powell, Dr. Jeffrey Caplan, Gerald Poirier, Dr. Rovshan Mahmudov for their technical

supports. I also would like to thank Dr. Donald Sparks, Gerald Hendricks, Dr. Joshua LeMonte, Dr. Chunmei Chen, Dr. Xuan Yu, Dr. Matt Siebecker, Dr. Jason Stuckey, Dr. Sherrem Inamdar, Weinan Pan, Zhixuan Qin, Ron Manelski, Dr. Anthony Aufdenkampe, Dr. Dianna Kirwan, Katie Clark, Dr. Sunendra Joshi, Dr. Jiying Li, Dr. Markus Flurry, Dr. Markus Tuller, and Dr. Lis de Jonge for their stimulating discussions and technical supports. My special thanks go to Dr. Sherry Kitto for her continuous encouragement and insightful advice as both a mentor and a friend.

I thank my fellow lab mates in the Environmental Soil Physics Lab: Dr. Volha Lazouskaya, Dr. Chao Wang, Dr. Wenjuan Zheng, Michael Doody, Taozhu Sun, Mohammad Zafar, Anna Jurusik, Saiqi Zeng, Dr. Dengjun Wang, for not only their professional skills and knowledge as scientists, but also their understanding and consideration as friends. In particular, I am grateful to Dr. Dengjun Wang for his insightful discussion and thoughtful advice. Also I would like to thank all my friends I met at the University of Delaware for sharing this wonderful journey with me.

I would like to thank my girlfriend, Liang Gong, for all her love and support. She not only brings joy and excitement to my life, but also motivates and challenges me to be a better scientist and person. Without her support and encouragement, I could not have finished this work.

Last but not the lease, I would like to sincerely thank my parents, Shufen Jia and Jinhe Yan, for bring me to this brilliant world and supporting me spiritually throughout my life. Their sacrifices make me come this far to be a scientist and a person.

TABLE OF CONTENTS

LIST OF TABLES

LIST OF FIGURES

ABSTRACT

Mobile colloids, 1-1000 nm particles, have attracted much research attention because they have small size and large specific surface area therefore the potential to facilitate the transport of contaminants in the subsurface environment. Despite colloids' potential importance, the role of mobile colloids in carbon cycling under varying redox conditions is largely unknown. This dissertation, combining laboratory investigations and field measurements, focused on (1) identification and understanding of the key processes and pathways leading to colloid and colloidal organic carbon (COC) release under dynamic redox conditions and (2) quantification of the actual colloidal load and assessment of colloids' role in organic carbon retention and mobilization in representative environmental systems.

In Chapter 2, I investigated the complex interplay of soil colloid release, organic matter (OM) content, and redox conditions via batch experiments. I found that reducing conditions promoted colloid release, but colloid release largely depended on the dynamic interactions between OM and colloids. Under aerobic conditions, the addition of dissolved OM (DOM) increased colloid release, while under anaerobic conditions, the release of indigenous DOM (DOM_{in}) by iron reduction inhibited colloid release. In Chapter 3, I developed a simple and efficient methodology to quantify mobile colloids in < 0.1, 0.1-0.45 and 0.45-1.0 μm fractions using size-dependent correlations between nephelometric turbidity and colloid mass concentration. I found that colloid size strongly affected concentration-turbidity correlations, while colloid composition played a less important role in shifting the

correlations. The relatively insignificant particle composition effect indicates the practically “universal” applicability of the reported correlations. The method developed in Chapter 3 was applied in Chapter 4 to quantitatively examine the actual colloidal load and COC pool in agricultural, forestry, wetland and estuarine systems. A special focus was on colloids in < 0.45 μm fraction, which has been operationally defined as part of the "dissolved" phase in most previous studies. I found that the amounts of colloids and COC in 0.1-0.45 μm fraction were substantial and COC accounted for 8-19% of the operationally defined dissolved organic carbon in < 0.45 μm fraction. Additionally, wetland was found to be a hotspot of both colloid and COC release and mobilization, compared to other investigated sites.

Chapter 1

INTRODUCTION, LITERATURE REVIEW AND RESEARCH OBJECTIVES

Mobile colloids, often defined as entities with sizes from 1 nm to 1.0 μm (Vold and Vold, 1983), have attracted much research attention because they have small size and large specific surface area therefore the potential to facilitate the transport of contaminants in the subsurface environment (de Jonge et al., 2004a; Kretzschmar et al., 1999; Mccarthy and Zachara, 1989; Sen and Khilar, 2006). In natural systems, colloids are a complex mixture of clay minerals, metal-oxides and oxyhydroxides, and organic substances (Baalousha et al., 2011; Buffle and Leppard, 1995). Compared to aqueous solution and large particles, colloids can play a more dynamic role in nutrient cycling and contaminant fate and transport, where colloids act either as shuttles to facilitate their transport, or form aggregates with, or serve as binding sites for them. Therefore, it is critical to quantify the colloidal pool and assess its quantitative contribution to the mobilization of colloid-associated-constituents and their environmental fate.

Among different colloid-associated-constituents, colloid-associated-organic matter, which are organic macromolecules in colloidal phase or organic compounds sorbed on the surface of inorganic colloids, commonly occur in natural environments. They can serve as either carbon source or sink depending on their nature and the changes in surrounding environments (Amon and Benner, 1996; Guo and Macdonald, 2006; Hama et al., 2004; Kang and Mitchell, 2013; Kleber et al., 2007). The release and mobilization of colloid-associated-organic matter may have profound significance

in carbon mobilization and stabilization and thus strongly impact global carbon cycles. Knowledge of colloid and colloid-associated-carbon transport, and the mechanistic understanding of carbon retention on colloids are therefore necessary to assess and manage transport of colloids and their facilitated organic carbon transport.

Changes in environmental conditions, such as pH, ionic strength, redox potential and human activities, can greatly impact the release and mobilization of colloids and organic matter, and thus alter the fate and transport of colloid-associated-organic matter (Kretzschmar et al., 1999; Mccarthy and Zachara, 1989; Sen and Khilar, 2006). Therefore, to better assess and predict the influence of environmental changes on organic matter mobilization and activity, identification of environmental systems and conditions that promote colloid release and mobilization is critical. The following provides a literature review on the current state of knowledge on colloid release and mobilization, as well as interactions between colloids and organic matter in the natural environments.

1.1 Colloids and Their Potential Role in Natural Ecosystems

1.1.1 Definitions and Properties of Colloids

1.1.1.1 Definitions and the Importance of Colloid Size

Soil colloids are heterogeneous and complex mixtures of organic and inorganic entities with supramolecular structure and properties, but small enough to remain in suspension. Colloids are often defined as entities with sizes from 1 nm to 1.0 μm (Vold and Vold, 1983). Because of their small size and large specific surface area leading to high reactivity with and the ability to facilitate the transport of contaminants in the subsurface environment, soil colloids have attracted much research attention (de

Jonge et al., 2004a; Kretzschmar et al., 1999; Mccarthy and Zachara, 1989; Sen and Khilar, 2006). In natural ecosystems, colloids are a complex mixture of clay minerals, metal-oxides and oxyhydroxides, and organic substances (Baalousha et al., 2011; Buffle and Leppard, 1995).

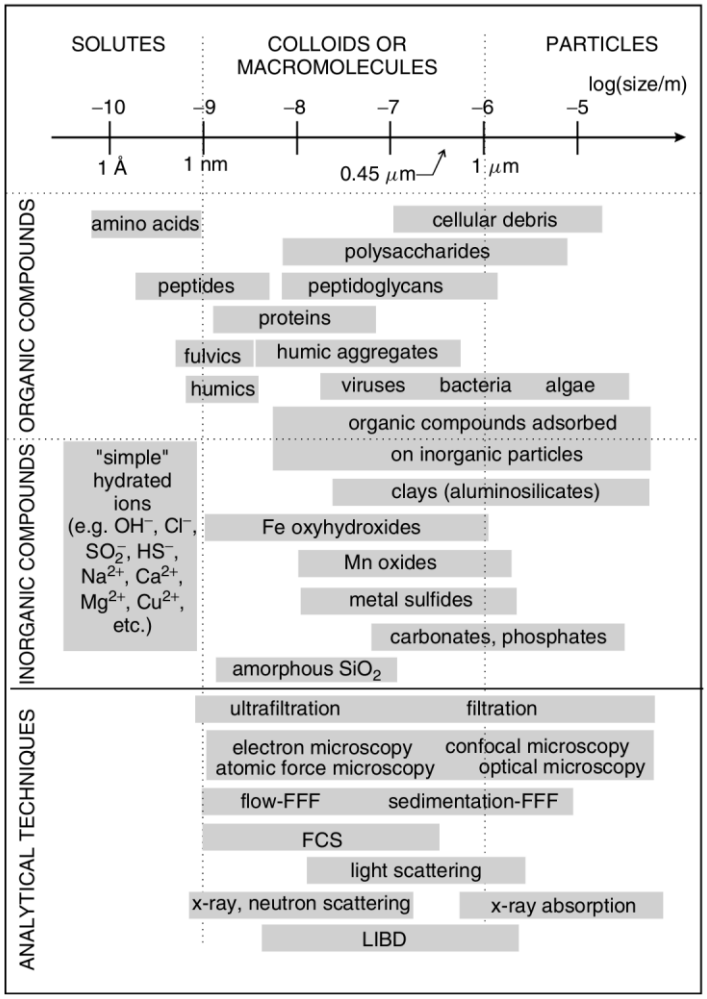

Figure 1.1 Size distribution of various types of environmental colloids and analytical techniques used to characterize them. Abbreviations: FFF = field-flow filtration; FCS = fluorescence correlation spectroscopy; LIBD = laser induced break down detection (adopted from Lead and Wilkinson, 2007).

According to the size-based definition, colloids are distinguished from aqueous solution and large particles. Thus, colloidal phase forms a critical transition zone between dissolved and particulate phases. The size range and chemical compositions of important colloidal and particulate species, along with the corresponding fractionation and analytical techniques are summarized in Figure 1.1 (Lead and Wilkinson, 2007). On the one hand, the lower size limit distinguishes colloids from aqueous solution and clusters, suggesting they are large enough to have supermolecular structures and properties that are significantly different from entities smaller than 1 nm. On the other hand, the upper size limit separates colloids from the larger particulate phase with interfacial properties less important than those of the colloidal phase. This size-based physical definition of colloids has been countered with a chemocentric definition by Gustafsson and Gschwend (1997). They proposed that colloids are constitutes possessing two main properties: (1) they offer molecular milieu into or onto which chemicals can escape from the aqueous solution and (2) its stabilization are dominated by coagulation or aggregation instead of gravitational sedimentation. Both the physical and chemical definitions of colloids signal the importance of the colloidal phase and its special properties compared with the aqueous or particulate phases. Generally, as they are small solid-phase materials, colloids are unique and dominated by their surface properties, such as large surface area and variable surface charges, rather than their chemical composition.

However, a generally accepted scientific definition to distinguish “dissolved” and “colloidal” phases does not exist. Traditionally, the dissolved or solution phase has been operationally defined as the filtrate through 0.45-μm filters, while colloidal and particulate phase are particles larger than the 0.45 μm cut-off size (Buffle, 1992;

Goldberg et al., 1952). This operational separation leads to the issue that large amounts of colloids may still be present as suspended particles in the ”dissolved” phase, and, consequently, an underestimation of colloidal activities. A recent publication on the studies of metal sorption on organic matter (OM) raised the question: “What if dissolved is not truly dissolved?” (Schijf and Zoll, 2011). This question is not new and has been raised and debated a decade ago (Hart et al., 1993; Martin et al., 1995; Vignati et al., 2005), but it has been largely ignored. As a result, the potentially significant quantities of < 0.45 μm colloidal particles have continually been treated as part of the “dissolved” phase.

1.1.1.2 Size Distribution of Natural Colloids

Natural colloids have been studied on their transport and association with micronutrients, trace metals, and OM in aquatic ecosystems (Buffle and Leppard, 1995). The generation and stabilization of natural colloids depend on their source, nature of the particles, and vary depending on the physical, chemical, and biological processes involved. As a result, colloid size distribution is highly related to where colloids are generated, such as in soil pore water, riverine and coastal or marine systems, and how they are being modified by biogeochemical parameters, such as pH, ionic strength, redox conditions, during their transport. Size distributions of natural colloids from three different main sources are summarized in the following paragraphs.

Ranville (2005) measured colloid mobilization from a soil profile and found a significant difference in colloidal size distribution among different soil horizons and the < 0.45 μm fraction consisted a large portion of the 0.08-1.0 μm colloidal pool. In another study where trace elements in different colloidal fractions were analyzed by

ultrafiltration and dialysis, Pokrovsky et al. (2005) found that trace elements from peat land soil water associated with various materials and distributed differently in different size fractions. They characterized them into three groups: (1) species that mostly present as dissolved inorganic species and form weak complex with organic materials, i.e. Ca, Mg, Li, Na, K, Sr, Ba, Rb, Cs, As, Mn, (2) species smaller than 1 kDa but form strong complex with fulvic acids, i.e. Co, Ni, Zn, Cu, and (3) species strongly associated with Al, Fe and OM in all ultrafiltrates and dialysis (10 kDa to 5 μm). Lu et al. (2013) also reported the presence of nanominerals, such as chlorite, vermiculite and ferrihydrite, whose size distributions displayed different ranges for nanosheets and nanorods of aluminosilicates (20 to 150 nm) and nanoparticles of iron-oxides (5 to 10 nm). Those observations indicate that colloids in soil solutions consist of three main components — clay minerals, iron-oxides and OM. The three components can exist in every size fractions and their size distributions largely depend on the physiochemical compositions and properties of soils.

It's well known that riverine colloids can be either sinks or vectors of trace metals, micronutrients, and OM. Recent applications of different fractionation methods, such as centrifugation and ultrafiltration, along with other analytical techniques, for studying the composition and partitioning of aquatic colloids have improved our understanding on mobilization of riverine colloids and cycling of the trace substances associated with the colloids.

Riverine colloids have high capacity in binding of trace elements, thus extensive research has been carried out on the interactions between colloids and trace metals. Measurements of trace metals associated with colloids in fresh water showed that colloid size distribution vary largely with changing hydrology, physiochemical

environments, and colloid composition. Size fractionations (< 0.45, 0.45 to 1.2, 1.2 to 2.0 μm) of stream water samples from Versoix River in Switzerland showed that < 0.45 μm colloids constituted 40% of bulk particle mass, while the other two fractions only made up 30% mass for each. Similar to those in soil pore waters (Pokrovsky et al., 2005; Pokrovsky and Schott, 2002), trace elements distributed differently within different fractions, where Al, Pb and Ti formed strong associations with particles from 0.45 to 1.2 μm, while other metal species varied in their affiliations on different size colloids (Vignati and Dominik, 2003). Ross and Sherrell (1999) arrived at the same conclusion that trace metals distribute differently in different size fractions. They found that colloids in < 0.45 μm filtrates from the samples from the Mullica River's drainage basins in New Jersey Pineland Streams included 65% Al, 82% Fe, 29% Mn, 66% Cu, 31% Zn, 46% Cd, and 88% Pb of the total concentration of these elements in bulk unfiltered samples.

Colloidal iron oxides, clay minerals, and OM have attracted much attention because of their potential role in trace element cycling. Pokrovsky and Schott (2002) reported that iron oxides are in general present as large size particles (0.22 to 5 μm), while natural organic matter (NOM) is concentrated in the fractions < 10 kDa. By using field flow filtration (FlFFF), Lyven et al. (2003) found OM has a narrow range of hydrodynamic size distribution (1 to 1.5 nm), while the distribution of iron-containing particles are centered at larger size up to 5 nm. Studies on natural organic carbon (OC) in fresh water also showed that colloidal organic carbon (COC) constituted a large portion of the bulk OC in the water. Dalzell et al. (2005) fractionated water samples from Big Pine Creek of west central India into particulate OC (POC; > 0.7 μm), COC (0.2 to 0.7 μm) and high-molecular-weight organic matter

(HMW-OC; 1 kDa to 0.2 μm). They found COC and HMW-OC together comprised 49% of the dissolved OC (DOC) during flooding and 40% of DOC during base flow. Similarly, another study on carbohydrate by Wang et al. (2013) reported that high-molecular-weight carbohydrates (HMW-CHO; 1 kDa to 0.45 μm) were the dominant species, representing 52-71% of the total carbohydrates (TCHO) pool, followed by low-molecular-weight carbohydrates (LHW-CHO; < 1 kDa), representing 14-44% of the TCHO, while the particulate carbohydrates (PCHO; > 0.7 μm) only accounted for 4-16% of the bulk TCHO.

Wells and Goldberg (1991, 1992) measured colloids in sea water samples collected from Pacific and off Nova Scotia and found that marine nanosize colloids (< 120 nm) are at least three orders of magnitude more abundant than larger submicron colloids (0.4 to 1.0 μm). Colloid concentrations varied as changing water depth and season, and the distribution of small colloids is substantially different from larger particles with increasing depth, where the concentration of large colloids (0.4 to 1 μm) decreased significantly with depth but the concentration of small colloids (< 120 nm) increased sharply near the lower thermocline (40-100 m). An additional study on sea water from Northern Atlantic and Southern Ocean confirmed their previous observations that small colloids (< 200 nm) varied in both concentration and size distribution with depth (Wells and Goldberg, 1994).

1.1.1.3 Surface Charge of Colloids

Natural colloidal particles are charged and the surface charges, which are either permanent or variable, depend on their chemical composition and surface properties (Baalousha et al., 2011; Buffle and Leppard, 1995; Ryan and Elimelech, 1996). Surface charges of soil particles are generated in four main ways: (1)

isomorphic substitution, defined as one atom replacing another with similar size in the mineral crystal lattice, e.g., the substitution of Si^{4+} by Al^{3+} in the tetrahedral layers or that of Al^{3+} by Fe^{2+}, Mg^{2+}, Zn^{2+} in the octahedral layers of clays; (2) ionization or dissociation of surface functional groups, such as protonation or deprotonation of M-OH in inorganic metal oxides or R-COOH, R-OH groups in COM; (3) dissolution of ionic solids, such as AgI; and (4) specific sorption of charged species, such as Ca^{2+}, or surfactants.

1.1.1.4 Surface Coating of Colloids

Surface coating formed between charged particles lead to complicated association of inorganic minerals and organic materials, and can significantly modify surface characteristics of the original uncoated particles (Baalousha et al., 2011; Stumm, 1993). The main components of soil colloids are layered silicates, metal oxides of Fe, Al and Mn, and OM. Large phyllosilicate minerals, such as kaolinite and montmorillonite, are usually coated with OM or inorganic Fe and Al oxides or oxyhydroxides from mineral weathering and deposition (Baalousha et al., 2011; Buffle and Leppard, 1995; Lead and Wilkinson, 2006).

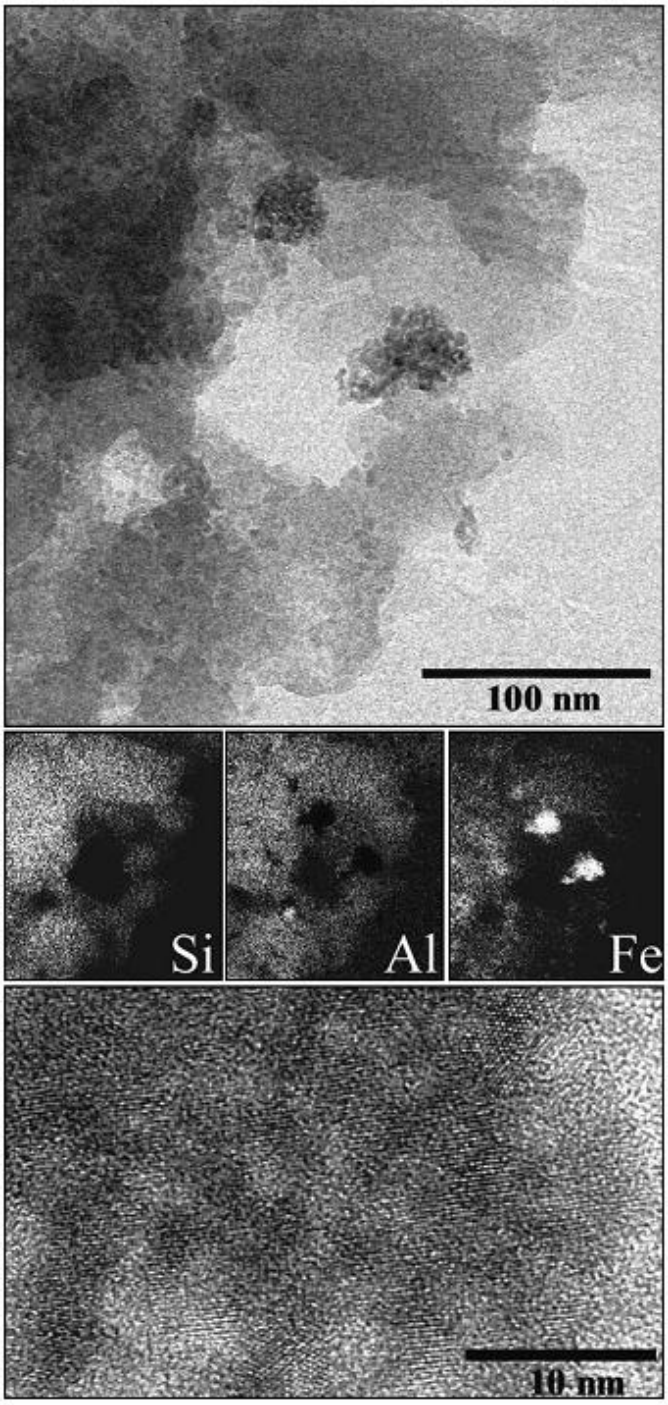

Figure 1.2 TEM images of sediments from Atlantic coastal plain, prepared using abrasion method. Top: zero-loss image; Middle: elemental images for Si, Al and Fe; Bottom: high resolution image of one goethite agglomerate from top image (adopted from Penn et al., 2001).

Iron oxides are ubiquitous in natural aquatic ecosystems and have been reported to act as a cement between clay minerals by Ryan and Gshwend (1990). They found that mobilization of soil inorganic colloids was largely affected by surface charge modification, which was induced by iron oxides and OM coatings on the surfaces of clays. Similarly, by using TEM, Penn et al. (2001) observed that sands from the Atlantic coastal plain aquifers displayed different surface electrostatic properties with coatings of goethite nanoparticles, Si and Al rich nanoscale minerals on the sand surface (Figure 1.2). Furthermore, shifting of point of zero charge (PZC) induced by surface coating of iron and aluminum oxides on soil minerals was also found on subsoil materials with different Fe and Al contents from southeastern United States and other tropical and subtropical areas around the world (Qafoku et al., 2000). Furthermore, studies of montmorillonite and kaolinite artificially coated with iron and aluminum oxides showed that the Fe and Al coatings affected not only PZC, but also other properties of minerals, such as specific surface area (SSA) and cation exchange capacity (CEC) (Sakurai et al., 1990). Iron and aluminum oxide coatings were found to affect PZC and CEC differently on different (Hendershot and Lavkulich, 1983) clay minerals, e.g., Al coating significantly shifted the PZC value of illite, but Fe coating had little effect on the mineral. (Hendershot and Lavkulich, 1983).

Compared to inorganic coatings, the effects of organic coatings on soil particles are more complex and vary with composition, such as different functional groups, and concentrations of OM. Mylon et al. (2004) reported that humic substance coatings on hematite stabilized hematite in the suspension. Similarly, removal of OM from water dispersible soil colloids led to their aggregation at lower electric conductivity of 91 $\mu S\ cm^{-1}$, while colloids with OM coating aggregated at a much

higher conductivity of 1023 μS cm^{-1} (Kjaergaard et al., 2004). However, OM coatings could also facilitate colloid aggregation via surface charge neutralization (Baalousha et al., 2008) as well as through bridging effects of high molecular weight OM (Baalousha, 2009).

1.1.2 Main Classes of Natural Colloids

1.1.2.1 Inorganic Colloids

Alumninosilicates are the most abundant colloids in soils and other natural aquatic ecosystems (Filella, 2007). Aluminosilicates are distinguished from other colloidal materials by their shape, surface morphology, charge property, and their broad particle size distribution. They are typically layered and have irregular platy shapes. Permanent negative charges can arise from isomorphic substitution in the octahedral sheet (e.g. Mg^{2+} for Al^{3+} of montmorillonite) or tetrahedral sheet (e.g. Al^{3+} for Si^{4+} of the vermiculites), while the charges on hydroxyls (e.g. Al-OH and Si-OH) on the "edges" of aluminosilicates are variable or pH-dependent. The stability of aluminosilicates in natural waters is mainly determined by the variable charge heterogeneity in combination with double-layer compression.

Ferric iron is present in soil and aquatic ecosystems as iron oxides, which are usually stable and do not dissolve in the presence of oxygen, while ferrous iron is only stable in the absence of oxygen or under reduced conditions (Cornell and Schwertmann, 2003b; Filella, 2007). The interchange between these two iron oxidation states leads to generation or removal of colloids or larger particles from different environment compartments. Compared to aluminosilicates, the release, dissolution and aggregation of colloidal iron oxides are highly controlled by the

dynamic physiochemical and biogeochemical processes that occur in natural ecosystems (e.g. microbial dissimilatory iron reductions). Natural iron oxide particles are complex with large variabilities in mineralogy, including goethite, hematite, magnetite, lepidocrocite, maghaemite and ferrihydrite (Cornell and Schwertmann, 2003b), and are generally recognized to act as cementing or coating agents on soil aggregates because they tend to possess net positive charges that can attract or stabilize negative charged aluminosilicates or OM.

1.1.2.2 Organic Colloids

Colloidal humic substances are heterogeneous in size and chemical composition. They are mixtures of plant and animals debris, which are structurally complex large macromolecules. Colloidal humic substances are typically resistant to degradation and are mainly consisted of carbon, oxygen, hydrogen, and small amounts of nitrogen, phosphorous and sulfur. While the unique chemical structure of humic substances has not been well developed, they are operationally defined by the technique used for their extraction and fractionation. The abundance and characteristics of humic substances vary among different environment compartments. Humic substances constitute 60-70% of soil OM (SOM) and 30-50% surface water OM. The numbers and types of active functional groups (e.g. COOH and OH) greatly influence the reactivity of humic substances in soils, where binding or complexation with minerals or metal ions occurs. The properties of colloidal humic substances have been reviewed by Jones and Bryan (1998). They reported that humic substances are naturally occurring organic colloidal particles, which interact with both naturally formed components (e.g. clays, metal ions) in the natural ecosystem and artificial materials (e.g. herbicides and pesticides) in agricultural fields.

Compared to humic substances, non-humic compounds are consisted of protein, carbohydrate, nucleic acids and small organic molecules, such as sugars and amino acids. The main components of non-humic compounds are carbohydrates because of their higher concentration and diverse composition (Jones and Bryan, 1998). Carbohydrates are normally excreted by algae and bacteria or released during cell lysis. Carbohydrates, especially polysaccharides, sometimes comprise 80-90% of the total extracellular release. The colloidal properties of polysaccharides largely depend on their macromolecular structure, from totally linear (e.g. cellulose) to strongly branched compounds (Baalousha et al., 2011; Filella, 2007).

1.1.3 Impact of Colloid Mobilization on Nutrients and Contaminants

1.1.3.1 Nutrients

Many laboratory and field investigations have found that colloids may influence nutrient movement, such as phosphorus (de Jonge et al., 2004b; Rick and Arai, 2011) and trace elements (Doucet et al., 2007; Lead and Wilkinson, 2006). The interaction between phosphorus and colloids and mechanism of colloid-facilitated transport of phosphorus are summarized as followed.

Phosphorus is frequently the limiting element in natural and agricultural ecosystems and its transfer is of great importance in controlling eutrophication. Colloid-facilitated transport plays a key role for the leaching of strongly sorbing phosphorus compounds from soils. de Jonge et al. (2004b) reported that the accumulated masses of particulate organic and inorganic phosphorus (< 2 μm) were linearly related to the accumulated mass of particles leached. And about 75% of the leached phosphorus was transported in a particle-facilitated manner. Experiments of

leaching using undisturbed soil cores by Vendelboe et al. (2011) also demonstrated the linear correlation between concentration of leached particles and particulate phosphorus concentration, which accounted for 70% of the total mass of leached phosphorus. Another soil leaching study with different phosphorus amendment by Kuligowski and Poulsen (2009) found that adsorption of phosphorus to soil particles (> 0.45 μm) contributed significantly to the total phosphorus pool.

Field studies have also demonstrated the importance of colloidal phosphorus in soil solution and aquatic ecosystems. Haygarth et al. (1997) fractionated river water and soil water samples into different size fractions and found that a considerable amount of reactive phosphorus was associated with organic colloids or mineral particles (1 kDa to 0.45 μm). The percentage of colloidal molybdate reactive phosphorous (3 kDa to 1.2 μm) varied in the lake and river samples, from 3% to 26% (Filella et al., 2006). Bauer et al. (1996) reported that 20-80% of total organic phosphorus pool was colloidal phosphorus (1 kDa to 0.2 μm) in the seawater samples collected from coastal Woods Hole.

1.1.3.2 Contaminants

Colloid-facilitating-transport of contaminants have attracted much attention and been examined in many laboratory and field studies involving radionuclides, heavy metals and organic contaminants (Kretzschmar et al., 1999; Mccarthy and Zachara, 1989; Sen and Khilar, 2006). The contaminants include cationic forms of metals (e.g., Cs^{+}, Cu^{2+}, Ni^{2+} etc.), anionic forms of metals (e.g. CrO_4^{2-}, AsO_4^{3-} etc.), nonpolar organic compounds (e.g. polycyclic aromatic hydrocarbons, polychlorinated biphenyls, DDT) and polar organic compounds. In general, the basic mechanisms of

contaminant's association with soil colloids are surface complexation, ion exchange, and hydrophobic partitioning (Sen and Khilar, 2006).

1.2 Colloid Mobilization and Stabilization

1.2.1 Colloid Generation and Mobilization in Aquatic Ecosystems

Three processes that affect colloid release and formation in subsurface environment include chemically induced release processes, precipitation, and hydrodynamically induced release (Kretzschmar et al., 1999; Mccarthy and Zachara, 1989; Sen and Khilar, 2006). Precipitation induced colloid release is mainly introduced by human activities, such as waste disposal, groundwater pumping or artificial recharge. Hydrodynamically induced release refers to colloid detachment by large hydrodynamic forces. Compared to chemical processes, neither precipitation nor hydrodynamically induced colloid release is common in a natural ecosystem. Previous studies have shown that mobilization of colloids and their subsequent behavior strongly depend on solution chemistry, such as pH, IS and presence or absence of NOM. The effects of pH and IS on colloid release and mobilization are reviewed in the following paragraphs, and the effect of OM will be discussed in section 1.3.

Shift in pH changes the surface charge of colloids and thus affects the attachment of colloids to soil porous medium. The surface of a colloid is negatively charged when pH is above the PZC value, while the surface is negatively charged if the pH is lower than the PZC value. When the pH is at the PZC, colloid tend to aggregate or coagulate (Hunter and White, 1987; Kretzschmar et al., 1998; Suarez et al., 1984). For soil colloids, pH is often more important for minerals with variably charged hydroxyl sites, such as iron-oxides, while is less important for permanently

charged clay minerals. This pH-effect has been clearly demonstrated in a study focusing on clay colloids passing through iron oxide-coated sand columns (Ryan and Gschwend, 1994a). They found that colloid release increased when the pH value exceeded the PZC of the iron oxide. Similarly, elevated pH effectively remobilized the attached bacteriophage PRD1 and silica colloids from iron oxide-coated sand aquifer (Ryan et al., 1999). Additionally, other than mineral colloids, studies on biological colloids, e.g. virus, have also observed similar impacts of pH on colloid mobilization (Chu et al., 2000; Jin et al., 1997).

Increasing solution IS compresses the electrical double layers around both colloids and collectors (e.g., a porous medium), and decreases the repulsive energy barrier between the colloids and collectors (Jin et al., 2000; Molnar et al., 2015; Ryan and Elimelech, 1996). Therefore elevated IS promotes both colloid-colloid aggregation and colloid attachments to collectors, and inhibit colloid mobilization. In other words, decrease in IS facilitates colloid mobilization. Ryan and Gschwend (1994b) investigated the IS-effect using columns containing hematite colloids and quartz sand grains. They found that both colloid release rate and extent increased with decreasing IS. Similarly, McDowell-Boyer (1992) observed the increase in mobilization of polystyrene latex colloids previously attached on sand grains when IS decreased. Similar impacts have been reported in studies on natural sediments, including studies on clay-containing Berea Sandstone (Khilar and Fogler, 1984; Kia et al., 1987; Vaidya and Fogler, 1990)

1.2.2 Colloid Mobilization under Anaerobic Conditions

1.2.2.1 Biogeochemistry of Anaerobic Ecosystems

Reduction reactions in soils take place as a result of oxygen being depleted from minerals or OM. Non-photosynthetic organisms tend to rebuild equilibrium by catalyzing oxidation of organic compounds back to inorganic forms in energy-yielding reactions. Compared to aerobic soils, anaerobic soils provide little or no oxygen as electron acceptors to produce energy but can provide alternative electron acceptors, either organics leading to fermentation or inorganics leading to anaerobic respiration (e.g. $NO3^-$, Fe or Mn oxides, $SO4^{2-}$ and CO_2). The sequences of reduction reactions as saturation time changes follow the order of decreasing change in free energy for the corresponding redox reactions, which are shown in Figure 1.3 as follows:

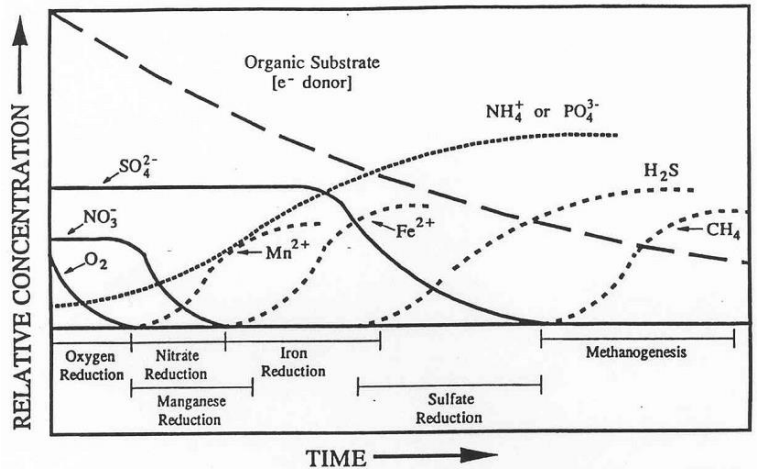

Figure 1.3 Sequence of reductions as time changes (adapted from Lorah et al., 2012).

Denitrification: $4NO_3^- + 5CH_2O + 4H^+ \rightarrow 2N_2 + 5CO_2 + 7H_2O$

Manganese Reduction: $2MnO_2 + CH_2O + 4H^+ \rightarrow 2Mn^{2+} + CO_2 + 3H_2O$

Iron Reduction: $4Fe(OH)_3 + CH_2O + 8H^+ \rightarrow 4Fe^{2+} + CO_2 + 11H_2O$

Sulfate Reduction: $SO_4^{2-} + 2CH_2O + 2H^+ \rightarrow H_2S + 2CO_2 + 2H_2O$

Methanogenesis: $2CH_2O \rightarrow CH_4 + CO_2$ or $4H_2 + CO_2 \rightarrow CH_4 + 2H_2O$

In soil systems, changes in moisture content strongly affect soil aeration status as well as soil redox conditions. Soil redox conditions are correspondingly dynamic and changes with soil depth and saturation time. Solution chemistry of anaerobic environments, such as pH, IS and OM concentrations, is also largely affected by reduction reactions. The indirect effects on transformation of key limiting nutrients play an important role in their cycling and mobilization. For example, phosphorus release is generated by iron reduction, chelation with metal ions and mineralization of organic phosphorus.

1.2.2.2 OM Effects on Iron Reduction

Many studies have reported the influence of NOM, such as humic substances, on iron bioreduction. Humic substances are complex organic polymers with diverse active functional groups, which are ubiquitous in the terrestrial ecosystem. Humic substances can chemically reduce ferric iron oxides without assistance from microorganisms (Szilagyi, 1971). In general, however, microbial dissimilatory iron reduction plays a key role in iron cycling by iron dissolution and organo-complexation. Enhancement of dissimilatory iron reduction depends on three strategies: (1) eliminate blockings of cell-oxide contact, (2) alleviate Fe(II) inhibition, and (3) make Fe(III) more available and bioreducible. Generally, NOM affects iron bioreduction in two main ways: electron shuttling and Fe(II) complexation (Figure

1.4.) (Lovley et al., 1996; Royer et al., 2002a; Royer et al., 2002b; Urrutia et al., 1999). In the presence of humic substances as redox mediators, enhancement of iron reduction has been reported in a study on monitoring the distribution of humic acid reduction and iron reducing bacteria in the freshwater sediments (Kappler et al., 2004). Rakshit (2009) showed that iron bioreduction was initially dominated by electron shuttling, while Fe(II) complexation dominated as Fe(II) concentration increased.

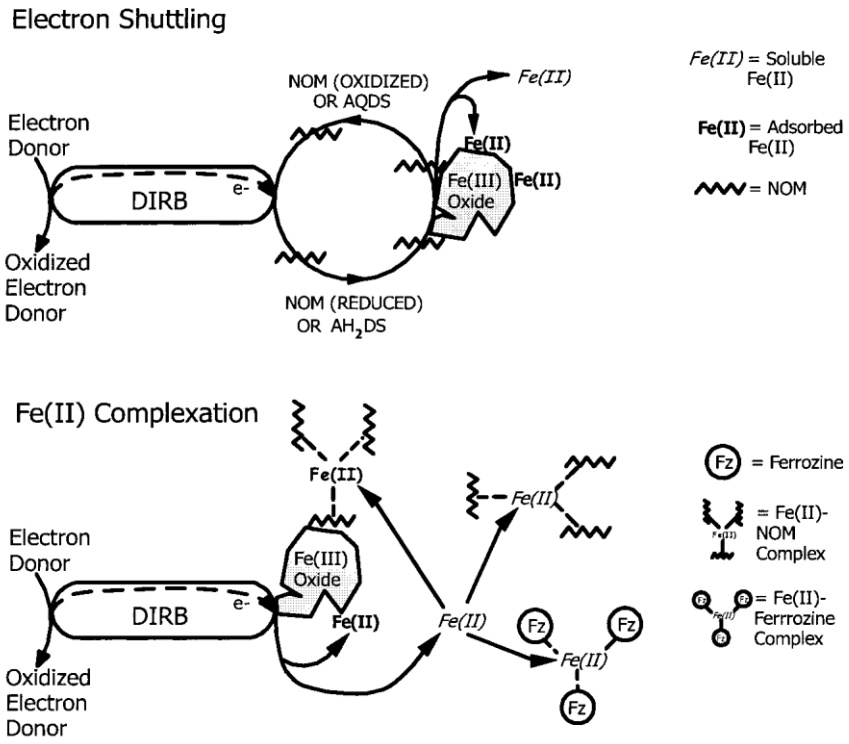

Figure 1.4 Proposed mechanisms for enhanced iron reduction by DIRB, electron shuttling and Fe(II) complexation. Abbreviations: DIRB = dissimilatory iron reduction bacteria; NOM = natural organic matter; AQDS = anthroquinone-2,6- disulfonate; AH_2DS = hydroquinone (reduced) form of AQDS (adapted from Royer et al., 2002b).

1.2.2.3 Iron Reduction Effects on OM Mineralization, Transformation or Retention

In addition to OM effects on iron reduction, iron reduction in turn can be a significant factor in controlling OM mineralization, transformation and retention on minerals in terrestrial ecosystems. When amorphous ferric iron oxides are present in river sediments, a wide range of fermentation products can be transformed and metabolized by iron reduction (Lovley, 1987; Lovley and Phillips, 1986). Dynamic redox reactions also affect the structure and characteristics of OM in forest soils (Fiedler and Kalbitz, 2003). The aromaticity and humic index of OM, which represent, respectively, the aromatic and humic substance content of the OM molecules, were higher in anaerobic soils than in aerobic soils. OM release and retention after mineral dissolution by soil reduction were also investigated (Fiedler and Kalbitz, 2003; Grybos et al., 2009; Hagedorn et al., 2000). Hagedorn et al. (2000) found a close correlation between DOC and dissolved iron concentration in forest soils, suggesting that reductive iron dissolution was a major factor for DOC release. Similarly, Fiedler reported that anaerobic conditions diminished the amounts of OM retained in soils (Fiedler and Kalbitz, 2003). The release of OM under reducing conditions was attributed to different processes, including reductive dissolution of Mn- or Fe- oxyhydroxides, pH induced desorption from organo-mineral associations, and organic metabolites produced by microorganisms. By conducting incubation experiments of soils under anaerobic conditions, Grybos et al., (2009) found that desorption of OM from clay as pH changed was more abundant than the OM from reductive dissolution from microbial metabolites.

1.2.2.4 Effects of Iron Reduction on Colloid Mobilization and Stabilization

Soil colloid mobilization and stabilization can be affected by the dynamic oscillation of redox conditions (Thompson et al., 2006), as shown in Figure 1.5. De-Campos et al. (2009) reported that short term reducing conditions disintegrated soil aggregates and resulted in particle mobilization. A strong positive correlation between soil redox potential (Eh) and soil aggregate stability, the ability of soil aggregates in remaining stable and not being disintegrated, indicated that aggregate stability decreased as Eh decreased (De-Campos et al., 2009). Studies on sediments and aquifers with high influxes of DOM also showed colloid release under reduced conditions (Fuller and Davis, 1987; Magaritz et al., 1990; Ronen et al., 1987; Ronen et al., 1992; Ryan and Gschwend, 1990). Shift in pH and iron dissolution as redox reactions proceed, both directly and indirectly, contribute to colloid release and stabilization. Calcareous cement dissolution as pH decreased, when CO_2 from degradation of OM dissolved into the soil water, induced colloid release and mobilization. Iron oxide cement dissolution can directly mobilize colloid from the solid matrix under reduced conditions (Ryan and Gschwend, 1990; Thompson et al., 2006). Ryan and Gschwend (1990)found that high concentrations of colloids (up to 60 mg colloids/L) were present in anoxic groundwaters, while much fewer colloids suspended in oxic groundwaters (< 1 mg colloids/L). However, incubation study of soils of high iron content with reduction and oxidation cycles showed that colloid mobilization dynamics depended on pH shifts accompanying the redox oscillations, rather than the reductive dissolution and oxidized formation of iron oxide cements (Thompson et al., 2006).

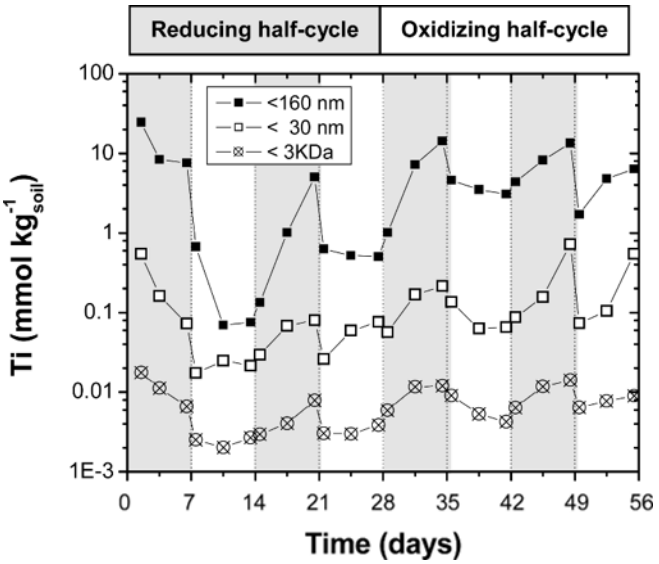

Figure 1.5 Colloidal Ti for the reactor with a full oscillation consisted of 7d of iron reduction followed by 7d of iron oxidation in logarithmic scales (adopted from Thompson et al., 2006).

1.3 Colloid Mobilization and Organic Carbon Stabilization

1.3.1 Carbon Stabilization in the Colloidal Phase

OM can be stabilized in soils by chemical protection via complexation or cation bridging with inorganic minerals, physical protection via occluded aggregation, and refractory stabilization due to its inert properties of OM (Bachmann et al., 2008; Kleber et al., 2007; Six et al., 2002). Generally, reactions of carbon stabilization depend on mineral composition, solution chemistry, and the varieties of functional groups that are on the OM. In physical stabilization, hydrophobic OM is stabilized by occluded aggregation with minerals following a decrease in wettability of soil aggregates (Bachmann et al., 2008). In chemical stabilization, abundance of hydroxyls on clay, iron and aluminum oxides (e.g. Al-OH, Fe-OH, Si-OH) stabilizes organic

carbon by forming organo-mineral complexes. A conceptual model of organo-mineral complexation was proposed by Kleber et al. (2007), which is shown in Figure 1.6

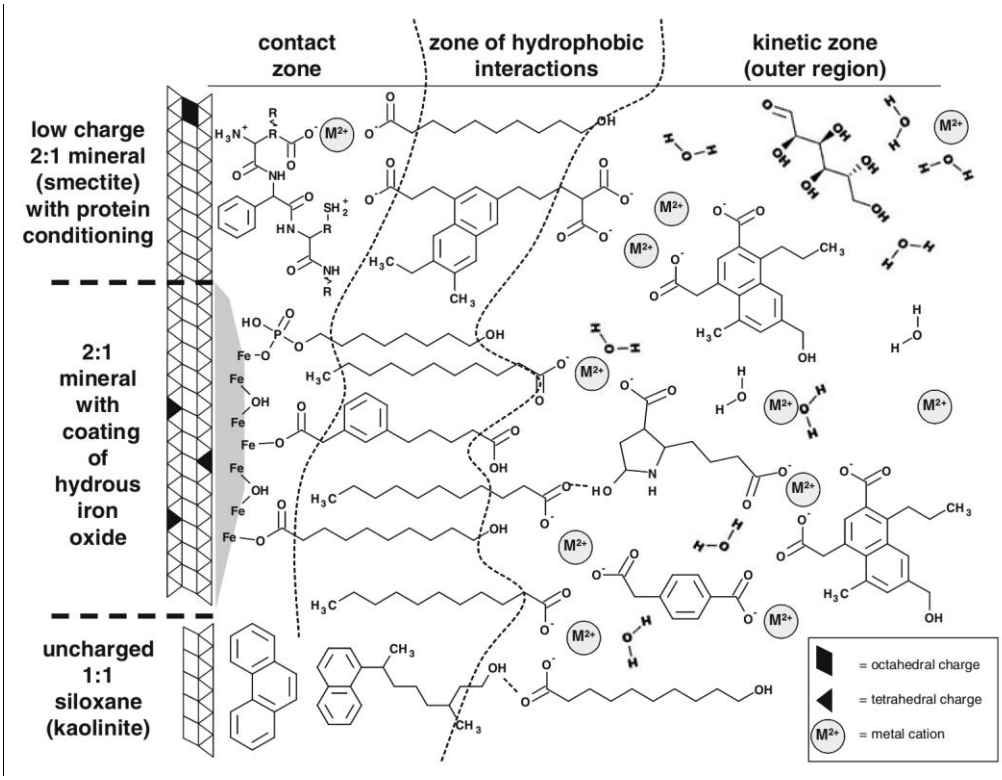

Figure 1.6 The zonal model of organo-mineral interactions. In the contact zone, amphiphilic fragments bind with charged surfaces through electrostatic interactions, directing hydrophobic portions outwards toward the polar aqueous solution; In the hydrophobic zone, entropically-driven self-organization to shield these non-polar organic matter from the polar aqueous medium through formation of a micelle; In the kinetic zone, interaction of organic molecular fragments and multivalent cations largely mediated the accumulation of organic matter (adopted from Kleber et al., 2007).

Compared to particulate and dissolved phases, the mechanism of carbon stabilization in the colloidal phase has not been thoroughly understood, despite

colloids' great potential in carbon retention. Both physical and chemical stabilization were observed in the particulate phase (> 1 μm) due to formation of micro-aggregates and macro-aggregates, while chemical stabilization dominated in the dissolved phase (Ellerbrock and Kaiser, 2005; Kaiser and Ellerbrock, 2005; Kayler et al., 2011; Kleber et al., 2007). However, the operational definition of "dissolved" phase used in these studies, which in fact contains both colloidal and truly dissolved phases, is not accurate. Therefore, it is reasonable to assume that while physical stabilization may be more significant in the particulate phase, chemical stabilization dominates in colloidal and truly dissolved phases. Nevertheless, this distinction still cannot differentiate and clarify the differences in carbon stabilization mechanisms between colloidal (1 or 10 kDa to 1 μm) and truly dissolved (< 1 or 10 kDa) phases. Many studies have reported that total organic carbon (TOC) in colloidal phase was comparable or greater than in truly dissolved phase, indicating that colloids can play a more significant role in carbon retention and stabilization compared to in truly dissolved phase (Guo and Santschi, 2007).

1.3.2 Effects of OM on Colloid Release and Stability

In natural ecosystems, OM tends to be associated with clay minerals and metal-oxides, especially iron-oxides. Specific adsorption and electrostatic attachment of OM on the surface of mineral colloids modify the colloids' surface properties, and thus greatly affect the dispersion of colloids. Previously, mobility and stability of colloids affected by OM were studied using: (1) synthesized crystalline or non-crystalline metal oxides, especially iron-oxides, such as goethite, hematite and magnetite, (2) isolated clay minerals or other metal oxides, such as quartz, aluminum oxides; and (3) natural riverine colloids or water dispersible soil colloids.

1.3.2.1 Synthesized Iron-oxides

Pure iron-oxides have PZC values from 6.3 to 9.5 (Cornell and Schwertmann, 2003b) thus they possess positive surface charge at natural pHs, while NOM are negative charged. The adsorption of OM modifies the surface charge of colloidal iron oxides and mobilizes or destabilizes them in different ways (Antelo et al., 2007).

Tipping and Higgins (1982) first reported that adsorbed humic substances enhanced the stability of colloidal hematite due to steric stabilization rather than electrostatic stabilization at high adsorption density. Building on these findings, another study concluded that surface charge neutralization and particle aggregation can be induced by small amount of humic acid adsorption on hematite, while surface charge reversion and particle stabilization are dominated by association with large amount of humic acid (Kretzschmar et al., 1995). Similarly, fulvic acid affected surface charge of hematite colloids and thus stabilized them in the suspension (Wilkinson et al., 1997). Herrera Ramos and McBride (1996) also found that low molecular weight OM, citrate and salicylate, and relatively high molecular weight natural humic substances both led to aggregation of goethite colloids at low concentration of organic carbon, while dispersion of colloids occurred at high concentration of organic carbon. Interestingly, disaggregation and mobilization of hematite nanoparticles from large aggregates have been found to occur due to repulsion forces as negative charged humic acid diffused inside the aggregates (Baalousha, 2009). Shift in PZC values has been used as an indicator for surface charge modification by adsorbed OM in many studies. Following the adsorption of OM, PZCs of iron-oxides shifting to lower values of pH have been reported (Baalousha, 2009; Herrera Ramos and McBride, 1996; Hu et al., 2010).

The adsorption of OM, along with IS, specific metal ion complexation and heteroaggregation with other inorganic particles, largely determine the aggregation behavior of colloids (Baalousha, 2009; Chen et al., 2006; Findlay et al., 1996; Herrera Ramos and McBride, 1996; Kretzschmar et al., 1995; Mylon et al., 2004). Findlay et al. (1996) found that heteroaggregation of quartz and hematite was dominated by electrostatic interactions, and was not influenced by absorbed OM. Kretzschmar et al. (1995) reported that stability of humic substances coated hematite was very sensitive to Ca^{2+} concentration; increasing Ca^{2+} concentration not only compressed the double layer, but also specifically complexed with the humic acid, and thus decreased colloid stability by forming large aggregates. Furthermore, both conformation and composition of adsorbed OM play a role in determining colloid stability, but it largely depends on the electrolytes in the given environment. One the one hand, electrostatic shielding of NaCl and neutralization of negative charge by $CaCl_2$ led to folding of adsorbed polysaccharide and retracting to hematite surface; on the other hand, the complexation of alginate with Ca^{2+} bridged hematite and alginate together (Herrera Ramos and McBride, 1996). Similarly, Chen et al. (2006) reported that citrate had profound effects on flocculation by forming intersphere complexes with Ca^{2+} and goethite.

1.3.2.2 Isolated Clay Minerals or Other Metal Oxides

Unlike iron-oxides, clay minerals possess an overall negative charge at natural pH. However, the oxy-hydroxy groups on the edge surfaces can be produced by breakup or disintegration of clay particles, which are more reactive in surface charge reactions and ion exchange than siloxane groups on the basal surfaces of clay minerals. Adsorption of humic acid was found to modify the surface properties and

facilitated the dispersion of kaolinite (Akbour et al., 2002). For concentrations of humic acid greater than 0.2 mg/L, kaolinite colloid stability increased as humic acid concentration increased; while for low concentrations of humic acid (< 0.2 mg/L), its stability decreased due to surface charge neutralization or bridging effects (Akbour et al., 2002). Similarly, adsorption of humic acid on the edge of montmorillonite increased its overall negative charge, increasing dispersion of montmorillonite particles in the suspension (Furukawa et al., 2009; Sondi et al., 1997).

Adsorption of OM is attributed to the formation of mononuclear bidentate or polynuclear surface complexes between metal centers, such as Al, Mg and Fe, and humic substances. Sondi et al. (1997) reported that the adsorption of small molecular OM affected the electrokinetic potential of silica, aluminum oxides and gibbsite. Johnson et al. (2005) also found that low or intermediate concentrations of small molecular organic anion covered the surface of colloids and formed a steric barrier, as a result, enhanced colloid stability. On the other hand, high concentrations of small molecular organic anion induced the formation of bridging Al(III)-organic surface precipitates, and thus decreased colloid stability (Johnson et al., 2005). Small and large molecular OM from different sources behaved differently in affecting colloid stabilization (Wilkinson et al., 1998). Fulvic acid enhanced the stability of montmorillonite colloids, while colloids aggregated by binding with aquagenic or autochtonous biopolymers, which had fibrillar nonramified structures. More interestingly, the colloids stabilized by adsorption of fluvic acid formed aggregates by addition of aquagenic biopolymer, suggesting small molecular OM stabilized colloid can be destabilized by the introduction of large molecular OM (Wilkinson et al., 1998).

1.3.2.3 Natural Riverine Colloids or Water Dispersible Soil Colloids

Natural colloids, composed of clay minerals, metal-oxides and NOM, are complex. Kretzschmar and Sticher (1997) reported that the natural soil colloids used in their study had complicated and various compositions and were composed of kaolinite, hydroxyl-Al-interlayered mineral, small amounts of gibbsite, goethite, hematite and NOM. By removing absorbed NOM with NaClO solution, they found that the attachment efficiency of colloids to matrix surfaces enhanced and thus decreased colloid mobility and stability. However, interestingly, by adding humic acid to NOM removed colloids, colloids regained their stability and mobility again (Kretzschmar and Sticher, 1997). As discussed above, mobility of natural colloids is largely affected by the presence of NOM in the natural aquatic ecosystems; however, it is also affected by many other factors, such as pH and the presence of specific cations.

1.4 Research Rationale and Objectives

1.4.1 Research Rationale

Despite the importance of the colloidal phase in binding elements or contaminants in soil and aquatic systems has been recognized, as indicated by the literature review above (Baalousha et al., 2011; Kretzschmar et al., 1999; Lead and Wilkinson, 2007; Vold and Vold, 1983), majority of the studies have not considered the role of mobile colloids in carbon cycling and colloidal organic carbon, especially those with sizes < 0.45 μm. This is the fraction that has been operationally defined as "dissolved" in most previous studies and, as a result, the < 0.45 μm remains a poorly quantified component of natural organic matter in both freshwater and seawater systems (Guo and Santschi, 2007). The operational definition of the “dissolved” phase

uses standard membrane filtration to produce "particulate" (> 0.45 μm in size) and "dissolved" (< 0.45 μm in size) fractions due largely to technical limitations and the rationalization that this size cutoff could lead to reduction of chemical complexity of filtrate, partial sterilization and improvement of data quality. This practice was based on an unjustified assumption and common believe that colloidal mass in the < 0.45 μm fraction was relatively low and their composition and behavior were similar to those of the solute or larger particles (Doucet et al., 2007). However, this operational practice likely leads to significant overestimation of dissolved pool thus underestimation of the actual colloidal loads. As a result, the practice would underestimate colloid-facilitated element transport as well as colloids' role in carbon transport. This underestimation and inability to accurately differentiate colloidal phase from particulate and dissolved phases would hinder our ability to assess the biological function and environmental fate and transport of colloid-associated-carbon. Therefore, it is critical to accurately quantify the colloidal pool and assess its actual contribution to the mobilization of colloid-associated-carbon.

Another reason that hindered our ability to quantify the < 0.45 μm colloidal fraction is the lack of economically feasible and technically effective methods to determine colloid concentration in field samples (Filella, 2007). Though previous studies have quantified colloids using a wide range of detection methods, including gravimetric determination, UV-Vis or fluorescent spectrophotometry, scanning electron microscopy (SEM) or transmission electron microscopy (TEM) microscopy, and laser-induced breakdown detection (Ledin et al., 1995), most of these methods have their limitations. For example, gravimetric method is greatly limited by its requirement for large volumes of samples where colloid concentrations in

environmental samples are in general low. In contrast, light scattering techniques, especially nephelometric turbidimetry, have the advantages of higher sensitivity, wider detection range, less interference, and smaller sample volume requirement, therefore, have been widely used in studies of sediment and colloid transport (de Jonge et al., 2004b; Jacobsen et al., 1997; Minella et al., 2008; Pfannkuche and Schmidt, 2003; Rugner et al., 2013; Schelde et al., 2002). However, most of the studies using the nephelometric turbidimetry method were conducted on larger particles (Minella et al., 2008; Pfannkuche and Schmidt, 2003; Rugner et al., 2013) with only a few studies focusing on colloid or nanoparticles (de Jonge et al., 2004b; Greswell et al., 2010; Jacobsen et al., 1997; Schelde et al., 2002). Therefore, evaluation of the turbidimetric method for its suitability to quantify mobile colloids, especially those < 0.45 μm is needed. A quick and simple method can significantly enhance our capability of quantifying colloids in natural samples in situ and to more accurately assess their role in affecting the fate and transport of colloid-associated constituents.

The alteration of environmental conditions can greatly impact the release and mobilization of colloids and organic matter, and thus changes the fate and transport of colloid-associated-organic matter. Therefore, identification of the environmental conditions or pathways that could potentially serve as hotspot of colloid and colloidal organic carbon (COC) mobilization is critical. Microbial dissimilatory iron reduction occurs under redox-dynamic conditions, commonly found in wetland soils, sediments, and natural waters (Kappler and Straub, 2005; Thamdrup, 2000; Weber et al., 2006), and can induce changes in solution chemistry, including ferric iron dissolution and pH shift (Ponnamperuma, 1972; Vepraskas et al., 2001). Recent studies have reported that the release of soil colloids and organic carbon can be induced by microbial-mediated

iron reduction (Buettner et al., 2014; Ryan and Gschwend, 1994a; Thompson et al., 2006), and external organic matter input accentuated the complexity of colloid and carbon mobilization through direct contacts with colloids or indirect influence on microbial iron reduction via electron shuttling and Fe(II) and Fe(III) complexation (Lovley et al., 1996; Roden and Urrutia, 2002; Royer et al., 2002a; Royer et al., 2002b; Straub et al., 2001). There is an interesting interplay between colloid mobilization, carbon release and changing redox conditions. Systematic investigation is necessary to understand the mechanisms of interactions between mobile colloids, organic matter and the potential role that colloids play in carbon cycling under dynamic redox conditions.

In addition, anthropogenic perturbations, such as agricultural practices and climate change, significantly influence environmental conditions, including primary production, physicochemical conditions, and microbial activities in natural systems. This would consequently influence colloid and colloid-associated-organic matter transport, and thus affect the allocation or input of organic matter from soils to inland water and marine systems (Bauer et al., 2013; Regnier et al., 2013). The ability of colloid-mediated-processes in affecting the mobility of OM varies depending on specific environmental systems or conditions. Therefore, to better assess and predict the influence of anthropogenic perturbation on OM mobilization and activity, environmental systems acting as potential hotspots of colloid and colloidal OM mobilization should be identified.

1.4.2 Research Objectives

The goal of the dissertation research was to investigate colloid mobilization and the colloids' role in carbon retention and transport. Both laboratory and field

experiments were conducted to quantify colloid release and mobilization under varying conditions and in different environments. Quantification and characterization of mobile colloids and the carbon associated with colloids were carried out. Specific objectives were:

1. To elucidate the mechanisms of colloid release affected by DOM under varying redox conditions;
2. To develop a methodology for quantifying mobile colloids < 0.45 μm fraction;
3. To quantify the environmental occurrence of mobile colloids, especially the < 0.45 μm fraction, and the OC associated with each size fraction;
4. To identify the environmental systems and conditions serving as hotspots of colloid and colloidal organic carbon release and mobilization among different natural and anthropogenic perturbed environments.

Chapter 2

SOIL COLLOID RELEASE AFFECTED BY DOM AND REDOX CONDITIONS

2.1 Introduction

Soil colloids (ca. 1 nm to 1 μm in size (Everett, 1972; Lead and Wilkinson, 2007)) are heterogeneous and complex mixtures of organic and inorganic entities with supramolecular structure and properties (Baalousha et al., 2011; Kretzschmar et al., 1999; Vold and Vold, 1983). Because of their small size and large surface area, and hence high reactivity and the ability to facilitate the transport of contaminants in the subsurface environments, mobilization and transport of soil colloids have attracted much research attention (Baalousha et al., 2011; Kretzschmar et al., 1999; Lead and Wilkinson, 2007). Soil colloid release, to a large extent, depends on solution pH, IS and natural OM (NOM) loadings, which affect the surface charge of colloids, and hence their inter-particle interaction and dispersion (McCarthy and McKay, 2004; Ryan and Elimelech, 1996; Suarez et al., 1984). Colloids tend to aggregate or coagulate when pH is at their point of zero charge (PZC), while dispersion of colloids is promoted at pH values both below and above the PZC (Hunter and White, 1987; Kretzschmar et al., 1998; Suarez et al., 1984). Adsorption of OM on colloid surfaces often changes the surface properties of colloids and determines their mobility (Hu et al., 2010; Kretzschmar et al., 1995; Tipping and Higgins, 1982; Wilkinson et al., 1997).

Microbial dissimilatory iron reduction occurs under redox-dynamic conditions, commonly found in wetland soils, sediments, and natural waters (Kappler and Straub, 2005; Thamdrup, 2000; Weber et al., 2006), and can initiate changes in solution chemistry, including ferric iron dissolution and pH shift (Ponnamperuma, 1972; Vepraskas et al., 2001). Dispersion of colloids under anaerobic conditions has been linked to iron dissolution and increase of suspension pH (Ryan and Gschwend, 1990, 1994a; Thompson et al., 2006). Ryan and Gschwend (1990) proposed a mechanism stating that iron oxides can act as cementing agents binding colloids together or to soil matrix, and colloids may be released when iron reduction and iron oxide dissolution cause inter-particle attraction forces to diminish or reverse. Some later experiments showed that transient pH shifts induced by iron redox chemistry principally controlled colloid dispersion (Ryan and Gschwend, 1994a; Thompson et al., 2006). These seemingly "inconsistent" explanations are the results of capturing only partially the very complex interactions between iron redox processes and colloid dispersion in each study. This complexity is further intensified by the coupling effects of OM through direct contacts with colloids or indirect influence on microbial iron reduction via electron shuttling and Fe(II) and Fe(III) complexation (Lovley et al., 1996; Roden and Urrutia, 2002; Royer et al., 2002a; Royer et al., 2002b; Straub et al., 2001). Previous research showed that OM could both disintegrate soil aggregates into colloids (Baalousha, 2009) or destabilize (i.e., cause formation of aggregates) suspended colloids depending on OM concentration or composition (Hunter and White, 1987). However, while the effects of pH and IS on colloid mobilization and transport have been studied extensively (Christian et al., 2008; Flury et al., 2002;

Grolimund and Borkovec, 1999; Tombacz et al., 1999), effects of OM and different redox conditions are less well understood.

Reducing conditions that result in dissolution of Fe and Mn oxides that could otherwise have served as sorption sites of DOM can also facilitate release of DOM in wetland soils (Kalbitz et al., 2000). Studies investigating the dynamics of DOM (operationally defined as OM passed through 0.22 or 0.45 µm (Karavanova, 2013; Nebbioso and Piccolo, 2013)) release in wetland soils reported positive correlations between DOM, Mn(II) and Fe(II) concentrations and increase in pH (Grybos et al., 2009; Hagedorn et al., 2000; Olivie-Lauquet et al., 2001). These processes can have significant impacts on mobilization and stabilization of colloidal carbon in soils. Therefore, a comprehensive understanding of colloid release in soils caused by coupling effects of OM and redox conditions is necessary.

This study focused on the interplay of colloid release, redox conditions, and effects of OM in soil. The research objective was to assess the coupling influences of iron reduction and DOM on the release of colloids. The complex dynamic interactions of soil colloids and OM under oxidizing and reducing conditions were examined under the following assumptions: (1) colloids and DOM are released during ferric iron reduction and dissolution processes; (2) colloid release over time is affected by changes in solution chemistry induced by iron reduction and presence of DOM. Batch experiments were conducted to quantify released colloids and to subsequently evaluate their mobility under aerobic and anaerobic conditions with different DOM concentrations. Relevant parameters, including pH, redox potential (Eh), IS, aqueous iron (Fe_{aq}) and OM concentrations, were measured, and colloid composition and morphology were also analyzed.

2.2 Materials and Methods

2.2.1 Soil Sample Collection and Preparation.

The soil used for this study was collected from a long-term 725-ha research watershed upstream of the Stroud Water Research Center (SWRC) in southeastern Pennsylvania, USA. The third-order watershed forms the headwaters of the White Clay Creek and is an intensively studied site for the established Christina River Basin Critical Zone Observatory (CRB-CZO). The soil is primarily Typic Hapludults (Newbold et al., 1997; Sloto, 1994). The soil was air-dried and hand-sieved through 2-mm sieves, and is classified as a sandy clay loam with sand = 51%, silt = 23%, clay = 26% using the hydrometer method (Bouyoucos, 1962). The soil had a pH of 6.2, its organic matter (SOM) content was 2.0% (loss on ignition method (Nelson and Sommers, 1996)), and total nitrogen content was 0.04% (Bremner, 1996). The exchangeable Fe, Ca, Al (determined by M3 extraction (Wolf and Beegle, 1995)) were 47.89 mg/kg_{soil}, 473.0 mg/kg_{soil} and 736.4 mg/kg_{soil}, respectively. The total "free" iron oxides and amorphous or poorly crystalline iron oxides were determined by dithionite-citrate-bicarbonate and NH_4-oxalate-oxalic acid extraction method (Loeppert and Inskeep, 1996), which were 9.4 g/kg_{soil} and 458 mg/kg_{soil}, respectively.

2.2.2 DOM Solution Preparation

DOM solution was extracted from a deciduous forest litter layer at the same field site where the soil samples were collected. The leaf litter was first washed using DI water and soaked for 24 h, and then the soaking solution was passed through a 0.2-mm sieve to remove leaf debris. To remove COM (colloidal organic matter, which is defined as OM from 10 kDa to 1 μm in this study) from the soaking solution, the

solution was filtered first through 0.45 μm MF-Millipore membrane filters (Millipore, Billerica, MA) and then through 10 kDa UF-Millipore membranes filters (Millipore, Billerica, MA). The resulting DOM solution was sterilized by pasteurization at 60°C for 1 h (Feachem et al., 1983; Vital et al., 2010); and total organic carbon (TOC) concentration was measured using a TOC analyzer (Elementar Americas, Vario TOC Cube) at the Soil Testing Lab at the University of Delaware. The major functional groups of 15 extracted DOM solutions from the same forest litter were characterized by EXAFS (extended X-ray absorption fine structure) spectroscopy previously (Chen et al., 2014). The C-NEXAFS (carbon near edge X-ray absorption fine structure) spectra of the extracted DOM showed a major band at 288.4 eV and two small peaks at 285.1 and 286.5 eV, respectively. These features correspond to carboxylic ($\pi^*_{C=O}$, 288.4 eV), aromatic ($\pi^*_{C=C}$, 285.1 eV) and phenolic ($\pi^*_{C=C-O}$, 286.5 eV) carbon (Chen et al., 2014).

2.2.3 Batch Experiments

Batch experiments were conducted to quantify the concentrations of colloids released over time at varying concentrations of added DOM under different redox conditions. The experiments consisted of a total of six treatments, including soil suspension in DI water, 5 and 20 mgC/L DOM solution, respectively, under both aerobic (oxidizing) and anaerobic (reducing) conditions, and with two replicates for each treatment. The soil samples for the anaerobic treatments were loosely spread out on clean glass plates and placed in a 95%:5% N_2:H_2 glovebox (Coy, Grass Lake, MI) for 96 h to thoroughly deplete oxygen. Afterwards, for each treatment, 14 g of soil and 140 ml of solution (DI water or 5 or 20 mgC/L DOM) were transferred into a 250 ml amber serum bottle (W. R. Grace and Company, Columbia, MA) to achieve a

soil:solution ratio of 1:10. To avoid re-oxidation of the soils when adding the solution, DI water was boiled while flushed with N_2 gas three times to deplete dissolved oxygen prior to use; DOM solutions were flushed with N_2 without boiling. Solid screw thread caps with interseal PTFE/silicone bonded septa (W. R. Grace and Company, Columbia, MA) were used to seal the bottles to avoid contact with air. Tightly sealed bottles were shaken outside the glovebox at 150 rpm in a water bath shaker (Eppendorf, Enfield, CT) for 14 d at 21 °C. The procedure for preparing the aerobic treatments was the same as for the anaerobic ones except that aerobic treatments were conducted in ambient air instead of in the glovebox.

2.2.4 Sampling Scheme & Sample Preparation

The reactors were sampled 7 times ($T_1 – T_7$) during the 14-d incubation: at 4, 68, 129, 197, 234, 306, 342.5 h after starting incubation for aerobic treatments and at 4, 72, 162, 208, 258, 306, 342.5 h for anaerobic treatments. At each sampling time, the reactors were allowed to sit for 3 h so that only < 1 μm colloids remained in suspension according to Stoke's Law (Krumbein and Pettijohn, 1938). The 3-h settling time was verified by measuring the size of particles that remained in suspension by dynamic light scattering analysis in a preliminary test, which showed a particle size range between 261 and 1084 nm. An aliquot of 1 ml of the suspension from each reactor was transferred into a microcentrifuge tube and then the same volume of DI water was added to each reactor to replenish the suspension to maintain a constant soil: solution ratio. Anaerobic reactors were sampled inside of the glovebox while aerobic reactors were sampled under ambient conditions.

2.2.5 Colloid Concentration

Concentration of < 1 μm colloids (after initial settlement by gravity and 30-min centrifugation at 4900 g to separate and remove the supernatant containing < 0.1 μm particles, if any, and dissolved ions) was determined gravimetrically. The centrifugation speed, time and the size of the particle settled by the centrifugation were selected based on the study of Gimbert et al. (2005). The collected colloids in each microcentrifuge tube were freeze-dried (Labconco, Kansa City, MO) for 24 h until a constant weight was achieved and then quantified with a microbalance. Colloid concentration was reported in a unit of mg/L (dry weight / volume of suspension). It should be noted that < 0.1 μm nano-sized colloids could be present in and hence were removed with the supernatant, however, the possible underestimation of colloid concentration should be insignificant due to the negligible mass of nano-sized colloids.

2.2.6 Chemical Analysis

Suspension pH, Eh and electrical conductivity (EC) were measured with corresponding probes (Fisher Scientific, Hampton, NH) at each sampling time; anaerobic samples were measured in the glovebox, while aerobic samples were measured in ambient air. Suspension IS was calculated from the measured EC values using the equation by Alva et al. and Griffin and Jurinak (Alva et al., 1991; Griffin and Jurinak, 1973; Morrisson et al., 1990):

$$IS = 0.013 \times EC \qquad (2.1)$$

where EC is the suspension electrical conductivity (ds/m).

The samples were centrifuged (30-min, 4900 g) to remove particles with sizes > 0.1 μm. Because Fe(III) is most likely to present in colloidal and particulate phase

due to its low solubility, aqueous iron concentration (Fe_{aq}) in the supernatant (< 0.1 µm) was assumed to be dominated by Fe(II) (confirmed by preliminary ferrozine colorimetric measurement, data not shown). To prevent Fe(II) from oxidation and precipitation, the supernatant was preserved by adding 1 N HCl to reduce its pH to < 1. Fe_{aq} concentration was measured by inductively coupled plasma mass spectrometry (ICP-MS, Intrepid II XSP, Thermo Elemental, Waltham, MA).

To determine DOM concentration under different redox conditions, for each treatment, TOC of < 0.45 µm soil suspension was measured using a TOC analyzer (Elementar Americas, Vario TOC Cube) at T_1 and T_7. Additionally, the < 0.45 µm OM in soil suspension under anaerobic conditions was characterized by UV absorbance and fluorescence-EEM (Excitation-Emission Matrix) at T_1 and T_7. The adsorption coefficient at 254 nm (a_{254} in m^{-1}) was obtained following the procedure of Green and Blough (1994) and specific UV absorbance (SUVA in L mgC^{-1} m^{-1}) of OM was calculated as its specific adsorption at 254 nm (m^{-1}) divided by the concentration of TOC (mgC/L) (Inamdar et al., 2011). Both a_{254} and SUVA provided a measure of OM aromaticity. The relative molecular weight of OM, which is inversely related to the S_R slope (the ratio of UV absorbance at 275-295 nm to 350-400 nm) (Helms et al., 2008), was evaluated. In addition, humification index (HIX), indicating the degree of humification of OM, was obtained by fluorescence-EEM analysis (Her et al., 2003).

2.2.7 Bacteria DNA Analysis

The denaturing gradient gel electrophoresis (DGGE) analysis was performed on selected samples to identify dominant bacteria community and evaluate differences in microbial activities under different experimental conditions using the DcodeTM Universal Mutation Detection System (Bio-Rad, Philadelphia, PA) at SWRC in

Avondale, Pennsylvania, USA. In brief, for each sample at the last sampling point (T_7), 1-mL of soil suspension was centrifuged at 11,800 g for 10-min and stored in a freezer at – 20 °C before DNA extraction. DNA was extracted using the UltraCleanTM Soil DNA Kit (MO BIO Laboratories, Carlsbad, CA). Polymerase chain reaction (PCR) amplification was performed with a Mastercycler (Eppendorf, Enfield, CT). The PCR primers used were 1070f and 1392r (GC clamp) (Ferris et al., 1996; Kan et al., 2006). DGGE was performed as previously described (Kan et al., 2006), except that the linear denaturant gradient used was 40-70% instead of 40-65%.

2.2.8 SEM-EDS Preparation and Analysis.

Colloid morphology and elemental composition were examined using scanning electron microscopy combined with an energy-dispersive X-ray spectroscopy microanalyzer (SEM-EDS). Soil colloids (< 1 μm) were isolated for direct examination by re-suspending the freeze-dried colloids in DI water to form a suspension, and then this suspension was dried on a silicon wafer and coated with Au/Pd. SEM microscopy was performed at the Delaware Biotechnology Institute BioImaging Center in Newark, Delaware, USA. SEM images were obtained using a Hitachi S-4700 with an accelerating voltage of 15 keV. The elemental compositions of the particles were determined with an energy-dispersive X-ray spectroscopy microanalyzer (Oxford INCAx-act Silicon Drift Detector) with a voltage of 15 keV and a live time of 180 s.

2.2.9 X-ray Diffraction (XRD) Preparation and Analysis.

Mineralogy of soil colloids for aerobic and anaerobic treatments at T_7 were analyzed by wide-angle XRD (WAXD). WAXD measurements were carried out under

ambient conditions operating at 40 kV and 40 mA with Cu Kα (λ=1.5418 Å) as the X-ray source. Scans were performed in a 2θ range of 5–70° with a sample step of 0.05° and counting times of 20 s.

2.2.10 Statistical Analysis

Each of the measured parameters, i.e. colloid concentration, pH, IS and Fe_{aq}, were analyzed using a one-way analysis of variance (ANOVA) combined with the Least Significant Difference (LSD) and DUNCAN analysis to test their significance of differences ($P < 0.05$) among treatments for the same sampling time as well as among different sampling times for the same treatment.

2.3 Results and Discussion

2.3.1 Colloid Release under Anaerobic Conditions

The concentrations of dispersed colloids as a function of incubation time, serving as an indicator of colloid release, are plotted in Figure 2.1. The significance of difference in colloid concentration and other parameters among different treatments and sampling times are summarized in Table 2.1. In general, more colloids were released at T_1 under anaerobic conditions, as indicated by the significantly higher colloid concentration. As incubation continued, however, colloid concentrations at later times, T_3 or T_4, under anaerobic conditions decreased to 10-20% of the concentration at T_1. The reduced colloid release and dispersivity may be explained by the modification of colloid surface properties by the dynamic changes in solution chemistry, especially pH, IS and OM, and the processes of dissimilatory iron reduction under anaerobic conditions.

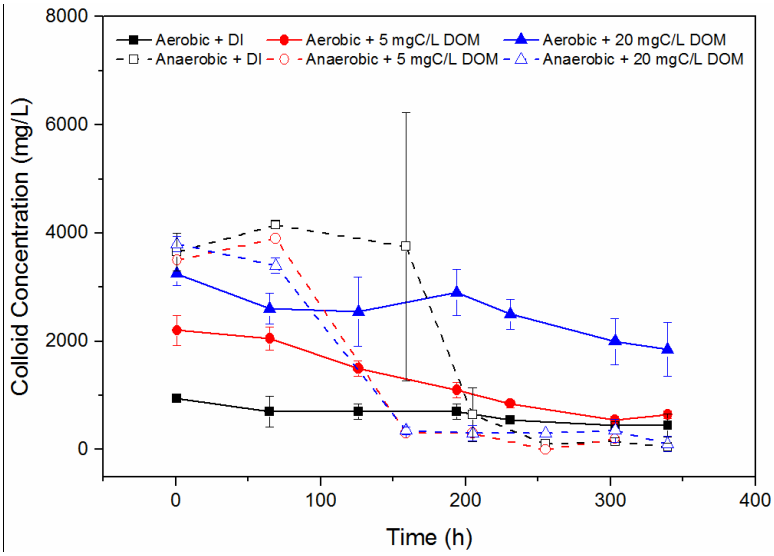

Figure 2.1 Colloid concentration as a function of time. Note: one anaerobic treatment with 5 mgC/L DOM had been exposed to air due to cracking of the sample bottle cap, the replicate results were not presented.

Table 2.1 Colloid concentration, pH, IS and Fe_{aq} dynamics under different redox conditions

Parameters	Treatments		Sampling time (Aerobic/Anaerobic)						
			T_1 (4/4 h)	T_2 (68/72 h)	T_3 (129/162 h)	T_4 (197/208 h)	T_5 (234/258 h)	T_6 (306/306 h)	T_7 (342.5/342.5 h)
Colloid concentration (mg/L)	Aerobic	DI	950c† ± 70.7§	700d ± 282.8	700 ± 141.4	700bc ± 141.4	550c ± 70.7	450b ± 70.7	450bc ± 70.7
		5 mgC/L DOM	2200b(a)‡ ± 282.8	2050c(a) ± 212.1	1500(b) ± 141.4	1100b(c) ± 141.4	850b(cd) ± 70.7	550b(d) ± 70.7	650b(d) ± 70.7
		20 mgC/L DOM	3250a ± 212.1	2600b ± 282.8	2550 ± 636.4	2900a ± 424.3	2500a ± 282.8	2000a ± 424.3	1850a ± 495.0
	Anaerobic	DI	3650a(a) ± 353.6	4150a(a) ± 70.7	3750(a) ± 2474.9	650bc(b) ± 495.0	100d(b) ± 0.0	150b(b) ± 70.7	50d(b) ± 70.7
		5 mgC/L DOM¶	3500a(a)	3900a(a)	300(b)	300c(b)	0d(b)	200b(b)	0d(b)

		20 mgC/L DOM	3800a(a) ± 141.4	3400a(b) ± 141.4	350(c) ± 70.7	300c(c) ± 141.4	300cd(c) ± 0.0	350b(c) ± 212.1	100bc(c) ± 141.4
pH	Aerobic	DI	6.71a† ± 0.01§	6.63a ± 0.04	6.70 ± 0.04	6.69 ± 0.06	6.71 ± 0.01	6.66a ± 0.03	6.64a ± 0.04
		5 mgC/L DOM	6.54bc(b)‡ ± 0.02	6.56a(b) ± 0.01	6.66(a) ± 0.01	6.64(a) ± 0.03	6.69(a) ± 0.00	6.67a(a) ± 0.00	6.68a(a) ± 0.04
		20 mgC/L DOM	6.35d(d) ± 0.03	6.41ab(c) ± 0.01	6.51(b) ± 0.04	6.63(a) ± 0.00	6.68(a) ± 0.01	6.63a(a) ± 0.01	6.65a(a) ± 0.01
	Anaerobic	DI	6.68ab ± 0.01	6.52a ± 0.18	6.94 ± 0.18	6.88 ± 0.13	6.74 ± 0.09	6.68a ± 0.04	6.61a ± 0.05
		5 mgC/L DOM¶	6.59abc	6.14bc	6.55	6.65	6.66	6.72a	6.68a
		20 mgC/L DOM	6.50c(a) ± 0.09	5.95c(d) ± 0.01	6.20(c) ± 0.05	6.41(ab) ± 0.03	6.38(b) ± 0.02	6.38b(b) ± 0.01	6.45b(ab) ± 0.02
IS (mM)	Aerobic	DI	0.37e†(c) ± 0.01§	0.83a(b) ± 0.13	0.84c(b) ± 0.12	0.88d(b) ± 0.18	0.96c(ab) ± 0.15	1.14c(a) ± 0.12	1.18c(a) ± 0.14

		5 mgC/L DOM	0.44d(c)‡ ± 0.01	0.83a(b) ± 0.06	0.83c(b) ± 0.06	0.94cd(a) ± 0.08	0.99c(a) ± 0.02	1.00c(a) ± 0.00	1.02c(a) ± 0.02
		20 mgC/L DOM	0.63c(b) ± 0.01	1.00ab(a) ± 0.18	1.19ab(a) ± 0.15	1.14bc(a) ± 0.01	1.15bc(a) ± 0.05	1.16c(a) ± 0.11	1.17c(a) ± 0.11
	Anaerobic	DI	0.65bc(e) ± 0.05	0.78a(de) ± 0.13	0.97bc(cde) ± 0.24	1.09bcd(cd) ± 0.11	1.34b(bc) ± 0.16	1.56b(b) ± 0.19	2.00b(a) ± 0.35
		5 mgC/L DOM¶	0.69a(d)	0.75bc(d)	1.01a(cd)	1.16a(c)	1.55a(b)	1.71a(ab)	2.03a(a)
		20 mgC/L DOM	0.71b(e) ± 0.03	0.90c(d) ± 0.06	1.16abc(c) ± 0.06	1.23b(bc) ± 0.09	1.28b(b) ± 0.08	1.31bc(b) ± 0.05	1.51bc(a) ± 0.02
Fe_{aq} (mg/L)	Aerobic	DI	0.08c† ± 0.03§	0.15c ± 0.21	0.09c ± 0.13	0.09a ± 0.13	0.07c ± 0.10	N. D. b	N. D. c
		5 mgC/L DOM	0.01c ± 0.04	0.01c ± 0.01	N. D. c	N. D. a	N. D. c	N. D. b	N. D. c

	20 mgC/L DOM	N. D. # c	N. D. c	N. D. c	N. D. a	N. D. c	N. D. b	N. D. c
Anaerobic	DI	1.92a(bc) ‡ ± 0.24	0.72b(e) ± 0.21	1.22a(cd) ± 0.21	1.07b(cd) ± 0.00	1.60b(cd) ± 0.54	2.57b(b) ± 0.54	4.73b(a) ± 0.41
	5 mgC/L DOM ¶	1.13b(c)	1.02ab(c)	1.30a(c)	1.50a(c)	4.28a(bc)	7.53a(ab)	11.03a(a)
	20 mgC/L DOM	1.07b(bc) ± 0.40	1.46a(ab) ± 0.18	0.85b(c) ± 0.10	0.82b(c) ± 0.14	1.05bc(bc) ± 0.11	1.32b(bc) ± 0.17	2.00bc(a) ± 0.33

† Statistical analysis on parameters of different treatments at same time ($P < 0.05$)

† Statistical analysis on parameters of same treatment at different time ($P < 0.05$)

§ Standard deviation of parameters

¶ Because only one replicate in anaerobic samples with 5 mgC/L DOM, one-way ANOVA analysis was conducted by assuming the standard deviation in parameters of anaerobic samples with 5 mgC/L DOM equals to the standard deviation of samples of all three treatments at same time. For example, the standard deviation in the colloid concentration of anaerobic samples with 5 mgC/L at T_1 equals to the standard deviation in those of anaerobic samples with DI, 5 and 20 mgC/L DOM at T_1.

N. D. stands for “not detectable” (?)

The mineralogical and elemental compositions of colloids under different redox conditions were similar according to XRD analysis and SEM-EDS microscopy. The colloids of the aerobic and anaerobic samples at T_7 were both composed of quartz, chlorite, biotite, and iron oxides (Figure 2.2). Iron oxides included mainly goethite and small amounts of hematite, magnetite and ferrihydrite. Elemental composition analysis of the colloids at T_3 (the time when colloid release was markedly reduced compared to at T_1 under anaerobic conditions) by SEM-EDS also showed that colloids from both aerobic and anaerobic samples had similar compositions (Figure 2.3). These observations indicate that colloid composition did not change significantly due to iron reduction during the short anaerobic incubation time in this study. However, the high initial colloid release followed by the decreased release over time under anaerobic conditions suggest that iron reduction led to modification of colloid surface properties therefore the interactions that control colloid release/dispersion.

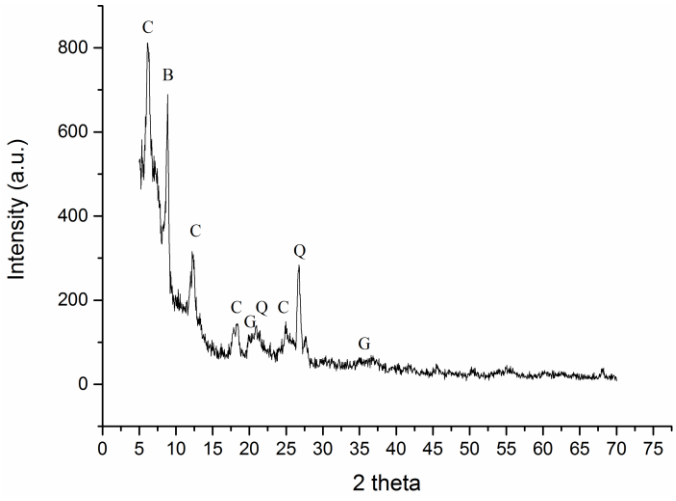

Figure 2.2 XRD analysis of colloids (Anaerobic + DI) at T_7.

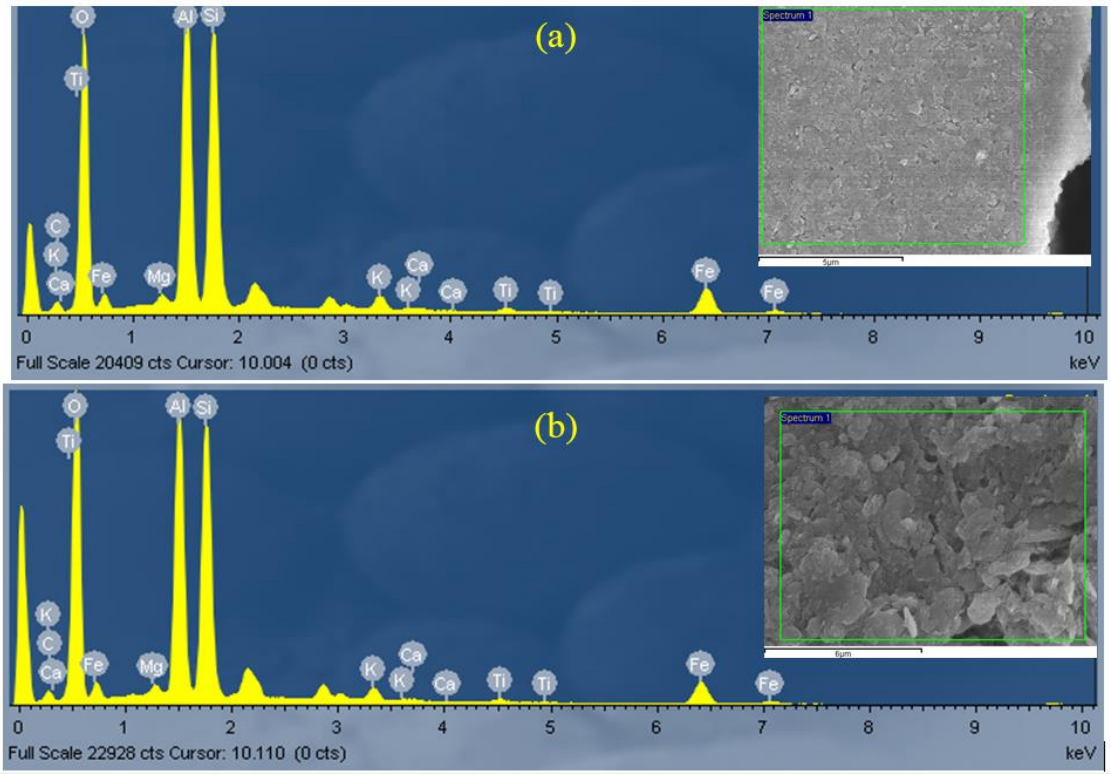

Figure 2.3 SEM-EDS elemental analysis of colloids without addition of DOM under aerobic (a) and anaerobic (b) conditions at T_3.

Dissolution of iron oxides changes solution pH and IS, which affect the magnitude or sign of colloid surface charge and hence inter-particle electrostatic repulsion (Bunn et al., 2002). To access the potential contribution of pH and IS to the initial colloid release, the pH and IS values at T_1 were compared between samples without the addition of DOM under aerobic and anaerobic conditions. No significant differences between pH (6.71 and 6.68, Figure 2.4a and Table 2.1, respectively) was observed. The PZC values of common iron oxides (Table 2.2) show that only the surface charge of magnetite could be affected at the sample pH values (Cornell and Schwertmann, 2003a), however, magnetite was largely absent from our experimental

soil, which further confirms that the effects of pH on the initial colloid release was limited. Small, although statistically significant, increase between the aerobic and anaerobic samples (0.37 and 0.65 mM, Figure 2.4b and Table 2.1, respectively) was observed. This small increase in IS likely played a minor role, if any, in affecting colloid release. Furthermore, increase in IS would have decreased colloid release rather than increasing it (Hunter and White, 1987; Ryan and Elimelech, 1996). Therefore, the observed greater initial release of colloids from the anaerobic samples was primarily caused by dissolution of iron oxides rather than changes in pH and IS.

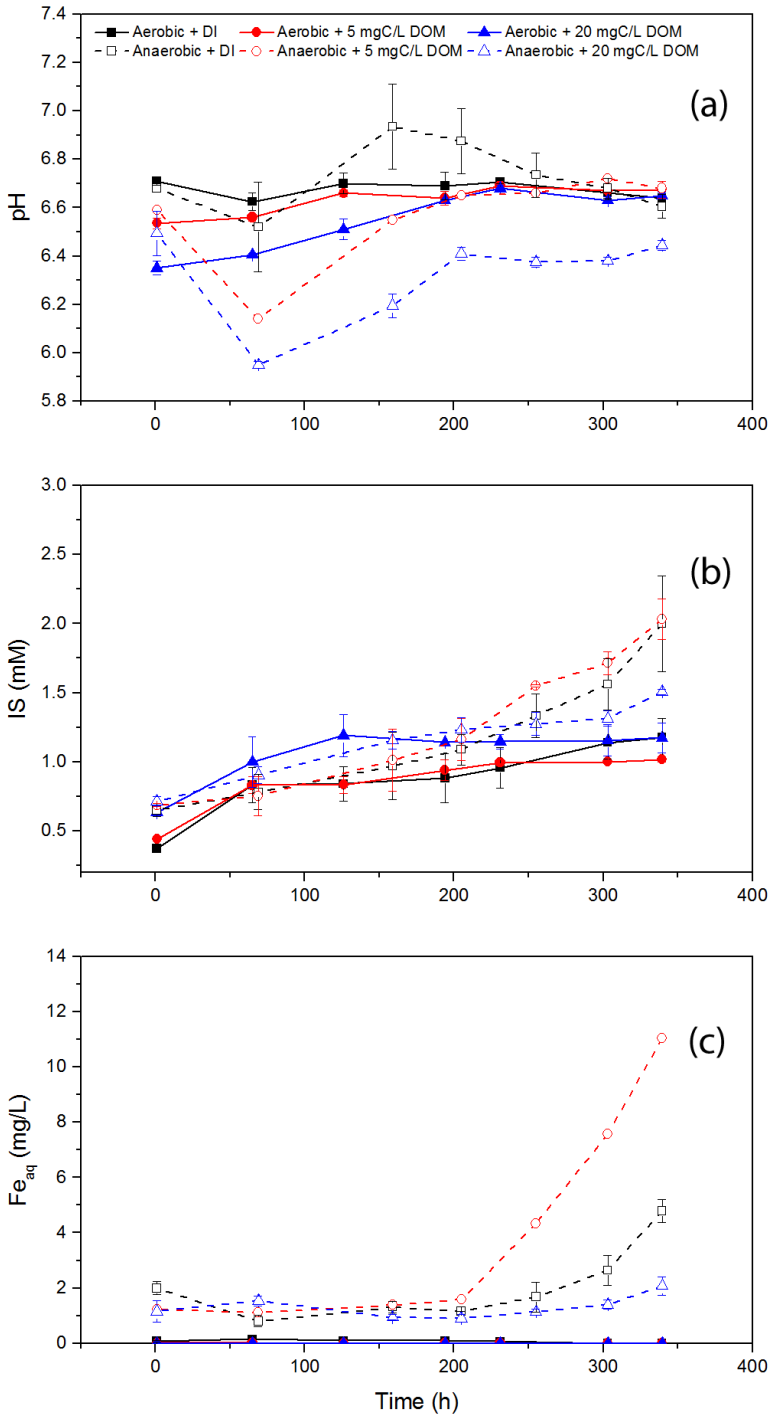

Figure 2.4 Solution chemistry dynamics as a function of time: (a) pH, (b) IS and (c) Fe_{aq} concentration.

Table 2.2 PZC (point of zero charge) of main iron-oxides in soils.

	Geothite	Ferrihydrite	Hematitie	Magnetite
PZC	7.5-9.5	7.8-7.9	7.5-9.48	6.3-7.1

To prove that colloid release was indeed due to iron reduction leading to dissolution of ferric iron oxides, Eh values and Fe_{aq} concentrations of the colloidal suspensions were measured (Figure 2.4c, Table 2.1). The Eh values generally remained stable in the aerobic samples during incubation at 400 to 600 mV but decreased to - 200 to - 400 mV in the anaerobic samples. The differences in Eh between the aerobic and anaerobic samples reflect the change in redox conditions and indicate that anaerobic samples were under strong reducing conditions. DGGE analysis showed that the microbial communities were also significantly different between the aerobic and anaerobic samples, and detected the presence of microbial iron reduction activities under anaerobic conditions (Figure 2.5). In addition, Fe_{aq} concentrations (1-2 mg/L) in the anaerobic samples at T_1 were significantly higher than in the aerobic samples (mostly below detection limit), providing convincing evidence that dissolution of ferric iron oxides occurred under anaerobic conditions ($P < 0.05$, Table 2.1). The higher Fe_{aq} concentration at T_1 coincided with more initial colloid release under anaerobic conditions. This observation is consistent with the previous study that attributed colloid release to iron reduction and dissolution of ferric iron oxides (Ryan and Gschwend, 1990). However, the fact that increase in Fe_{aq} concentration did not facilitate colloid release beyond T_3 suggests that other factors, i.e., DOM_{in}, IS and cations, may have contributed to the observed lower colloid concentrations in the anaerobic samples at longer incubation times, as discussed below.

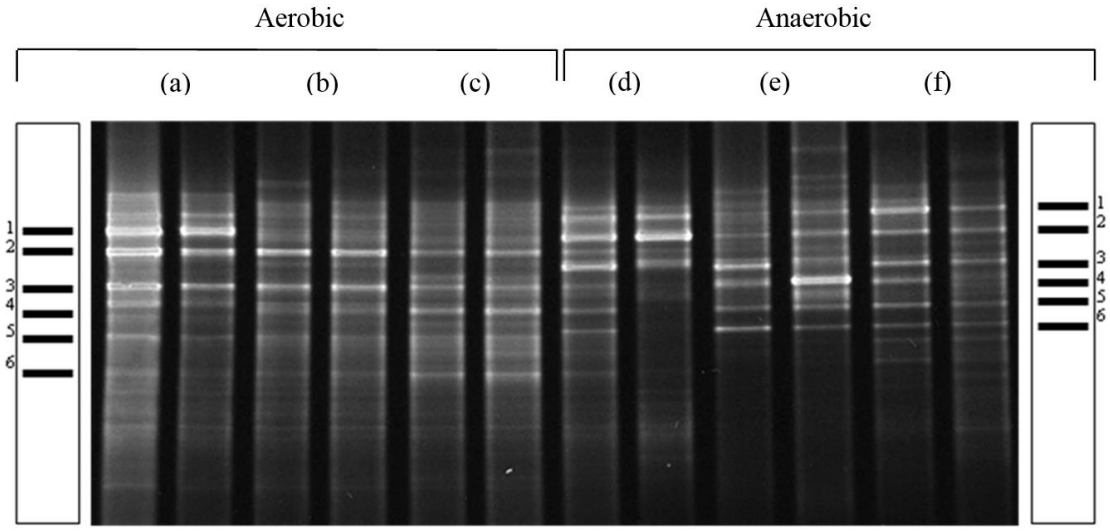

Figure 2.5 PCR-DGGE analysis of bacteria community at T_7. Bacteria community analysis under aerobic and anaerobic conditions for (a), (d) with DI water, (b), (e) with 5 mgC/L DOM solution, and (c), (f) with 20 mgC/L DOM solution. For each treatment, two replicates of samples were analyzed. Representative bands are listed and illustrated in the boxes for aerobic (left) and anaerobic samples (right).

2.3.2 OM-induced Dispersion of Colloids

The addition of DOM enhanced the initial release of colloids at T_1 under aerobic conditions (Figure 2.1, Table 2.1), which is likely caused by direct interactions between the colloids and DOM rather than the slight shifts in pH and IS due to the addition of DOM (Figure 2.4a, Table 2.1). The decrease in pH and increase in IS between the aerobic sample without DOM and samples with 5 and 20 mgC/L DOM at T_1 both would have inhibited colloid release due to the decrease in repellent negatively surface charge and double layer suppression by shifting in pH and IS, respectively. (Ryan and Elimelech, 1996) Previous studies reporting DOM's stabilizing effects on dispersed colloids have attributed the effects to inter-particle steric repulsion and electrostatic stabilization caused by adsorption of negatively

charged OM on colloid surfaces, especially at high concentrations of OM (Hu et al., 2010; Kretzschmar et al., 1998; Ryan and Gschwend, 1990; Tipping and Higgins, 1982).

Release of colloids over time was also influenced by the concentration of added DOM in the aerobic samples. As shown in Figure 2.1 and Table 2.1, most of the dispersed colloids in the treatment with 20 mgC/L DOM remained in suspension from T_1 to T_7, while colloid concentration in the sample with 5 mgC/L DOM treatment decreased gradually after T_2. Suspension pH and IS in samples with 5 and 20 mgC/L DOM both slightly increased from T_1 to T_3, but neither changed significantly between T_4 and T_7 ($P < 0.05$, Table 2.1). These insignificant shifts in pH and IS did not correspond to the considerable decrease in colloid concentrations of samples with 5 mgC/L DOM from T_4 to T_7. These observations suggest that the surface interaction between colloids and DOM played a more important role than suspension pH and IS in determining colloid release both initially and over time. There are several possible mechanisms that could explain the observations. DOM can stabilize a colloidal suspension through two mechanisms: steric repulsion and electrostatic interactions, both due to DOM adsorption to the colloids and the effects tend to depend on DOM concentration (Kretzschmar et al., 1997; Kretzschmar et al., 1998; Philippe and Schaumann, 2014; Tipping and Higgins, 1982). Therefore, at higher DOM concentration (i.e., 20 mgC/L DOM), greater DOM adsorption would possibly result in more complete coverage of colloid surfaces thus stronger steric repulsion and/or electrostatic interactions. On the other hand, the 5 mgC/L DOM concentration was likely not sufficiently high to provide enough surface coverage to cause more complete steric repulsion. In this case, it is also possible that DOM adsorption

occurred mainly on the positively charged sites (e.g. goethite), which gradually neutralized the surface charge leading to diffusion-limited coagulation (Hunter and White, 1987; Zhang and Buffle, 1995). This explanation is consistent with the observation that colloid concentration decreased gradually with time, as shown in Figure 2.1. It should be noted that, according to studies with well controlled systems, the relative importance of electrostatic and steric repulsion on colloid dispersion might be evaluated by monitoring the shifts in zeta potential, electrophoretic mobility of colloids or simulating and comparing the thickness of the diffuse double layer and OM adsorption layer on colloids. (Kretzschmar et al., 1998; Philippe and Schaumann, 2014; Tiller and Omelia, 1993) In this soil incubation study, these parameters were not measured or calculated due to the complexity in changes of solution chemistry and microbial activities, therefore either of the possible mechanism cannot be ruled out. To further this study, extracted soil colloids with controlled solution chemistry should be used in the future work.

Unlike aerobic conditions, addition of DOM did not increase colloid release at T_1 (Figure 2.1, Table 2.1) under anaerobic conditions, suggesting that most of the colloids were released initially due to iron dissolution rather than OM-induced disintegration of soil aggregates. In addition, high concentrations of DOM_{in} and corresponding significant decreases in colloid concentrations over time under anaerobic conditions were observed (Figure 2.6). Long-chain aquagenic biopolymers (Wilkinson et al., 1998; Wilkinson et al., 1997) or high-molecular-weight OM (Herrera Ramos and McBride, 1996; Lafuma et al., 1991) can form "bridges" with colloidal particles leading to aggregation under anaerobic conditions (Hunter and White, 1987). A supplemental TOC analysis of the same soil

suspension without the addition of DOM showed that the TOC concentration at T_1 under anaerobic conditions (29.48 mgC/L) was much higher than that under aerobic conditions (4.13 mgC/L) and gradually increased as incubation continued, which resulted in the bridging effects of DOM_{in} at T_3 or T_4. SEM images show that colloids in the samples without DOM addition under anaerobic conditions had more distinct patterns of "cracks", which are characteristic of OM coatings on soil particles (FitzPatrick, 1993) compared to the colloids from the aerobic samples (Figure 2.7).

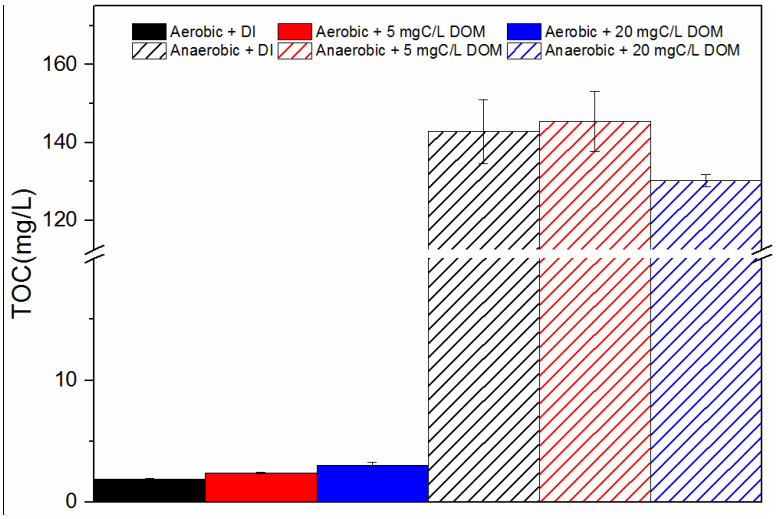

Figure 2.6 TOC concentrations of DOM in soil suspension at T_7.

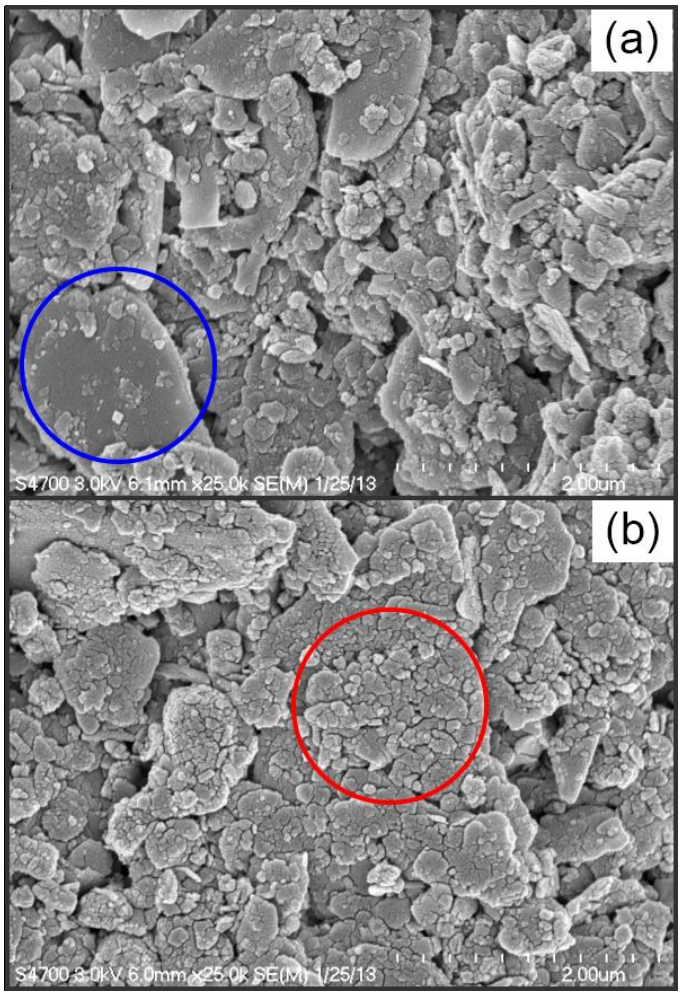

Figure 2.7 SEM images of aerobic (a) and anaerobic (b) samples without the addition of DOM at T_1. In (a), smooth morphology is circled out in blue; in (b), patterns of cracks are circled out in red.

To further validate the influence of bridging effects on colloid aggregation, a_{254}, SUVA, S_R slope and HIX of DOM_{in} of the anaerobic samples were characterized at T_1 and T_7 with UV absorbance and fluorescence-EEM, respectively (Table 2.3). The changes in these parameters of DOM_{in} suggest that OM with high aromaticity (a_{254}, SUVA), high degree of humification (HIX) and large relative molecular weight (S_R

slope) tend to absorb on colloids and settle out by forming large aggregates with the colloids (Bolt et al., 1991). In addition to direct bridging effects of DOM_{in}, cation bridging could also play an important role. A SEM-EDS analysis showed that re-sorption of Ca^{2+} or Fe^{2+} could form cation bridges between negatively charged particles and OM (Chen and Elimelech, 2007; Dong and Lo, 2013; Liu et al., 2011).

Table 2.3 DOM_{in} characterization under anaerobic conditions

Treatment: Anaerobic + DI	a_{254} (m^{-1})	SUVA ($L\ mgC^{-1}\ m^{-1}$)	S_R slope	HIX
T_1 (4 h)	36.39	0.54	1.28	0.31
T_7 (342.5 h)	4.38	0.01	20.00	0.18

2.3.3 Colloid Release/Stabilization Mechanisms and Environmental Significance

Based on the results from this study, the complex processes of colloid release as influenced by changing redox conditions and DOM concentration were summarize and possible mechanisms were proposed in Figure 2.8. Under aerobic conditions, the released colloids were either be stabilized in suspension or formed aggregates over time depending on the DOM concentration, suggesting possible mechanisms that steric and/or electrostatic repulsion dominate at higher concentrations of DOM, whereas surface charge neutralization occurs at low concentrations of DOM. Under anaerobic conditions, the initial release of colloids was primarily due to microbial iron reduction. Iron reduction induced changes in solution chemistry: the increase in IS suppressed the electric double layer of colloids. Iron reduction also facilitated release of high-molecular-weight DOM_{in}, which possibly bridges colloids together directly or

indirectly through cation bridges leading to formation of new aggregates and thus destabilizes colloid suspension.

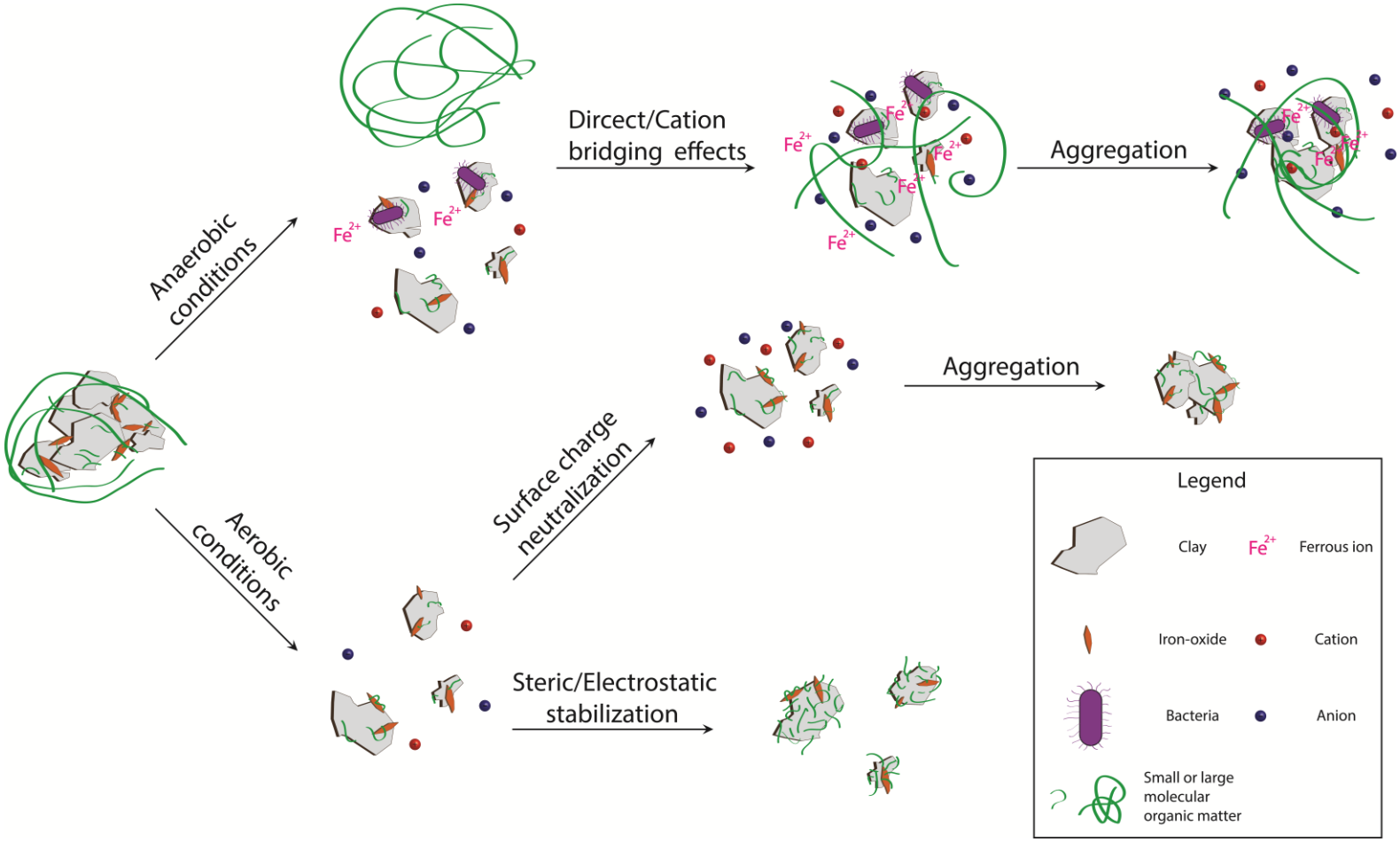

Figure 2.8 Scheme of colloid mobilization and stabilization in the batch system.

It should be noted that although supporting evidences for all the proposed mechanisms could not be completely provided due to the complex nature of the interactions involved, the diagram in Figure 2.8 represents a more complete conceptualization of potential processes involved in colloid release and stabilization in aerobic and anaerobic soil environments and can serve as a useful guide for additional studies to further elucidate the mechanisms.

The release and dispersion of colloids have significant environmental implications in natural reducing environments (e.g. sediments, wetland soils). Released colloids are mobile and hence could possibly act as vectors to facilitate the transport of nutrients and contaminants in surface water and the subsurface environments. In environments that are subject to variations in OM flux and redox status, the coupling effects of OM and redox conditions may regulate the mobility of colloid and the fate of strongly sorbing constituents. The OM associated with colloids could be mobilized and potentially contribute to the carbon pool in surface water, freshwater catchments, and soil solutions (Guo and Santschi, 2007). Anoxic iron reduction can also induce the release of colloidal carbon (2.3-430 nm) (Buettner et al., 2014). Although quantitatively to what extent does the role of colloid affect carbon cycling cannot be answered, these results, together with the observations from our study, suggest that colloids could play an important role in carbon retention and transport under both oxidizing and reducing conditions through association with OM. Therefore, studies on the quantification and characterization of OM, especially characterizing the reactivity and bioavailability of organic carbon, on colloids should be explored in future studies.

2.4 Conclusions

In this study, the complex interplay of colloid release, OM content, and redox conditions was investigated via batch experiments to quantify and characterize soil colloid release after the addition of dissolved OM (DOM). These results demonstrate that (i) DOM stabilized the colloids released under aerobic conditions but had minimal effects on colloids released under anaerobic conditions and (ii) high concentrations of DOM_{in} released under anaerobic conditions decreased subsequent colloid release due to DOM_{in}–colloid association. These findings have strong implications for colloid release and colloid-associated nutrient and contaminant mobilization and transport in redox-dynamic environments such as wetlands. On the other hand, these observations also suggest that colloids can play an important role in carbon retention and transport through association with OM, and carbon retention on colloids goes through different pathways depending on redox state. The OM's tendency to form aggregates with colloids may stabilize carbon under certain redox conditions depending on the properties and concentration of OM. For example, under reducing conditions, aggregation of colloids with high-molecular-weight OM can stabilize the OM by blocking its surface and preventing interactions with microorganisms, which has been proposed in previous studies (Bachmann et al., 2008; Kleber et al., 2007). Additionally, these observations can provide insight for predicting OM release in climate sensitive areas such as the Arctic Peatlands where coupling effects of anaerobic respiration, particularly iron reduction, and humic substances play an important role in carbon mineralization and emissions of CH_4 and CO_2 (Lipson et al., 2010).

Chapter 3

SIZE-DEPENDENT TURBIDIMETRIC QUANTIFICATION OF SUSPENDED SOIL COLLOIDS

3.1 Introduction

Soil colloids (ca. 1 nm to 1 μm in size) (Everett, 1972; Lead and Wilkinson, 2007) are complex mixtures of organic and inorganic entities with supramolecular structure and properties (Baalousha et al., 2011; Kretzschmar et al., 1999; Vold and Vold, 1983). Because of their small size and large surface area, hence high reactivity and the ability to facilitate the transport of contaminants in the subsurface environments, mobilization and transport of colloids have attracted much research attention (Baalousha et al., 2011; Kretzschmar et al., 1999; Lead and Wilkinson, 2007). While many studies have identified and analyzed the behavior of soil colloids in aquatic samples, quantitative information of the environmental occurrence of the colloids, especially those in the size fraction of < 0.45 μm, is scarce. The main reasons for this scarcity are: (1) < 0.45 μm colloids are considered as "dissolved" by the operational practice of filtration in most studies therefore not quantified (Doucet et al., 2007; Lead and Wilkinson, 2007) and (2) lack of economically feasible and technically effective methods to determine colloid concentration in field samples (Filella, 2007). The operational definition of colloids (i.e., > 0.45 μm) together with the lack of reliable quantification methods could greatly underestimate the colloidal pools in natural systems. As a result, concentrations of chemical and biological constituents (e.g., carbon, nutrients, organic contaminants and heavy metals,

and microbial pathogens etc.) in the "dissolved" pool would be overestimated because they would include the constituents that are sorbed onto the < 0.45 μm colloidal particles. The overestimation and the inability to distinguish accurately the "state" (sorbed vs. dissolved) of these constituents hinder our ability to access their environmental fate. Therefore, it is essential to quantify the small colloidal fractions (< 0.45 m) and to examine the role of these fractions on the fate and transport of colloid-associated-constituents.

Quantification of colloid concentration has been accomplished by a variety of methods, including gravimetric determination (Ledin et al., 1995; Yan et al., 2016), light scattering (Filella et al., 1997), UV-Vis or fluorescent spectrophotometry (Haiss et al., 2007; Koynov and Butt, 2012), scanning electron microscopy or transmission electron microscopy (Mavrocordatos et al., 2007), and laser-induced breakdown detection (Kim and Walther, 2007; Walther et al., 2006). Among these methods, gravimetric, UV-Vis and fluorescent, light scattering methods are more frequently used due to their relative simplicity and lower cost. However, the use of gravimetric method is greatly limited by its requirement for large volumes of samples where colloid concentrations in environmental samples are in general low. While sample-volume requirement is less a limiting issue for UV-Vis and fluorescent methods, these analyses are greatly interfered by light-absorbing dissolved substances and thus are not suitable for samples with colored background, e.g. samples containing humic substances (Gippel, 1995). In contrast, light scattering techniques, especially nephelometric turbidimetry, have the advantages of higher sensitivity, wider detection range, less interference, and smaller sample volume requirement, therefore, have been widely used in studies of sediment and colloid transport (de Jonge et al., 2004b;

Jacobsen et al., 1997; Minella et al., 2008; Pfannkuche and Schmidt, 2003; Rugner et al., 2013; Schelde et al., 2002).

Success of the nephelometric turbidimetry method depends on reliable correlations between turbidity and particle concentration. While various linear correlations between turbidity and particle concentration have been used in the quantification of total suspended solids (TSS) or suspended particulate matter (SPM) in freshwater lakes and rivers (Minella et al., 2008; Pfannkuche and Schmidt, 2003; Rugner et al., 2013), these correlations were developed based on and for measurements of larger particles (2~100 μm). Only a few studies have attempted quantification of smaller particles (< 2 μm) such as soil colloids (de Jonge et al., 2004b; Jacobsen et al., 1997; Schelde et al., 2002) and industrial nanoparticles (Greswell et al., 2010). Furthermore, these correlations are generally regarded as particle- or field site-specific therefore have been applied as such. To date, no 'universal" correlations, to the best of our knowledge, exist. Indeed, effects of particle size and composition, especially size, on turbidity-sediment concentration correlations have been reported in previous studies (Foster et al., 1992; Gippel, 1995). However, detailed and systematic evaluation and quantification of the effects of particle size and composition on turbidity measurement, especially for < 1.0 μm soil colloids, have not been carried out to date.

The objective of this study was to develop size-dependent turbidimetric correlations to quantify soil colloids in different size fractions in environmental samples. For this purpose, a large number of soil samples were collected (37 soils from the U.S. and Denmark). Soil colloids were dispersed and fractionated into different size fractions (< 0.1, 0.1-0.45 and 0.45-1.0 μm) to generate correlations

between mass concentrations of dispersed soil colloids and turbidity for different fractions. Then these correlations were tested by comparing estimated values from turbidity measurements against gravimetric measurements of additional environmental samples. Furthermore, concentration-turbidity correlations measured from model colloids (latex, silica, iron-oxide particles) were analyzed and compared to these from dispersed soil colloids, and the effects of colloid size and composition on shifting in these correlations were examined.

3.2 Materials and Methods

3.2.1 Model Colloids

Carboxylate modified latex (CML, Molecular Probes, Thermo Fisher, Waltham, MA), silica (Nissan Chemical America Corporation, Houston, TX), goethite and hematite were used as model colloids (e.g., uniform size and pure composition) to investigate the effects of particle size and composition on concentration-turbidity correlations. Purchased CML with diameters of 0.04, 0.1, 0.35, 0.42, 0.6, 1.2 μm and silica particles of 0.2 μm were directly dispersed in deionized water after sonication for 5 min. Goethite (length: 1-2 μm, width: 0.09 μm) and hematite (0.25 μm) particles were synthesized following the method of Schwertmann and Cornell (2007) and then dispersed to obtain colloid suspensions. More details of the synthesis method and particle characteristics were provided in previous studies (Wang et al., 2015a, 2015b). Mass concentrations of goethite and hematite suspensions were determined gravimetrically, while the concentrations of CML and silica suspensions were calculated based on the original stock concentrations and dilution factors. Suspension

turbidity was determined using a nephelometer (HACH, Loveland, CO) and reported in nephelometric turbidity units (NTU).

3.2.2 Soil Samples

A total of 37 soil samples, 15 from the U.S. and 12 from Denmark were collected or obtained from colleagues. The soils represent different elemental composition (e.g. organic carbon, iron content) and soil texture, were air-dried, and passed through 2-mm sieves prior to use. Soil texture was determined based on particle size analyses using the hydrometer method (Bouyoucos, 1962) and laser diffraction method (Eshel et al., 2004). Soil organic carbon (SOC) content was determined with a LECO analyzer coupled with an infrared CO_2 detector (Thermo Fisher Scientific Inc., MA) or converted from soil organic matter (SOM) content (i.e., the loss on ignition method, (Nelson and Sommers, 1996) using the "Van Bemmelen factor" of 0.58 (i.e., SOC = 58% SOM) (Van Bemmelen, 1890). The content of total "free" iron oxides, which affects the light scattering properties of particles (Ishida et al., 1991; Lafon et al., 2006), was determined by the dithionite-citrate-bicarbonate extraction method (Loeppert and Inskeep, 1996). Characteristic properties of these soils are summarized in Table 3.1.

Table 3.1 Characteristic properties of soils

Soil	Soil Texture	Sand	Silt	Clay	OC	Free Iron Oxides
					%	
CZO-R†	Sandy Clay Loam	51.0	23.0	26.0	1.16	0.99
BV-R†	Sandy Loam	76.0	12.0	12.0	0.7	3.08
BV-G†	Sandy Clay Loam	66.0	8.0	26.0	0.35	0.16
CM-Ag†	Silt Loam	29.0	51.0	20.0	2.21	0.64
CM-Pa†	Loam	43.0	43.0	14.0	3.55	1.06
CM-Fo†	Loam	50.0	38.0	12.0	2.97	0.52
Conrad†	Fine Sand	90.0	8.0	2.0	2.38	0.49
Potts†	N. A. ‡	N. A.	N. A.	N. A.	0.70	0.49
Palouse†	Silt Loam	13.2	68.6	18.2	1.22	0.52
Walla Walla†	Silt Loam	8.3	78.4	13.3	1.05	0.34
Royal†	Silt Loam	30.7	63.1	6.2	0.47	0.31
Salkum†	Silt Clay Loam	11.9	59.7	28.4	2.97	1.02
Red Bluff†	Clay	17.9	36.5	45.6	1.40	2.09
Øbakker#101	N.A.	N.A.	N.A.	N.A.	1.44	0.37
Øbakker#107	N.A.	N.A.	N.A.	N.A.	21.2	0.41
Øbakker#115	N.A.	N.A.	N.A.	N.A.	30.9	1.18
Øbakker#117	N.A.	N.A.	N.A.	N.A.	10.6	0.22
Norwegian FF	Sandy Loam	56.1	33.4	10.5	5.49	0.49
Greenland#1	Loamy Fine Sand	84.2	12.5	3.3	2.04	0.26
Greenland#3	Sandy Loam	66.1	29.1	4.8	7.01	0.38
Greenland#24	Loamy Fine Sand	77.3	18.2	4.6	2.24	0.31
Greenland#28	Sandy Loam	54.9	37.4	7.7	5.31	0.38
Greenland#39	Loam	43.1	49.5	7.4	2.57	0.32

Greenland#47	Sandy Loam	65.9	30.8	3.4	4.95	0.23
Jyndevad#6	Fine Sand	90.3	4.9	4.8	1.69	0.57
Jyndevad#7	Fine Sand	90.8	4.5	4.7	1.61	0.56
Jyndevad#11	Fine Sand	90.4	4.9	4.6	1.93	0.59
Jyndevad#67	Fine Sand	90.8	5.0	4.2	1.97	0.36
Jyndevad#73	Fine Sand	90.8	5.0	4.2	1.99	0.35
Jyndevad78	Fine Sand	90.8	5.0	4.3	2.11	0.35
Estrup#5	Loamy Fine Sand	79.6	14.7	5.7	2.07	0.15
Estrup#6	Sandy Loam	75.7	17.6	6.8	2.07	0.17
Estrup#17	Sandy Loam	68.3	23.8	7.9	4.47	0.15
Estrup#53	Sandy Loam	62.1	28.6	9.3	5.69	0.16
Tylstrup#13	Sandy Loam	73.4	22.2	4.4	N.A.	0.20
AZ13†	Sandy Loam	58.1	15.4	10.5	1.60	0.89
AZ18†	Sandy Clay Loam	51.4	21.6	27.0	2.31	2.33

† Soils from the U.S.A, others are from Denmark.

‡ N.A.: not analyzed.

3.2.3 Colloid Fractionation and Quantification

Air-dried soil samples were gently crushed and passed through a 0.05-mm sieve. Prior to particle size fractionation, all soil samples were dispersed in deionized water at a soil:water ratio of 1:10, shaken for 24 h and sonicated for 15 min to disintegrate aggregates and obtain water dispersible soil colloids. The dispersed colloids were fractionated into three size fractions (< 0.1, 0.1-0.45 and 0.45-1.0 μm) by sequential centrifugation, which is briefly described as follows. Firstly, colloids < 1.0 μm in the supernatant were separated from bulk soil suspensions by centrifugation at 221 g for 8 min and syphoned out into 50 ml centrifuge tubes. The supernatant was further centrifuged at 884 g for 10 min to settle out the fraction of 0.45-1.0 μm. Finally, colloids < 0.1 and 0.1-0.45 μm were separated from the < 0.45 μm suspension from the previous step at 22,095 g for 8 min. These selected centrifugation speed and time combinations were determined based on the study of Gimbert et al. (2005). To avoid alteration of the scattering characteristics of colloids from drying, fresh colloids settled by centrifugation were immediately re-suspended with deionized water and used as stock suspensions. The mass concentration of colloids in the stock suspension was determined by weighing the dry mass of the settled colloids after drying 10-40 ml aliquots from the suspension at 105 °C. From those measurements, concentration-turbidity calibration curves were generated for each size fraction.

3.2.4 Field Sampling, Preparations, and Measurement

To evaluate the applicability of size-dependent concentration-turbidity calibrations, soil pore water samples were collected from a field site at Blackbird State Forestry in New Castle County, DE (39°20’ N 75°40’ W), Delaware, USA. To

minimize sampling artifact, a peristatic pump (Geotech, Denver, CO) was used at a low flow rate of 100 ml/min (Ryan and Gschwend,1990) to extract water from wells located at different soil depths. Samples were first fractionated into < 0.1, 0.1-0.45 and 0.45-1.0 μm size fractions by centrifugation at the prescribed centrifuge force and time as given earlier. Colloid concentrations in each size fractions were determined by the size-dependent concentration-turbidity correlations by measuring turbidity as well as directly measured gravimetrically (i.e., by weighing oven-dry samples on glass slides at 105 °C with a microbalance) and compared.

3.2.5 Statistical Analysis

Linear regressions between turbidity and colloid mass concentration, 95% confidence and prediction interval were obtained using the Origin Software Program (Origin Lab, Northampton, MA). To examine the size- and composition-effect on concentration-turbidity correlations, Pearson's correlation coefficients were calculated between scattering properties of colloids, i.e. specific turbidity, and the content of soil clay, free iron oxides, and organic carbon, respectively. Changes in specific turbidity of colloids with changing colloid size was also analyzed using a one-way analysis of variance (ANOVA) combined with the Tukey-Kramer HSD to test the significance of differences in specific turbidity among different size fractions. Both Pearson's correlation and one-way ANOVA analyses were performed using JMP Pro 12.1.0 (SAS Institute Inc., Cary, NC). Additionally, linear regression analysis between gravimetrically measured and predicted colloid concentration from the correlations was performed, and absolute and relative errors were used to evaluate the performance of correlations in predicting colloid concentration.

3.3 Results and Discussion

3.3.1 Concentration-Turbidity Correlations of Model Colloids

Measured concentration and turbidity values for the suspensions of all model colloids, including CML of various sizes, silica, and iron oxy-hydroxides, are presented in Figure 3.1. Strong correlations between colloid concentration and turbidity were observed for all colloids. Figure 3.1 clearly shows that, for the same type of colloids (e.g., CML), concentration-turbidity correlations strongly depend on particle size, as reflected by the increase in the slopes of those curves from ~0.1 to ~6.3 as particle size decreased from 1.2 to 0.04 μm. The dependence is much more pronounced for smaller particles with sizes < 0.1 μm or 100 nm, which is the cutoff size used to define nanoparticles (Baalousha et al., 2011), indicating that nanoparticles have very different light scattering properties compared to their larger counterparts.

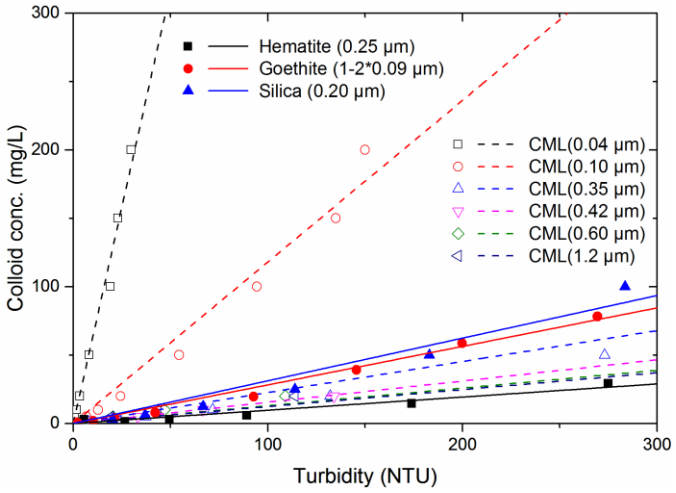

Figure 3.1 Correlations between suspension turbidity and mass concentration of model colloids with different sizes and compositions.

The effect of particle composition can also be observed in Figure 3.1 when the slopes of the concentration-turbidity curves of 0.09-μm goethite and 0.1-μm CML, and those of 0.25-μm hematite and 0.35-μm CML and 0.2-μm silica colloids, at the same concentrations, are compared. The goethite curve has a much smaller slope than the 0.1-μm CML curve, and the hematite curve has a much smaller slope than the 0.35-μm CML and 0.2-μm silica curves. It should be noted, however, that the comparison between goethite and CML may not be fully justified because goethite's shape is also different.

The effects of both particle size and composition on concentration-turbidity correlations are due to the differences in their light scattering intensities. Increased slopes correspond to decreased light scattering intensity. This trend is clearly seen in Figure 3.2 where the measured specific turbidity values T_m (i.e., the light scattering intensity per unit mass of colloids), which have been used in previous studies (Foster et al., 1992; Gippel, 1995), are shown for different types of model colloids: iron oxy-hydroxides have larger T_m values than silica and CML particles, and hematite has a T_m value larger than all other particles. Furthermore, Figure 3.2 also shows the size-effect on light scattering intensity as indicated by decreased T_m values of CML with decreasing sizes.

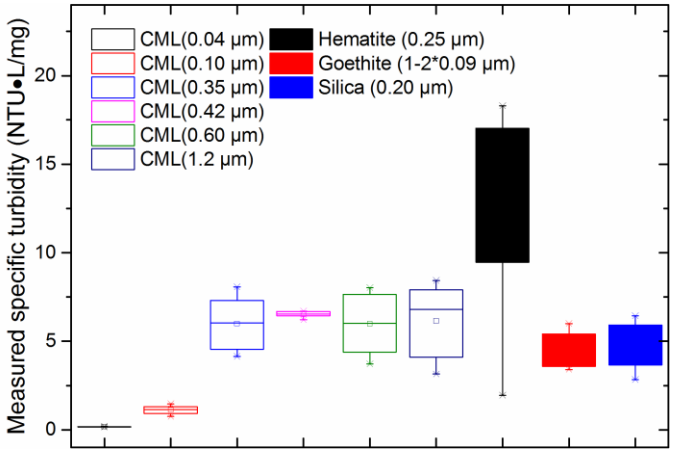

Figure 3.2 Measured specific turbidity, T_m, of model colloids of different sizes.

The dependence of concentration-turbidity correlations on particle size and composition has been reported in other studies as well (Foster et al., 1992; Gippel, 1995). Our results indicate that the effect of size is more significant than the effect of composition. Moreover, the size-effect is much more pronounced for nanosize particles, especially those with diameters < 0.2 μm. This observation emphasizes the need to develop size-depended concentration-turbidity correlations when quantification of nanoparticles in environmental samples is needed.

3.3.2 Concentration-Turbidity Correlations of Soil Samples

Measured concentration and turbidity values for the 37 soil samples are plotted along with linear regression lines in Figure 3.3 for soil colloids in size fractions of 0.45-1.0, 0.1-0.45, and < 0.1 μm. The mass concentrations of colloids correlate well with turbidity measurements although there are variations among different soils. Overall, most data from the 37 soils can be fitted by the same curve within the size fraction of 0.45-1.0 μm and 0.1-0.45 μm, respectively, but not for the < 0.1 μm

fraction. Similar to the observations with the model colloids, the concentration-turbidity curves of soil colloids are also size dependent, as indicated by the changes in slope with different size fractions (0.77 and 1.45 for 0.45-1.0 and 0.1-0.45 μm colloids, respectively). The size-dependence is further reflected by the significant increases in T_m values with increasing colloid size ($p < 0.0001$ for One-way ANOVA with Tukey-Kramer HSD, Figure 3.4). Size-effect on turbidity measurement in environmental samples have been reported in previous studies on 0.45-100 μm sediments (Baker et al., 2001; Foster et al., 1992; Gippel, 1995; Landers and Sturm, 2013; Lewis, 1996; Schelde et al., 2002; Wass and Leeks, 1999). Our results further stress the importance of taking the size effect into consideration when turbidimetric quantification of colloids is used, especially for those < 0.45 μm.

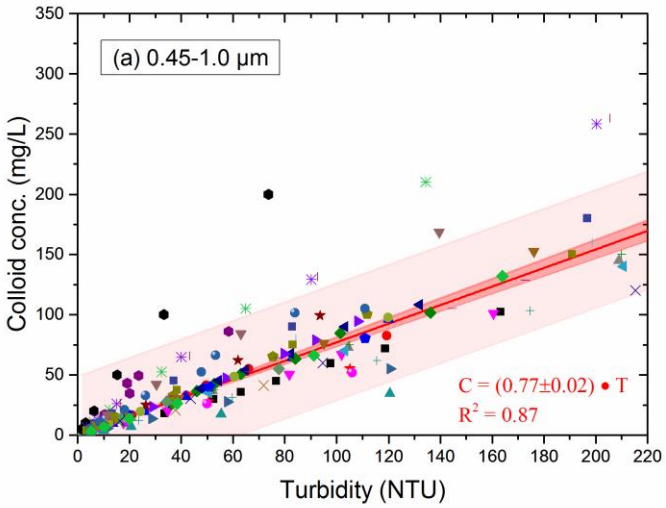
(a) 0.45-1.0 μm
Colloid conc. (mg/L)
Turbidity (NTU)
C = (0.77±0.02) • T
R² = 0.87

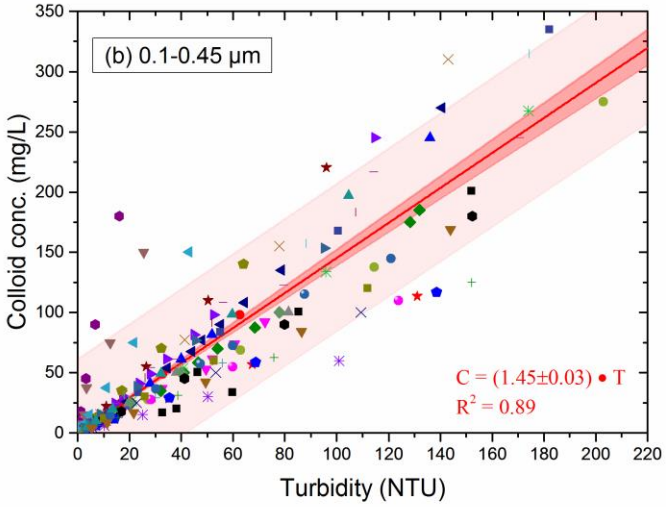
(b) 0.1-0.45 μm
Colloid conc. (mg/L)
Turbidity (NTU)
C = (1.45±0.03) • T
R² = 0.89

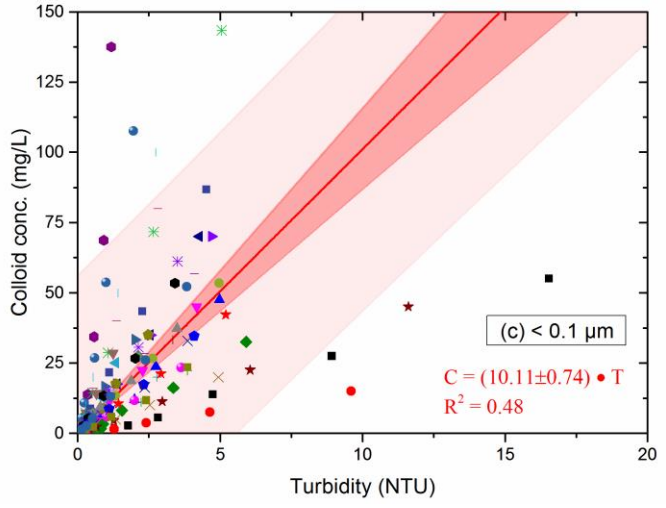
(c) < 0.1 μm
Colloid conc. (mg/L)
Turbidity (NTU)
C = (10.11±0.74) • T
R² = 0.48

Figure 3.3 Scatter plots and regression analyses between suspension turbidity and mass concentration of soil colloids extracted from 37 soils for size-dependent correlations: (a) 0.45-1.0, (b) 0.1-0.45 and (c) < 0.1 μm colloids. Note: C, T in correlation equations represent colloid concentration in mg/L, suspension turbidity in NTU, respectively, and R^2 represents the coefficient of determination.

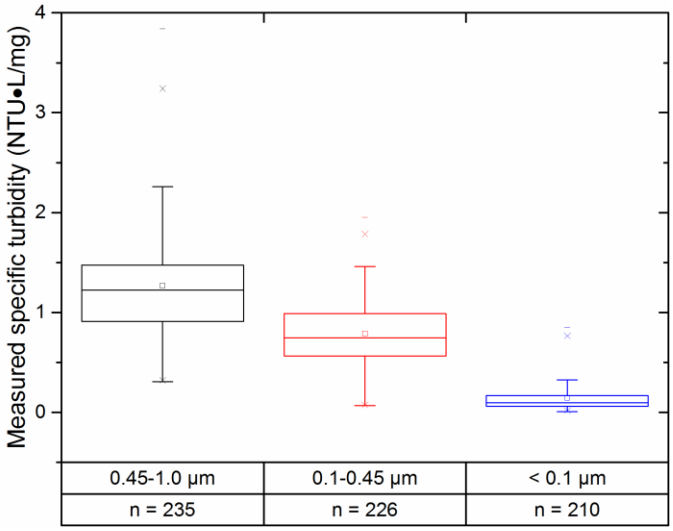

Figure 3.4 Measured specific turbidity (T_m) of soil colloids from 37 soils in different size fractions. Note: n represents the number of samples

The effects of colloid composition on concentration-turbidity correlations were assessed by Pearson's correlation analyses between T_m and chemical parameters of soils, including free iron oxide, clay and organic carbon content (Fe%, Clay% and OC% in Table 3.2). Table 3.2 shows that Fe% and clay% positively and OC% negatively, respectively, correlated with T_m, but statistical significances between T_m and these parameters were only observed for < 0.1 μm fraction ($p < 0.05$), not for size fractions of 0.45-1.0 μm and 0.1-0.45 μm. The limited composition-effect within size fractions of 0.45-1.0 μm and 0.1-0.45 μm is likely due to the similarity in refractive

index (RI) values of the major mineral compositions of the colloids. In soil systems, RI values of different clay minerals are similar, ranging from 1.5 to 1.6 (Table 3.3), and thus significant shifting in concentration-turbidity correlations with increasing clay% is not expected. Similarly, although changes in the curve slopes is more likely in soils with higher Fe% due to the considerably higher RI values of iron oxy-hydroxides (Table 3.3), Fe% in the colloid fractions of 0.45-1.0 μm and 0.1-0.45 μm was not be high enough to significantly increase the colloids' RI values. For example, Lafon (2006) found that when volumetric content of iron oxides increased from 0 to 10.9%, RI values of aggregates only slightly increased from ~1.5 to ~1.6, which are very similar to the RI of pure clay minerals (Table 3.3).

Table 3.2 Pearson correlation coefficient (r) between soil properties, and specific turbidity of colloids within different size fractions

		OC%	Fe%	Clay%	T_m (NTU·L/mg)		
			%		0.45-1.0 μm	0.1-0.45 μm	< 0.1 μm
OC%		1.00	-0.11	-0.17	-0.07	-0.07	-0.30
Fe%		-0.11	1.00	0.54**	0.11	0.09	0.78**
Clay%		-0.17	0.54**	1.00	0.18	0.00	0.43*
T_m (NTU·L/mg)	0.45-1.0 μm	-0.07	0.11	0.18	1.00	0.25	0.13
	0.1-0.45 μm	-0.07	0.09	0.00	0.25	1.00	0.31
	<0.1 μm	-0.30	0.78**	0.43*	0.13	0.31	1.00

* $p < 0.05$, ** $p < 0.01$

N.A. represents "not applicable"

Table 3.3 Specific gravity and refractive index of common soil minerals

Minerals		Specific Gravity†	Refractive Index†
Clay	Kaolinite	2.60	1.54-1.60
	Halloysite	2.60	1.50-1.60
	Chlorite	2.70	1.50-1.60
	Vermiculite	2.50	1.50-1.60
	Smectite	2.35	1.40-1.54
Iron oxides	Goethite	3.80	> 1.9
	Lepidocrocite	4.00	> 1.9
Others	Quartz	2.63	1.54-1.60
	Gibbsite	2.35	1.54-1.60
	Calcite	2.71	1.48-1.65
	Dolomite	2.85	1.50-1.68
	Gypsum	2.30	1.52-1.53

† Summarized from reference (FitzPatrick, 1993)

The effect of OM on concentration-turbidity correlation is also limited: the correlations between OC% and T_m values within the 0.45-1.0 μm and 0.1-0.45 μm fractions are not statistically significant (Table 3.2). To further evaluate the effects of OM, turbidity values were measured for concentrated OM suspensions prepared using Suwannee River humic acid (SRHA) at 75 and 150 mg-C/L < 0.1 μm SRHA. The SRHA suspensions were found both < 0.2 NTU. Furthermore, addition of 75 mg-C/L SRHA into 1 and 43 mg/L CML suspension only slightly decreased the turbidity of CML from 4.5 to 4.2 NTU and 377.0 to 371.6 NTU, respectively (Figure 3.5). These observations confirm that OM-effect on turbidity measurement is negligible over a wide range of OM concentrations.

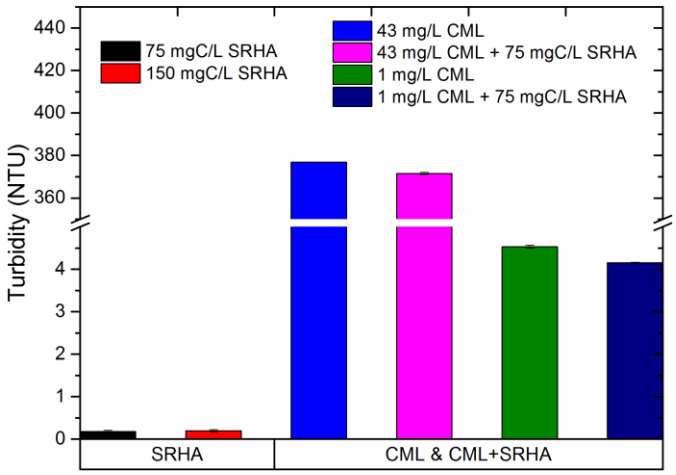

Figure 3.5 The turbidity of < 0.1 μm Suwannee River humic acid (SRHA) and mixture of 1.2 μm CML and SRHA.

Compared to colloids in the size fractions of 0.45-1.0 μm and 0.1-0.45 μm, concentration-turbidity correlations of < 0.1 μm colloids varied significantly and could not be fitted by a single correlation curve (Figure 3.3c). The large variations are likely due to the significant differences in chemical composition within the < 0.1 μm fraction. Unlike for the larger colloid fractions discussed above, the correlations between Fe%, Clay% and T_m are statistically significant, at $p < 0.01$ and $p < 0.05$, respectively (Table 3.2). These results imply that the relative importance of composition-effect increases as the specific turbidity decreases when particle size approaches the nano-size range. Thus, concentration-turbidity correlations for nanoparticles could be more composition-specific than their larger counterparts. On the other hand, it should be noted that both colloid concentration and turbidity are much lower in the < 0.1 μm fraction, compared to fractions of 0.45-1.0 μm and 0.1-0.45 μm, giving rise to larger measurement errors. In addition, as shown in Figure 3.5, the relative impacts of OM-effect also became more pronounced with decreasing

colloid concentration and turbidity. All the factors discussed above could have contributed to the larger variations in the concentration-turbidity correlations, as shown in Figure 3.3c.

3.3.3 Application of Correlation Curves to Field Samples

The size-dependent concentration-turbidity correlations were applied to the additionally collected water samples to calculate colloid concentrations within the size fractions of 0.1-0.45 and 0.45-1.0 μm. Then the calculated values were compared with gravimetrically measured concentrations. As shown in Figure 3.6, the calculated values agreed well with the measured concentrations, with most data fell on the 1:1 line, with only a few outliers. Calculated-to-measured concentration ratios are summarized in Figure 3.7, most ranging from 0.95 to 1.26. The ratios suggest that predictions from the size-dependent concentration-turbidity correlations are reliable for most samples, although there could be exceptions.

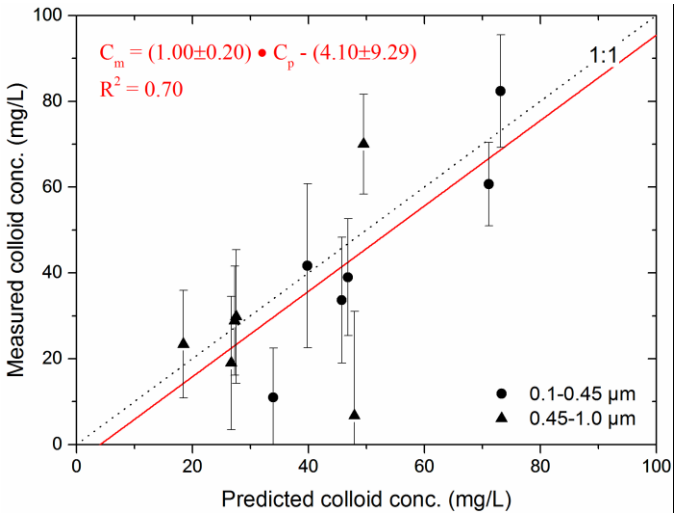

Figure 3.6 Regression analysis between measured and predicted colloid concentrations for field samples. Note: C_m, C_p in correlation equations represent measured, predicted colloid concentration in mg/L, respectively, and R^2 represents the coefficient of determination.

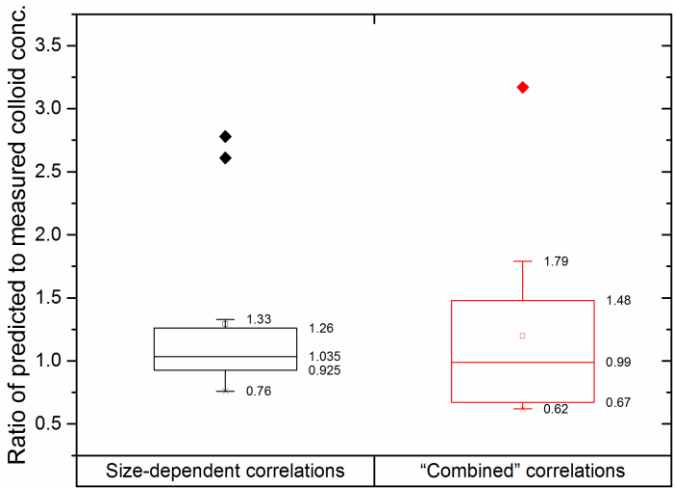

Figure 3.7 Ratio of predicted to measured colloid concentrations from size-dependent and "combined" correlations.

Additionally, colloid concentrations of these samples were separately calculated from the correlation curves for 0.1-0.45 and 0.45-1.0 μm colloids (Figure 3.3a, 3.3b), and a 'combined' curve, i.e. the curve of < 1.0 μm (Figure 3.8, a curve typically used) and compared. The size-dependent correlations provide more accurate estimation and less uncertainty in colloid concentrations than the combined curve as reflected by smaller absolute and relative errors (Table 3.4), and lower calculated-to-measured ratios (Figure 3.7). This implies that size-dependent correlations should be promoted to quantify colloid concentration in environmental samples.

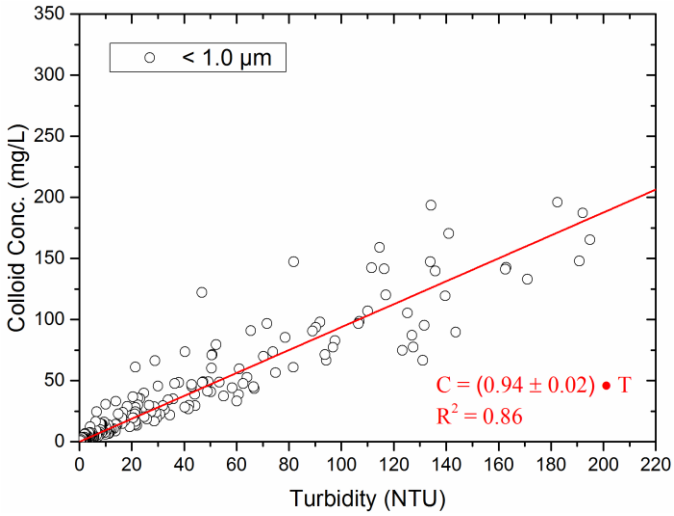

Figure 3.8 Scatter plots and regression analyses between suspension turbidity and mass concentration of soil colloids extracted from 37 soils for "combined" correlations: < 1.0 μm colloids. Note: C, T in correlation equations represents colloid concentration in mg/L, suspension turbidity in NTU, respectively, and R^2 represents the coefficient of determination.

Table 3.4 Comparison between calculated and measured colloid concentrations from size-dependent correlations (SDC) and "combined" correlation (CBC) and error analysis.

Size	Measured colloid concentration mg/L.	Calculated colloid concentration mg/L		Absolute error* mg/L		Relative error†	
		SDC	CBC	SDC	CBC	SDC	CBC
0.1-0.45 µm	70.7 ± 13.4	73.1 ± 1.5	47.2 ± 2.0	2.4	23.5	0.0	0.3
	38.3 ± 13.4	45.7 ± 0.9	29.5 ± 1.3	7.4	8.8	0.2	0.2
	73.4 ± 9.5	71.1 ± 1.5	45.9 ± 2.0	2.3	27.5	0.0	0.4
	44.9 ± 13.6	46.8 ± 1.0	30.2 ± 1.3	1.9	14.6	0.0	0.3
	41.7 ± 19.1	39.8 ± 0.8	25.7 ± 1.1	1.9	16.0	0.0	0.4
	12.2 ± 5.6	33.9 ± 0.7	21.9 ± 0.9	21.7	9.7	1.8	0.8
All 0.1-0.45 µm‡	46.9	51.8	33.4	4.9	13.5	0.1	0.3
0.45-1.0 µm	18.4 ± 24.4	47.9 ± 1.2	58.4 ± 2.5	29.5	40.0	1.6	2.2
	30.5 ± 15.2	27.5 ± 0.7	33.5 ± 1.4	3.0	3.0	0.1	0.1
	57.4 ± 11.4	49.5 ± 1.3	60.3 ± 2.6	7.9	2.9	0.1	0.1
	24.7 ± 12.7	27.3 ± 0.7	33.2 ± 1.4	2.6	8.5	0.1	0.3
	20.1 ± 14.2	26.7 ± 0.7	32.5 ± 1.4	6.6	12.4	0.3	0.6
	24.2 ± 3.3	18.4 ± 0.5	22.4 ± 1.0	5.8	1.8	0.2	0.1
All 0.45-1.0 µm‡	29.2	32.9	40.0	3.7	10.8	0.1	0.4

***** Calculated from the absolute difference between the mean values of calculated and measured colloid concentration.

† Calculated from the absolute error divided by the measured colloid concentration

‡ Only average values are provided for measured and calculated colloid concentrations

3.4 Conclusions

In this study, the reliability of using turbidimetric measurement were tested to quantify colloid concentration in aquatic environmental samples and developed size-dependent turbidity-concentration correlations curves for three colloidal size fractions (< 1.0, 0.45 – 1.0, 0.1-0.45, and < 0.1 μm) based on measurements from a large number of soil samples. The results demonstrated that particle size is the dominant factor affecting the correlation between turbidity and colloid concentration while effects of particle composition and OM are largely negligible. The size-dependent concentration-turbidity correlations provide more accurate estimations when tested against gravimetric measurements using field samples compared to the combined curve of < 1.0 μm, which is more commonly used. The relatively insignificant particle composition effect indicates the practically "universal" applicability of the reported correlations. In addition, the correlations, for the first time, allow quantification of colloids in different size fractions in environmental samples, especially colloids that are < 0.45 μm, which are traditionally considered as part of the dissolved phase and hence underestimated. This would enhance our capability to more accurately quantify the colloidal pools in natural systems. Furthermore, size-dependent correlations provide size-specific quantification of colloids within the fraction of < 1.0 μm, thus improve our understanding in biogeochemical cycling of constituents involving colloid contribution, especially if the contribution is colloid size-dependent. For example, colloids of varying sizes have different surface areas available for the constituents to sorb on and they differ in mobility. This colloid quantification method developed in our study will enhance our capability in quantifying colloidal pools in natural systems, especially < 0.45 μm fractions, therefore provides more accurate

assessment in the mobility of colloid-associated-constituent, such as nutrients, contaminants and trace elements.

Despite the large number of samples used in this study to develop the size-dependent turbidity-concentration correlations for colloid quantification, it should be noted that caution must be taken applying these relationships. Because of the extremely heterogeneous nature of soil and sediment materials, situations are expected to exist (e.g., sample compositions are significantly different from the soils used in this study) where these correlations may not apply. Therefore, potential users are encouraged to verify the correlations using their own samples whenever possible.

Other issues that may limit the applicability of the proposed correlations include: (1) large variability in concentration-turbidity correlations for soil colloids in < 0.1 μm fraction thus the correlation is not reliable for quantification of nano-sized colloids and (2) an appropriate range of suspension turbidity is required (1 to 300 NTU) for a better correlation. Issue (1) could be partially explained by issue (2), in which low suspension turbidity was observed in the < 0.1 μm fraction. The observed low suspension turbidity was close to or below the detection limit and thus caused large measurement errors for samples in < 0.1 μm fraction. Furthermore, effects of organic matter could have a much more significant effect on turbidity measurement when the suspension turbidity is < 1 NTU, as shown in Figure 3.5. Similarly, if the suspension turbidity is > 300 NTU, multiple scattering from overlapped scattering of colloids could underestimate the actual value of suspension turbidity. Multiple scattering at high suspension turbidity may be less important, compared to the effect of organic matter at low suspension turbidity, due to the limited amounts of colloids in

natural samples. Therefore, specially cautions should be taken if the correlations are to be used for samples with high organic matter and low suspension turbidity.

Chapter 4

SIZE-BASED FRACTIONATION AND QUANTIFICATION OF MOBILE COLLOIDS AND COLLOIDAL ORGANIC CARBON IN NATURAL SYSTEMS

4.1 Introduction

Natural colloids, i.e., particles with sizes between 1-1000 nm (Everett, 1972; Lead and Wilkinson, 2007), are heterogeneous and complex mixtures of organic and inorganic entities. They include nano-size macromolecules to micro-size fragments of clay, metal oxides and other solids. Mobile colloids have attracted much research attention due to their small size, large surface area and hence high reactivity and the ability to facilitate transport of nutrients and contaminants in the subsurface environments (Baalousha et al., 2011; Kretzschmar et al., 1999; Vold and Vold, 1983). While behavior of colloids in some aquatic systems (e.g. ocean) have been extensively studied, quantitative information of environmental occurrence of colloids and colloid-associated-constituents, especially those with sizes < 0.45 μm, is scare. The scarcity is mainly due to the practice that uses 0.45-μm filters to separate colloidal and dissolved phases thus operationally defines the "dissolved" phase as filtrates < 0.45 μm. This practice overestimates the dissolved pool while underestimates the actual colloidal loads, and as a result, underestimates the mobile fractions of any constituents associated with the colloids. Furthermore, inability to accurately differentiate colloidal phase from "dissolved" pool also hinders our ability to provide accurate assessment of the biological functions and environmental fate and transport of colloid-associated-

constituents. Therefore, it is critical to quantify the extent of underestimation on colloidal pool and assess its actual contribution to the mobilization of colloid-associated-constituents and their environmental fate.

Quantification of dissolved organic matter (DOM) follows the same practice, which operationally defines DOM as the fraction that passes 0.45 μm filters. DOM constitutes one of the largest pools of mobile and reactive carbon in global carbon cycles, and serves as either carbon source or sink depending on their nature and the changes in surrounding environments (Kleber et al., 2015). In natural aquatic systems, the mobility and stability of dissolved organic matter are significantly impacted by the interactions with mobile colloids, such as sorption on or coagulation with colloids. On one hand, organic matter (OM) coating on inorganic colloids produces negatively charged surface and promotes colloid dispersion and OM mobilization (Hu et al., 2010). On the other hand, OM transformation and decomposition are also affected when sorbed on colloids since OM can be chemically stabilized via organo-mineral-complexation or physically protected by forming microaggregates (Amon and Benner, 1996; Guo and Macdonald, 2006; Hama et al., 2004; Kang and Mitchell, 2013; Kleber et al., 2007). These complex processes may have profound significance in carbon mobilization and stabilization and thus strongly impact global carbon cycles. However, most previous studies monitoring DOM in natural systems, especially studies on inland aquatic or terrestrial systems, have not considered the role of mobile colloids, and the quantitative contribution of colloid-associated-carbon to the mobile carbon pool still remain scarce. In addition, similar to that of colloid quantification, considering < 0.45 μm colloidal OM (COM) as DOM would lead to incorrect quantification of the actual mobility and reactivity of organic carbon and thus

inaccurate assessment of the carbon sink or sources. Therefore, a study quantifying and characterizing COM and their size distribution, especially in the < 0.45 μm size fraction, is needed.

Additionally, anthropogenic perturbations, such as agricultural practices and human-induced climate change, significantly influence environmental conditions, including primary production, physicochemical conditions, and microbial activities in natural systems. The alterations of environmental conditions can greatly impact the release and mobilization of colloids and OM, and thus changes the fate and transport of colloid-associated-OM. This would significantly influence the allocation or input of OM from soils to inland water and marine systems. The ability of colloid-mediated-processes in affecting the mobility of OM varies depending on specific environmental systems or conditions. Therefore, to better assess and predict the influence of anthropogenic perturbation on OM mobilization and activity, environmental systems acting as potential hotspots of colloid and COM mobilization should be identified.

This study focused on quantification of colloid and COM of different size fractions (0.1-0.45, 0.45-1.0 μm) in samples collected from different natural systems, i.e. agricultural, forestry stream, freshwater wetland, and estuarine field sites. The forestry stream represents a system with little anthropogenic perturbation, while both agricultural and estuary field sites withstand extensive perturbations due to agricultural practices. The wetland represents a natural system that undergoes dynamic redox oscillations that commonly occur due to soil moisture change, which is likely to intensify due to human induced climate change. The objectives were to (1) identify environmental hotspots of colloid and COM mobilization and release; (2) examine the colloid-OM relationships and evaluate the ability of carbon retention on colloids; (3)

quantify natural colloids and COM of different sizes with a special emphasis on the < 0.45 μm fraction (the fraction currently being considered as part of the dissolved phase) and assess the contribution of colloidal organic carbon (COC) to total mobile organic carbon pool.

4.2 Materials and Methods

4.2.1 Study Sites Description

Water samples were collected from four types of watershed or natural ecosystems, i.e. agriculture, forest, freshwater wetlands and estuary, aiming to represent natural colloids from different sources under varied hydrological and physicochemical conditions. The locations of the study sites are presented in Figure 4.1.

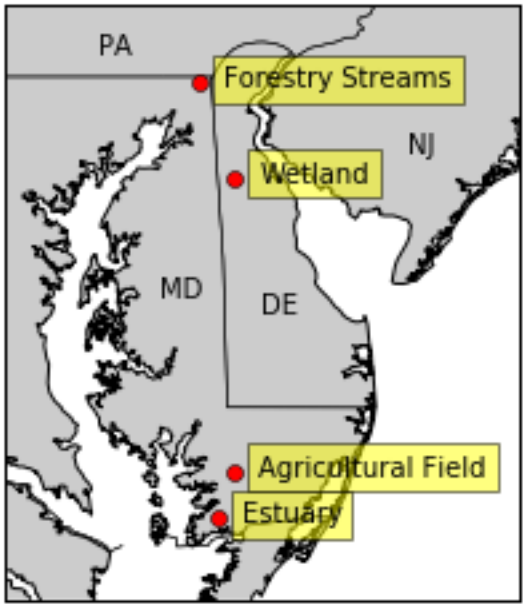

Figure 4.1 Locations map of sampling sites in this study

4.2.1.1 Agricultural Site

The agricultural site is located at the University of Maryland Eastern Shore (UMES) Research Farm in Princess Anne, MD (38° 12’ N and 75° 40’ W). The UMES farm is part of the Manokin River Watershed and is approximately 10 km from the Chesapeake Bay. This farm has a series of small field ditches (0.3-1.0 m deep) that drain into larger ditches (1.0-3.0 m deep) and ultimately drain into the Manokin River and the Chesapeake Bay (Vadas et al., 2007). The mean annual precipitation is ~1110 mm and mean annual temperature is ~13 °C (Kibet et al., 2016; Kleinman et al., 2007). The surface soil horizon (0.5 to 0.75 m deep) is dominated by poorly-drained Quindocqua silt loam (fine-loamy, mixed, active, mesic Typic Endoaquult), which is underlain by a silty clay subsoil horizon that overlays coarse marine sediments (0.1 m deep) (Kibet et al., 2016; Vadas et al., 2007). The field site is managed with conventional tillage and planted with corn and soybeans since its purchase by the UMES in 1997. Prior to 1997, the site had been a commercial broiler operation for more than 20 years, as a result excessive amounts or concentrations of soil phosphorus (Mehlich-3 P > 60 mg/kg) were measured due to continuous application of poultry litters (Kleinman et al., 2007). This site was chosen to represent the environmental system under long-term human and agricultural activities. Water samples were collected from both surface and subsurface horizons (small ditches, 0.6 and 1.2 m deep wells).

4.2.1.2 Forestry Site

The forestry streams are located in the Fair Hill Natural Resources Management Area (FH-NRMA) in Cecil County, MD (39°42’ N, 75°50’ W), and are part of an ongoing study on organic matter (Dhillon and Inamdar, 2014; Inamdar et al.,

2011). The FH-NRMA is managed and protected by the State of Maryland's Department of Natural Resources after its purchase from Mr. William duPont, Jr. since 1975. Prior to 1975, this site had been used for both farming and recreational hunting. The FH-NRMA is part of the Big Elk River Watershed and streams of FH-NRMA ultimately drain into the northeastern portion of the Chesapeake Bay. The mean annual precipitation is ~1200 mm and mean annual temperature is ~12 °C. The soils are mainly coarse loamy, mixed, mesic, Lithic and Oxyaquic Dystrudept. The study area is mostly covered with deciduous forest, including Fagus grandifolia (American beech), Liriodendron tulipifera (yellow poplar), and Acer rubrum (red maple) (Dhillon and Inamdar, 2014; Levia et al., 2010). This site was chosen to represent an environmental system that is primarily covered with forest and thus perturbations from human and agricultural activities are limited. Surface water samples were automatically collected with ISCO samplers at the outlets of 12 and 76 ha catchment when precipitation intensity was > 2.54 mm per hour. More details of sampling locations and site descriptions can be founded in Dhillon and Inamdar (2013) and Inamdar et al. (2011).

4.2.1.3 Wetland Site

The freshwater wetland is located in Blackbird State Forestry in New Castle County, DE (39°20’ N 75°40’ W). It is part of the Blackbird Creek watershed that drains into Blackbird Creek and ultimately flows into the Delaware Bay. The mean annual precipitation and mean annual temperature in this area are ~1200 mm and ~ 14 °C. This wetland is a seasonally-saturated mineral soil flat wetland, where inundation mostly occurs outside of the growing season. For most of the growing season the water table is below 30 cm, however, the water table depth fluctuates often in response

to major precipitation events. Water is supplied directly through precipitation and also by groundwater flow through a sand lens. The soils in the wetland are mainly fine-loamy, mixed, active, mesic, Typic Endoaquults. The dominant trees include the Nyssa sylvatica (black tupelo), Liquidambar styraciflua (American sweetgum), Acer rubrum (red maple), Quercus phellos (willow oak), Quercus lyrata (overcup oak). This site was chosen to represent an environmental system that is under dynamic redox conditions, which is indirectly affected by anthropogenic perturbations. Water samples were collected from shallow (0-40 cm), deep (64-127 cm) and sand lens (130-203 cm) sampling wells along the transect from inlet to outlet (upland, soil mineral flat, depression wetland, and wetland outlet) as shown in Figure 4.2.

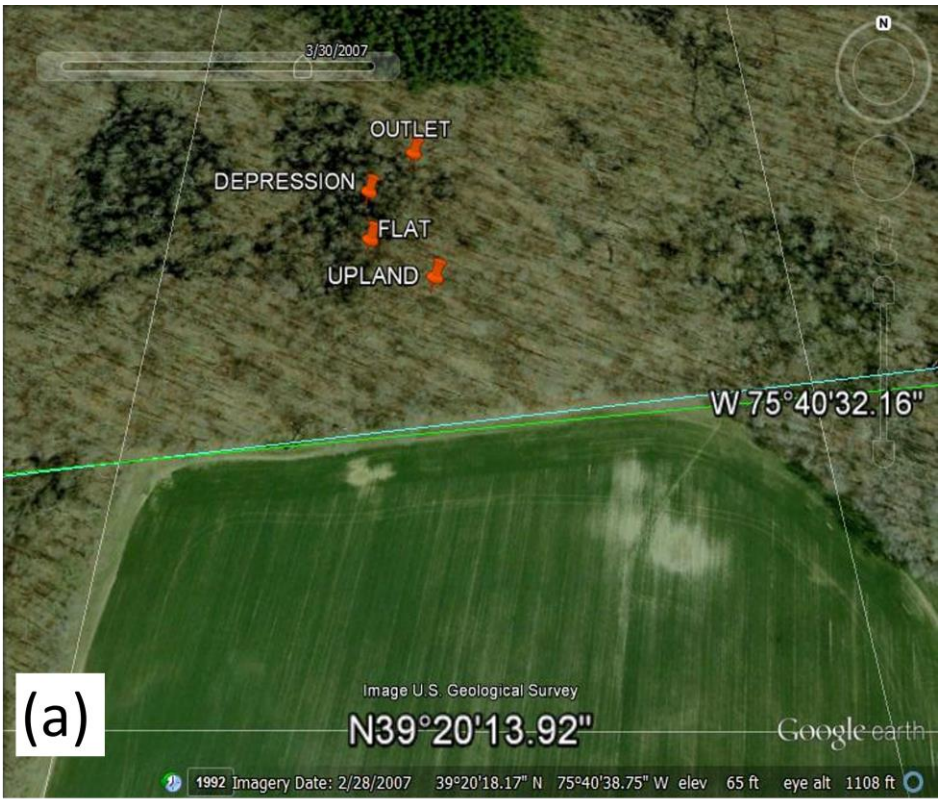

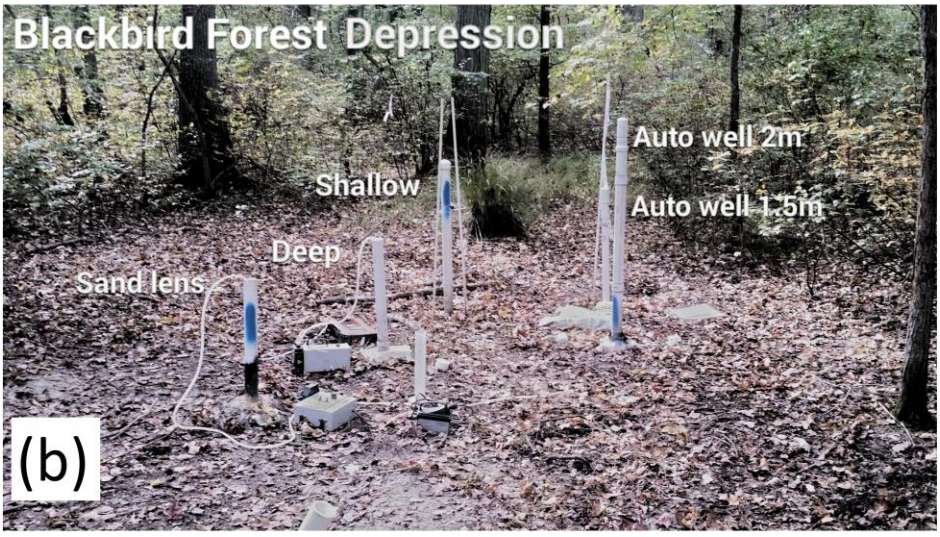

Figure 4.2 Location of sampling wells along the transect (a) and the picture of sampling well setup at depression wetland (b)

4.2.1.4 Estuary Site

East Creek, a coastal tributary, is part of the lower Chesapeake Bay watershed on the eastern shore of the Delmarva Peninsula in Somerset County, MD (38°03’ N, 75°78’ W). The upper part of the watershed is primarily occupied by poultry operations and agricultural fields with corn-soybean rotations, while the lower part of the watershed is mainly surrounded by brackish tidal marsh (Upreti et al., 2015). The mean annual precipitation and mean annual temperature in this area is ~1000 mm and ~ 15 °C, respectively. The creek is approximately 10 km long, primarily drains from the open ditches in agricultural and poultry farms, and ultimately drains into the Chesapeake Bay. Because of the long-term poultry operation and the over-application of inorganic fertilizer and manures on the agricultural farms in surrounding areas (Sims et al., 2000), the upper region has been significantly impacted by agricultural activities. This site was chosen to represent an environmental system in the estuarine region. Water samples were collected along the creek from a drainage ditch near an agricultural farm to the mouth of the creek at the Chesapeake Bay. The sampling locations are shown in Figure 4.3. More details of sampling locations and site descriptions can be founded in Upreti et al. (2015) and Stout et al. (2016).

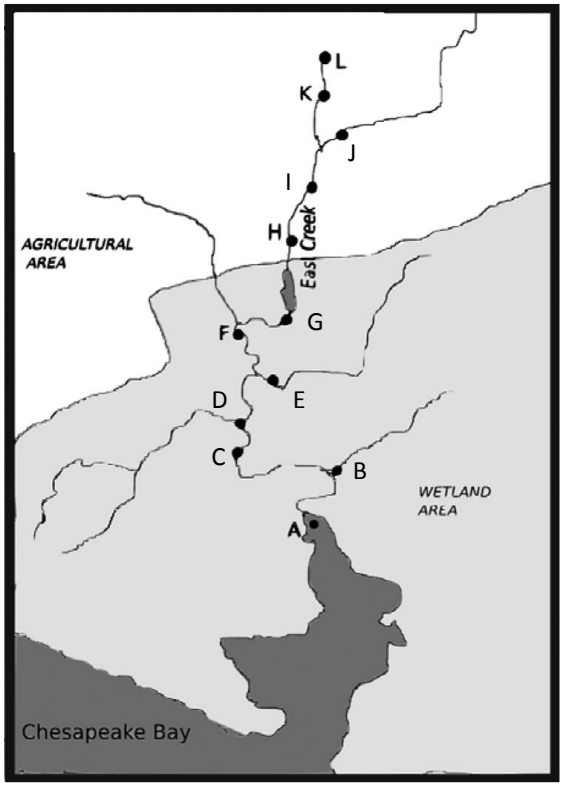

Figure 4.3 Location of sampling sites from A to L along East Creak (adopted from Stout et al. 2016).

4.2.2 Sample Collection

Sampling at multiple wells at the different locations referred above was performed from 2013 to 2015; detailed schedule is summarized in supplemental materials (Table 4.1). Surface water samples were collected directly from estuarine tributary, ditches and sample wells at the agricultural field, while stream water was automatically sampled by ISCO auto-sampler at the forestry watershed. For the freshwater wetland, special wells and techniques were designed for sampling water containing soil colloids under anaerobic conditions. Briefly, the wells were filled with sand and sealed with polyurethane to eliminate bentonite contamination. After purging for 3 well volume, sampling was performed with a peristatic pump (Geotech, Denver,

CO) at ~100 ml/min, suggested by Ryan and Gschwend (1990), to minimize suspending colloids from surrounding soils. The water samples were collected in acid-washed 250-ml serum bottles, flushed with argon gas, and sealed PTFE silicone septa to avoid oxidation. All samples were kept at 4 °C during transportation to the lab and size fractionations were performed within 48 h.

Table 4.1 Sample time for colloid and TOC determination for different sites

Samples	Sample Time	
	Colloid concentration*	Colloid and TOC conc.†
Agricultural Field	Mar 10th, 2015T	N/A
Forestry Stream	Nov 28th, 2013; Mar 11th, Apr 16th, 2014T	Aug 14th, 29th, 2013G
Wetland	N/A	Apr 1st, 3rd, 13th, May 14th, 28th, June 3rd, 2015T
Estuary	Jun 4th, Aug 25th, 2014T	Jun 15th, 2015T

* Only colloid concentration was determined for these samples
† Both colloid and TOC concentration were determined
T, G Colloid concentration determined by turbidity (T) or gravimetrically (G)

4.2.3 Colloid Fractionation and Quantification

Water samples with suspended particles were hand shaken thoroughly and then sonicated for 5 min to homogenize the suspensions. The samples from the agricultural field, estuary and wetland were syphoned out from the supernatant after centrifugation (Thermo Scientific, MA) at 22,095 g for 8 min, 884 g for 10 min, 221 g for 8 min, respectively to fractionate out colloids of < 0.1, 0.45 and 1.0 μm size fractions. Freshwater stream samples were centrifuged as described above and sequentially filtered with 0.7, 0.45 and 0.1 μm membrane filters. The 0.7 and 1.0 μm cutoff sizes were selected to collect total or close-to-total colloidal pool below 1.0 μm, according to the IUPAC definition (Lead and Wilkinson, 2007). The 0.45 μm cutoff size was

used to be consistent with the commonly used and operationally defined size to distinguish between colloidal and dissolved phases (Buffle and Leppard, 1995; Lead and Wilkinson, 2007). The 0.1 μm cutoff was selected to separate the nanosized particles from the rest of the colloidal materials. The centrifugation speed and time duration were determined based on Stokes' Law (Gimbert et al., 2005). To confirm accuracy of particle fractionation using centrifugation, particle size distribution of supernatants was measured with a laser diffraction size distributor (Bechman Coutler, CA) and found to be consistent with their designed size range in a previous study. The colloid concentration were mostly determined by measuring turbidity in each size fractions and convert it to colloid mass concentration with predetermined colloid-turbidity relationships, while other samples were determined gravimetrically (detailed summary is given in Table 4.1). To determine the < 0.1 μm nano-size COC in samples from the estuary site, following centrifugation, 15-ml of < 0.1 μm aliquots were removed and subjected to ultrafiltration (10 kDa) at 53 psi with Amicon ulfiltraiton stir cell (EMD Millipore, NJ).

4.2.4 Chemical Analyses

Sample pH and electrical conductivity (EC) were measured with corresponding probes (Fisher Scientific, Hampton, NH) in the lab; measurements for wetland samples were performed in a glovebox and were done in the ambient air for samples from the other sites. Suspension OC concentration in each size fractions (< 10 kDa, 0.1, 0.45, 0.7 and 1.0 μm) after fractionation was measured by using a catalyst facilitated high temperature combustion following acidified samples with phosphoric acids (Teledyne Tekmar, OH). The COC concentration in 0.45-1.0, 0.45-0.7, 0.1-0.45 μm size fraction were calculated from the difference between < 0.1, 0.45, 0.7 and 1.0

μm fractions. The OC content on colloid (%OC) was also calculated from the ratio of OC concentration to colloid mass concentration in different size fractions.

4.2.5 Data and Statistical Analyses

Sample average, standard deviation were provided for each of the measured parameters, i.e. colloid concentration, OC concentration, %OC and the ratio of DOC_{tr} to DOC_{op}. Statistical analysis was performed by one-way analysis of variance (ANOVA) combined with Turkey-Kramer HSD analysis to test their significance of differences ($p < 0.05$) among different sampling sites as well as different size fractions (JMP®, Version Pro 12. SAS Institute Inc., Cary, NC). Pearson's correlation coefficients between solution pH, EC, salinity and OC and colloid concentration in different size fractions were provided ($p < 0.1$, 0.05 and 0.001). To examine the relationships between OC concentration and colloid mass concentration, linear regressions between OC and colloid mass concentration were obtained using the Origin (OriginLab, Northampton, MA).

4.3 Results and Discussion

4.3.1 Colloid Concentration

Colloid concentrations in 0.1-0.45 and 0.45-0.7/1.0 μm fractions in the samples from different field sites were measured; < 0.1 μm fraction was assumed as dissolved phase in this study. Figure 4.2a show that colloid concentrations in both size fractions range from 0 to 20 mg/L in most samples, but can be as high as 250 mg/L in some samples. Measured colloid concentrations in 0.1-0.45 and 0.45-0.7/1.0 μm size fractions as well as the total concentration (0.1-0.7/1.0 μm) are listed in Table 4.2. As shown, the average concentration of 0.1-0.45 μm and 0.45-0.7/1.0 μm colloids of all

sampling sites are statistically equivalent, which are 6.88 ± 17.54 mg/L and 4.74 ± 19.66 mg/L, respectively. Furthermore, no significant difference in colloid concentration is observed between 0.1-0.45 µm and 0.45-0.7/1.0 µm size fractions, when they are compared for agricultural, forestry and wetland sites. Colloid concentration are slightly higher in 0.1-0.45 µm than 0.45-0.7/1.0 µm size fraction in estuarine sites (Figure 4.2a and Table 4.2). These results suggest that 0.1-0.45 µm colloids could play at least equally important roles as their larger size counterparts in colloid-facilitated-transport regardless of differences in their environment conditions. Although changes in colloid composition within these size fractions could influence their ability in colloid-facilitated-transport, these results clearly show that the amounts of colloids in < 0.45 µm fractions are substantial, and therefore should not be neglected and considered as dissolved matter.

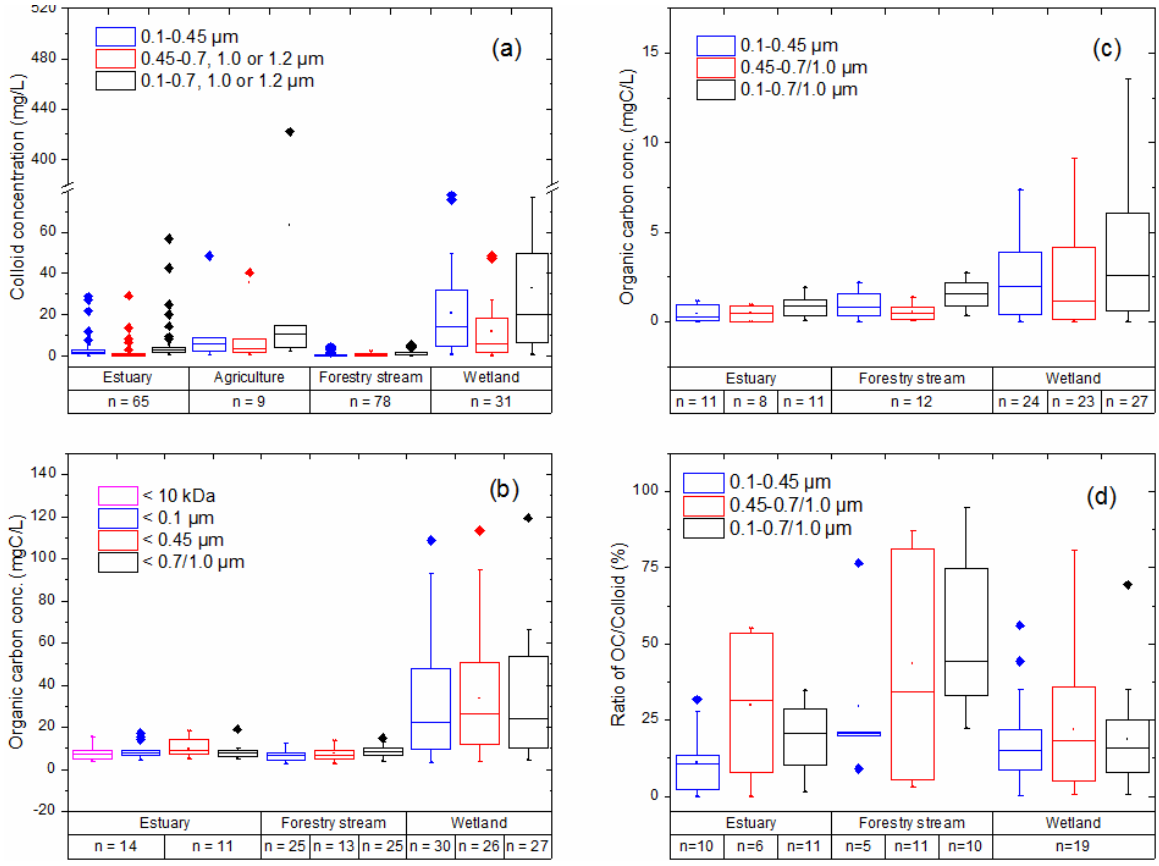

Figure 4.4 Colloid and organic carbon concentrations among different natural systems: (a) the concentration of colloids within size fractions of 0.1-0.45, 0.45-0.7/1.0/1.2 and 0.1-0.7/1.0/1.2 µm; (b) organic carbon concentration within size fractions of < 10 kDa, 0.1, 0.45 and 0.7/1.0 µm in different natural systems; (c) COC concentration, and (d) the ratio of OC to colloids (%OC) within size fractions of 0.1-0.45, 0.45-0.7/1.0 and 0.1-0.7/1.0 µm.

Table 4.2 Colloid concentrations in 0.1-0.45, 0.45-0.7/1.0, and 0.1-0.7/1.0 μm size fractions in samples from different sites.

Samples	Sample Number	Colloid concentration in mg/L		
		0.1-0.45 μm	0.45-0.7/1.0 μm	0.1-0.7/1.0 μm
Agricultural field	9	27.65a*(a)† ± 54.99	35.49a(a) ± 82.56	63.14a ± 137.29
Estuary	65	3.60b(a) ± 5.43	1.73bc(b) ± 4.06	5.33b ± 9.03
Forestry streams	78	0.79b(a) ± 0.98	0.78c(a) ± 0.63	1.47b ± 1.28
Wetland	31	20.89a(a) ± 21.09	12.07b(a) ± 12.79	32.95a ± 33.74
All	183	6.88(a) ± 17.54	4.74(a) ± 19.96	11.83 ± 37.29

* Statistical analysis on parameters of different sampling sites within the same size fraction ($P < 0.05$).
† Statistical analysis on parameters of different size fractions at the same sampling site in parentheses ($P < 0.05$).

While the relative contribution of 0.1-0.45 and 0.45-0.7/1.0 μm fractions to the total colloidal pool are generally equivalent, the absolute colloid concentration within each size fractions change significantly depending on the conditions of each sampling site (Figure 4.4a). This implies that differences in environmental conditions largely determine the total colloidal load, therefore identification of environmental systems and conditions that promote colloid release and mobilization is critical. Total average colloid concentration (0.1-0.7/1.0 μm fraction) in samples from the different field sites are significantly different and follows the order (high to low): agricultural field or wetland (63.14 ± 137.29 mg/L and 32.95 ± 33.74mg/L) > estuary or forestry streams (5.33 ± 9.03 and 1.47 ± 1.28 mg/L) ($p < 0.05$ for one-way ANOVA with Tukey-Kramer HSD test, Table 4.2).

As expected, colloid concentrations in forestry stream samples are lower than in samples from the other sites, presumably due to lack of influence of human activities. For samples from estuarine sites, on the other hand, although human activities could have some impacts, high solution ionic strength promotes colloid

aggregation thus limit colloid release and mobilization, which is confirmed by the negative correlation between salinity and colloid concentration ($p < 0.05$ for Pearson's correlation analysis, Table 4.3). The highest colloid concentrations are measured in samples from the agricultural field, suggesting that agricultural practices could strongly enhance colloid release and mobilization. However, the number of samples from the agricultural fields is limited, and given the high variability associated with field samples, the measured average colloid concentration may not be accurate. To minimize this uncertainty, only concentrations in the first and third quartile of the boxes were compared in Figure 4.4a (only data points inside the rectangular boxes). The re-analyzed results show a similar colloid concentration order as shown above and Table 4.4, which is generally "wetlands or agricultural fields > estuary or forestry stream", and they further support the conclusion about the impact of agricultural activities. Additionally, promotion of colloid release and mobilization by agricultural activities is further supported by the observations in the estuarine sites, where colloid concentrations in the upper stream samples are much higher due to direct input from erosion or discharge from agricultural fields, and these observations are consistent with results of a previous study (Upreti et al., 2015). These results indicate that agricultural practices/human activities could significantly affect colloid-mediated-processes in field sites.

Table 4.3 Pearson's correlation coefficient between pH, EC and colloid and OC concentration among different size fractions

	pH						EC					
	Colloid concentration			OC concentration			Colloid concentration			OC concentration		
Size fractions (μm)	0.1-0.45	0.45-0.7/1.0	0.1-0.7/1.0	0.1-0.45	0.45-0.7/1.0	0.1-0.7/1.0	0.1-0.45	0.45-0.7/1.0	0.1-0.7/1.0	0.1-0.45	0.45-0.7/1.0	0.1-0.7/1.0
Agricultural field	0.57	0.54	0.56	NA	NA	NA	-0.76*	-0.69**	-0.73**	NA	NA	NA
Estuary	0.04	0.04	0.05	0.28	0.31	0.37*	-0.81**	-0.57***	-0.80***	-0.89**	-0.82***	-0.68***
Wetland	0.33*	0.35*	0.34*	-0.47*	-0.45**	-0.46**	0.09	0.09	0.09	-0.16	-0.14	-0.15

* $p < 0.1$
** $p < 0.05$
*** $p < 0.001$

Table 4.4 Colloid concentrations in 0.1-0.45, 0.45-0.7/1.0, and 0.1-0.7/1.0 μm size fractions in samples from different sites after removing the outliers (removal of data outside 1.5 times interquartile range).

Samples	Sample Number	Colloid concentration in mg/L		
		0.1-0.45 μm	0.45-0.7/1.0 μm	0.1-0.7/1.0 μm
Agricultural field	7	10.00a*(a)† ± 15.87	8.28a(a) ± 13.27	18.28a ± 29.03
Estuary	50	2.09b(a) ± 1.33	0.84b(a) ± 0.71	2.95b ± 1.53
Forestry streams	69	0.45b(a) ± 0.26	0.73b(a) ± 0.61	1.05b ± 0.65
Wetland	28	17.03a(a) ± 15.43	9.60a(b) ± 8.81	26.63a ± 24.06
All	154	4.71(a) ± 9.80	2.71(b) ± 5.84	7.51 ± 15.69

* Statistical analysis on parameters of different sampling sites within the same size fraction ($P < 0.05$).

† Statistical analysis on parameters of different size fractions at the same sampling site in parentheses ($P < 0.05$)

Compared to agricultural fields, wetlands, although with little direct anthropogenic perturbation, also have a large and comparable total colloidal load ($p < 0.05$ for One-way ANOVA with Tukey-Kramer HSD test, Table 4.2). Consistently, colloid concentrations in 0.1-0.45 and 0.45-0.7/1.0 μm fractions of samples from the wetland are also higher than those in estuary and forestry stream samples ($p < 0.05$ for One-way ANOVA with Tukey-Kramer HSD test, Table 4.2). High colloid concentrations in wetland samples could be due to prolonged periods of water saturation and inundation that induce iron dissolution and changes in solution chemistry under anaerobic conditions, and thus promote soil disaggregation (De-Campos et al., 2009) and colloid mobilization (Chin et al., 1998; Ryan and Gschwend, 1990; Thompson et al., 2006; Yan et al., 2016). This is partially supported by the positive correlation between pH and colloid concentrations ($p < 0.05$ for Pearson's correlation analysis, Table 4.3). These observations suggest that indirect perturbations such as changes in soil moisture content and redox dynamics associated with climate change events, e.g., intense precipitation and sea-level rise, could have profound impacts on colloid release mobilization from wetlands.

4.3.2 Organic Carbon Concentration

OC concentrations in size fractions of < 10 kDa, 0.1, 0.45, 0.7 and 1.0 μm were measured to examine the size distribution of OC and to evaluate the contribution of truly dissolved and different size colloidal OC to the total OC pool in samples from the different sites. In this study, truly dissolved, colloidal, and total OC were defined as DOC_{tr} < 10 kDa or 0.1 μm, COC in 0.1-0.7/1.0 μm and TOC < 0.7/1.0 μm, respectively.

Figure 4.4b shows that, across all sampling sites, DOC_{tr} consistently dominated the TOC pool, contributing 82.08-87.38% (with 95% certainty) whereas COC generally accounts for ~10-20% of the TOC pool. Despite the relatively small percentage compared to DOC, the absolute concentrations of COC can be substantial, e.g. ~ 15 mgC/L in systems such as wetlands and water bodies affected by agricultural operations. Similar to distribution of colloid concentrations in different size fractions, Figure 4.4c and Table 4.5 show that the average COC concentration in 0.1-0.45 μm fraction is similar to the concentration in 0.45-0.7/1.0 μm fraction (no significant difference for One-way ANOVA with Tukey-Kramer HSD test, Table 4.5). These results clearly demonstrate that the role of < 0.45 μm colloids in carbon retention and transport is as significant as their larger size counterparts, and thus COC in < 0.45 μm fractions should not be treated as dissolved organic carbon.

Table 4.5 COC concentration in 0.1-0.45, 0.45-0.7/1.0, and 0.1-0.7/1.0 μm size fractions from different sites

Samples	Sample Number	COC conc. in mgC/L		
		0.1-0.45 μm	0.45-0.7/1.0 μm	0.1-0.7/1.0 μm
Estuary	11	0.46b*(a)† ± 0.43	0.46b(a) ± 0.43	1.02b ± 0.47
Forestry streams	12	1.00 b(a) ± 0.76	0.55 b(a) ± 0.43	1.54b ± 0.78
Wetland	24	2.36a(a) ± 2.00	2.02a(a) ± 2.45	4.94a ± 3.72
All	47	1.73(a) ± 1.76	1.38(a) ± 1.98	3.14 ± 3.21

* Statistical analysis on parameters of different sampling sites within the same size fraction ($P < 0.05$).
† Statistical analysis on parameters of different size fractions at the same sampling site in parentheses ($P < 0.05$).

Also similar to measured colloid concentrations, COC concentrations change significantly with changing environmental conditions as well (Figure 4.4c). Among the different sampling sites, the average COC concentration in 0.1-0.7/1.0 μm fraction

follows the order: wetland > forestry streams or estuary, indicating that wetlands produce or release more COC than estuary and forestry streams. Consistently, in terms of 0.1-0.45 and 0.45-0.7/1.0 μm fractions, comparable or higher colloid concentrations within these fractions are observed in wetlands than other sites ($p < 0.05$ for One-way ANOVA with Tukey-Kramer HSD test, Figure 4.4c, Table 4.5). The higher COC release and mobilization in wetlands demonstrate that colloid-facilitated-carbon-transport is an important process in systems under reducing conditions, which have been reported in previous studies (Chin et al., 1998; Ryan and Gschwend, 1990; Thompson et al., 2006; Yan et al., 2016). One possible reason is the release or desorption of colloidal organic matter from soil aggregates when solution chemistry changes during microbial dissimilatory iron reduction. Indeed, increase in pH significantly increases COC mobilization in wetlands, which is reflected by the positive correlation between pH and COC concentration ($p < 0.05$, Table 4.3). Compared to wetlands, COC concentrations in samples from the estuarine site correlate negatively with salinity ($p < 0.05$, Table 4.3). It is perceivable that COC formed aggregates and deposited during their transport from inland upstream to offshore downstream where ionic strength is significantly higher. These results clearly demonstrate that different factors and pathways control COC release and mobilization in different natural systems. Field sites under reducing conditions, i.e., wetland in this study, can be considered a hot spot of COC release and mobilization.

4.3.3 Correlation between Organic Carbon and Colloids

To examine the correlation between COC and colloid concentration and quantify carbon retention on colloids in different size fractions, Pearson's correlation analyses were performed between COC and colloid concentration, combining all

samples from estuary, wetland, and forestry streams, for each size fraction. Significant and positive correlations are observed between COC and colloid concentration for all size fractions, although Pearson's correlation coefficients, r, are relatively low (Table 4.6). This result suggests at least some released COC are in the form of mineral-OC complexes and are subject to the same influences as other types of colloids regardless which size fraction they belong. To further examine the quantitative relationship between COC and colloid concentration, linear regression analyses were performed (Figure 4.5). As expected, COC proportionally increases with increasing colloid concentration, and most of the data points can be fitted by the linear regression curve, except several outliers. The reason for the observed outliers could be because of the heterogeneity in colloid composition having different affinity for OC.

Table 4.6 Pearson's correlation coefficient between colloid and COC concentration among different size fractions

	Colloid concentration in mg/L		
	0.1-0.45 µm	0.45-0.7/1.0 µm	0.1-0.7/1.0 µm
COC conc. in mgC/L	0.27*	0.36**	0.33**

* $p < 0.1$
** $p < 0.05$

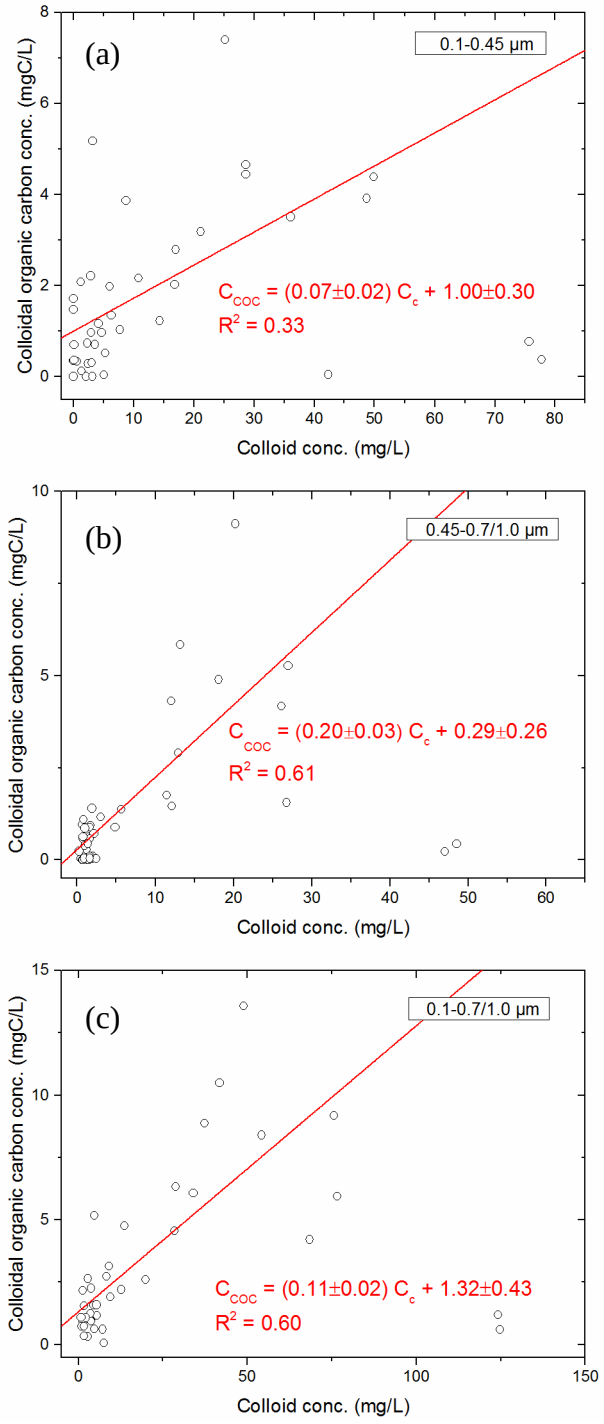

Figure 4.5 Linear regression analyses between COC and colloid concentration within size fractions of (a) 0.1-0.45, (b) 0.45-0.7/1.0 and (c) 0.1-0.7/1.0 µm for data points combined from all natural systems.

The changes in OM contents on colloids in different size fractions were examined by calculating OC contents on colloids (%OC), respectively, for size fractions of 0.1-0.45, 0.45-0.7/1.0 and 0.1-0.7/1.0 μm. Figure 4.4d shows that %OC of colloids varied in all size fractions, ranging from 0 to 70% with a median %OC of ~ 20% after removing the outliers. Much higher %OC on 0.1-1.0 μm colloids than on > 1.0 μm particulate matter has been reported in previous studies (Bergamaschi et al., 1997; Dhillon and Inamdar, 2014; Rostad et al., 1997). For example, Bergamaschi et al. (1997) found %OC of 2-500 μm sediment particles from the Peru Margin ranged from 1.5-9.8%, and Rostad et al. (1997) reported %OC of > 3.6 μm suspended particles in Mississippi River and its tributaries were 1.26-16.8%. More convincingly, Dhillon and Inamdar (2014) sampled the same forestry streams in this study, and found much lower %OC on > 0.45 μm particulate matters, i.e. 0.3-8.9%. These values are much lower than measured in this study on 0.1-1.0 μm colloids, as discussed above. These results suggest that colloidal OM could be more carbon-dense than particulate OM, presumably due to (1) they have larger surface area and sorption capacity, and (2) they form from detachment/transformation of particulate OM or from sorption of or coagulation with branched high molecular weight OM (Guo and Santschi, 1997). Furthermore, increase in carbon loading suggests changes in the stability or lability of organic matter (Feng et al., 2014; Gu et al., 1994). According to the zonal model (Kleber et al., 2015), as carbon content or loading increase, weak organic-organic interactions become more dominated than strong organo-mineral interactions. This could decrease the stability of OC sorbed on 0.1-1.0 μm colloids with increasing carbon loading, compare to > 1.0 μm particulate matter. On the other hand, OM coating on particles could significantly influence both the availability of

sorption sites on mineral surface, and selective composition of sorptive organic compounds in the hydrophobic and kinetic layers on particles (Gschwend and Wu, 1985). These results suggests COM could behave differently from POM in carbon mineralization and stabilization, and thus the biological reactivity or bioavailability of COC should be investigated in future study.

4.3.4 Relationship between Operationally Defined and Truly Dissolved Organic Carbon

To extensively evaluate the contribution of COC to the operationally defined DOC (DOC_{op}), OC concentrations in different size fractions were summarized from this study and reported results in the literature of measurements of samples from numerous rivers, estuary and marine sites across the globe, and then calculated the ratio of DOC_{tr} (< 10 kDa or 0.1 μm) to DOC_{op} (< 0.2 to 0.45 μm). Among all samples, the average OC concentration is 8.1 ± 14.7 mgC/L, and the ratio of DOC_{tr} to DOC_{op} is 86.4% ± 9.6% (Figure 4.6a, Table 4.7), indicating that most of the OC in DOC_{op} is in truly dissolved phase and only 12-15% of DOC_{op} is in colloidal phase. The ratios of DOC_{tr} to DOC_{op} are relatively constant, compared to the large variations in OC concentrations, as reflected by their variance coefficient, 0.11 and 1.82, respectively. This observation seems to suggest that the DOC_{tr} to DOC_{op} ratio is largely independent of changes in OC concentrations (Table 4.7, Figure 4.6b)

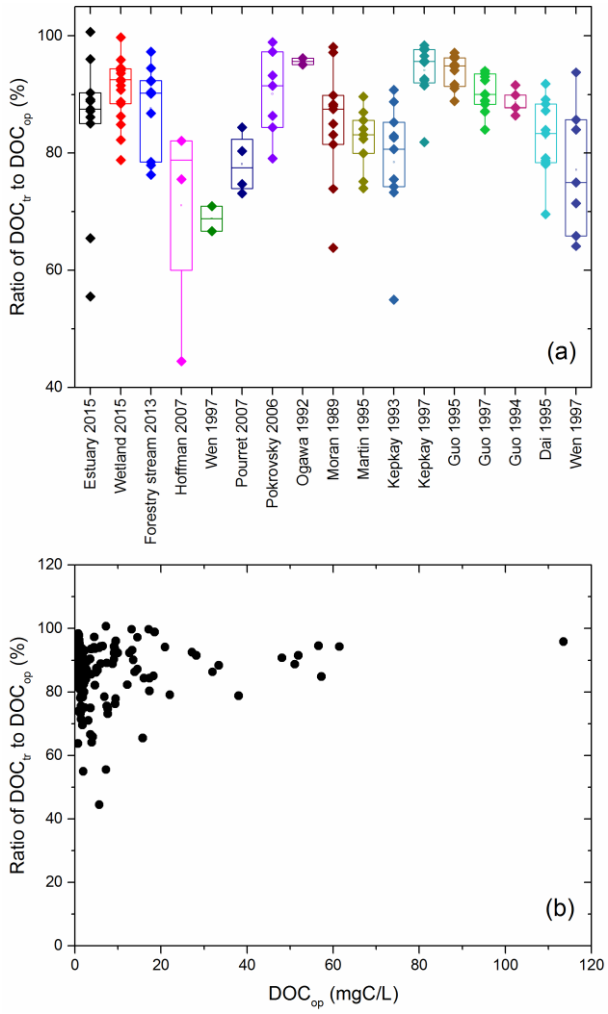

Figure 4.6 Ratio of DOC_{tr} to DOC_{op} (a) and its relationship with DOC_{op} (b) of samples from this study and literature.

Table 4.7 The ratios of DOC_{tr} to DOC_{op} from this study and literature

Samples	Sample Number	Lower/Upper cutoff size	Site description	DOC_{tr} mgC/L	DOC_{op} mgC/L	Ratio of DOC_{tr}/DOC_{op} %
Estuary	14	10 kDa/0.45 µm	Chesapeake Bay, MD	15.53 ± 6.39	20.11 ± 9.44	84.71 ± 13.00
Wetland	18	0.1/0.45 µm	Wetlands, DE	39.49 ± 30.55	36.86 ± 29.48	91.43 ± 5.46
Forestry streams	12	0.1/0.45 µm	Forestry streams, MD	7.53 ± 3.38	6.53 ± 3.01	87.64 ± 7.52
Hoffmann et al. (2007)	4	10 kDa/0.4 µm	Rivers, WI and MI	326.50 ± 104.27	463.75 ± 107.09	71.05 ± 17.97
Pourret et al. (2007)	4	10 kDa/0.2 µm	Groundwater, Central Brittany, France	9.96 ± 4.97	12.48 ± 5.57	78.13 ± 5.20
Pokrovsky et al. (2006)	7	10 kDa/0.22 µm	River, central Siberia, Russia	16.21 ± 4.86	18.06 ± 5.41	90.09 ± 7.16
Ogawa and Ogura (1992)	2	10 kDa/0.45 µm	Pacific ocean, Honshu, Japan	75.40 ± 11.03	78.90 ± 12.16	95.65 ± 0.78
Moran and Moore (1989)	11	10 kDa/0.45 µm	Sea water, Nova Scotia, Canada	53.32 ± 10.35	62.62 ± 9.59	85.12 ± 9.79
Martin et al. (1995)	9	10 kDa/0.4 µm	Venice Lagoon, Italy	165.28 ± 52.28	198.74 ± 54.65	82.32 ± 5.20
Kepkay et al. (1993)	11	10 kDa/0.4 µm	Bedford Basin, Nova Scotia, Canada	83.03 ± 12.71	107.87 ±23.84	78.47 ± 9.82
Kepkay et al. (1997)	12	10 kDa/0.2 µm	Bedford Basin, Nova Scotia, Canada	66.32 ± 11.58	70.67 ± 13.18	94.12 ± 4.63
Guo et al. (1994)	5	10 kDa/0.2 µm	Gulf of Maxico and Mid Atlantic Bay	85.26 ± 29.36	96.60 ± 34.29	88.68 ± 2.06
Guo et al. (1995)	12	10 kDa/0.2 µm	Chesapeake Bay and Galveston Bay	105.73 ± 107.58	114.83 ± 122.26	93.79 ± 2.93

Guo and Santschi (1997)	14	10 kDa/0.2 µm	Gulf of Maxico	230.51 ± 121.67	253.21 ± 129.73	90.36 ± 3.13
Dai et al. (1995)	11	10 kDa/0.4 µm	Rhone Delta, Switzerland	97.36 ± 16.08	11.89 ± 22.52	82.52 ± 6.46
Wen et al. (1997)	2	10 kDa/0.45 µm	Rivers, TX	2.30 ± 0.14	3.35 ± 0.35	68.85 ± 3.04
	7	10 kDa/0.4 µm	Gulf of Maxico	2.04 ± 0.65	2.74 ± 1.12	77.12 ± 11.04
All results	151	10 kDa/0.2 to 0.45 µm		9.32 ± 16.48	8.17 ± 15.33	86.44 ± 9.57

Additionally, the linear regression between DOC_{tr} and DOC_{op} shows that majority of the data fall on the same regression line with a slope of 0.92 and a high R^2 value (Figure 4.7a). This seems to indicate the existence of a constant distribution between DOC_{tr} (92%) and COC (8%) in DOC_{op} regardless of sampling source and location. The "universal" nature of this observation suggests the possibility of predicting COC concentrations from DOC_{op} concentrations.

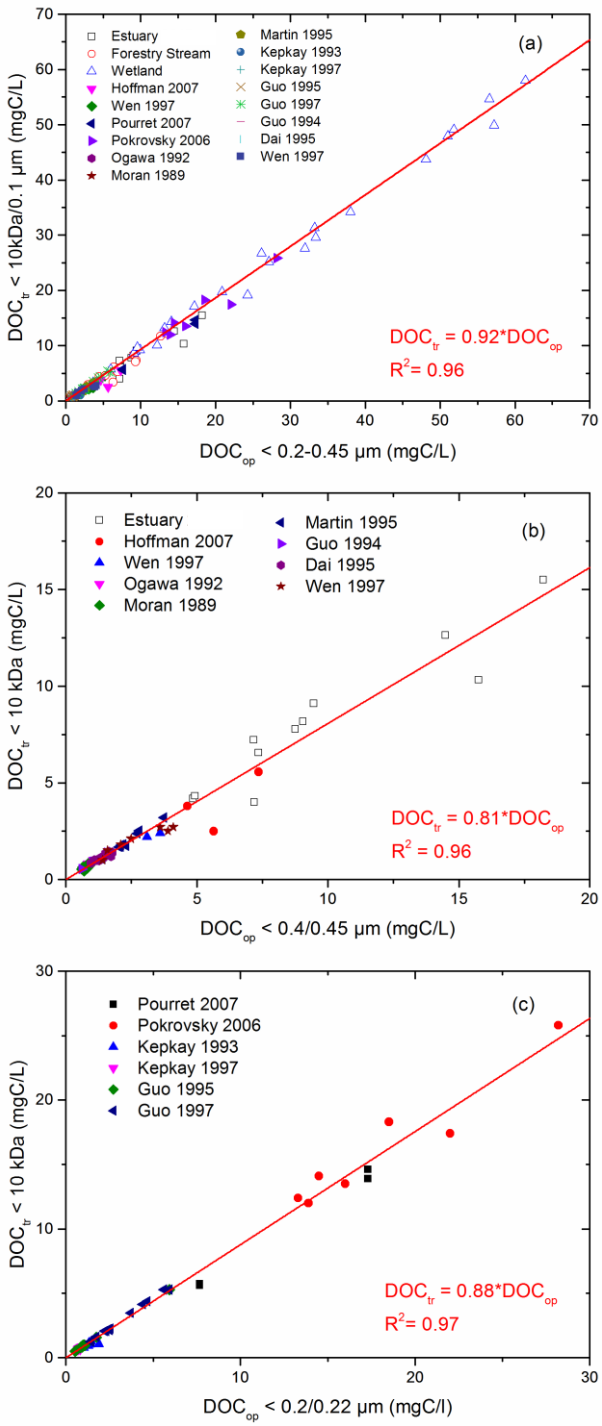

Figure 4.7 Relationships between DOC_{tr} and DOC_{op}: (a) for all data together; (b) DOC_{tr} < 10 kDa and DOC_{op} < 0.4/0.45 µm and (c) DOC_{tr} < 10 kDa and DOC_{op} < 0.2/0.22 µm.

Because the results presented in Figure 4.7a are from different studies that used different cut-off sizes for colloid definition, additional regression analyses were performed using < 10 kDa OC as DOC_{tr} and < 0.2/0.22 μm or < 0.4/0.45 μm OC, respectively, as DOC_{op}. Figure 4.7b and c show that the ratio of DOC_{tr} to DOC_{op} is 0.81 for samples of < 0.4/0.45 μm OC and 0.88 for samples of < 0.2/0.22 μm OC. Results in Figure 4a, 4b, and 4c collectively indicate that there is at least 8% but can be up to 12-19% of COC that has been regarded as dissolved OC when using the operational defined cut-off size of either 0.2/0.22 μm or 0.4/0.45 μm. This result is consistent with Benner and Amon's estimation that ~77% of total OC in the ocean are low molecular weight OC (Benner and Amon, 2015). It represents more than the marine environment because it also included terrestrial samples. Furthermore, it considered different size fractions separately thus providing a range of size-dependent estimations.

4.4 Conclusions, Implications, and Environmental Significance

In this study, mobile colloids and colloid-associated-organic-carbon were quantify in 0.1-0.45, 0.45-0.7/1.0 and 0.1-0.7/1.0 μm fractions in samples collected from different natural systems, including agricultural, forestry stream, freshwater wetland, and estuarine field sites. Our results demonstrate that (1) colloid and COC, especially those in < 0.45 μm fraction, are substantial in natural systems, and thus are largely being underestimated in current operationally defined practices; COC could account for 8-19% of DOC in < 0.45 μm fraction; (2) positive correlations between OC and colloid concentration were observed, and COC proportionally increase with colloid concentration in all size fractions; (3) wetland and agricultural fields were

found to be hotspots of colloid and COC mobilization and release, compared to forestry and estuary sites.

These findings clearly demonstrate that results from analyzing operationally defined "dissolved" matters are misleading for studies aiming at "truly" dissolved materials, and thus a more accurate boundary between colloidal and dissolved phase need to be defined. The results in this study provide important guidance in quantitatively differentiating colloidal materials from "truly" dissolved matter in < 0.45 μm fraction and determining total colloidal loads in natural systems. This ultimately have strong implications in assessing biological function and environmental fate and transport of dissolved- and colloid-associated-constituents in natural systems. Besides, these findings fill the gap in the quantification of < 0.45 μm COC and provide the basis for possibly considering COC as a separate phase in carbon cycling and assessment of carbon budget in different natural environments, as COC is likely to behave differently from truly dissolved or particulate organic carbon in these systems (Benner and Amon, 2015; Guo and Santschi, 2007).

The seemingly "constant" contribution of COC in DOC < 0.2 or 0.45 μm following the current practice provide us the capability for estimating the underestimated COC pool in global carbon cycles. According to studies on estimation of global DOC flux (Bauer and Bianchi, 2011; Bauer et al., 2013), riverine DOC flux to the ocean ranges from 0.17 to 0.4 PgC $year^{-1}$ and total DOC pool in the world's ocean is 662 ± 32 PgC (Hansell et al., 2009). As a result, based on our conservative estimation, COC may account for at least 13.6 to 32 TgC $year^{-1}$ as a riverine flux and 530 ± 25 TgC of global DOC pool in ocean (calculated based on COC accounts for 8% of DOC pool). The significant, but underestimated amount of COC could

represent a substantial and dynamic pool of biodegradable OC and thus contribute to the carbon emission by mineralization and microbial respiration (Amon and Benner, 1996; Hama et al., 2004). Furthermore, nano- or micro-size colloid can aggregate to form macro-size particles and thus the OC complexed or sorbed on colloids could be settled out and stored as sediments during their transport. This study shows that the COC is a significant component in the global carbon pool, and thus its contribution should not be neglected and should be considered in models of carbon budget estimation.

Additionally, the findings signify the importance of colloid-facilitated-transport on carbon cycles in environments that are subjected to variations in redox status and the influence of human and agricultural activities. Colloid and COC formation and mobilization are extremely sensitive to the physicochemical changes of the environments as the alteration of climate and anthropogenic changes, indicating the contribution of COC to the global carbon pool could be more intensive in regions undergoing significant environmental changes, including intermittent anoxia in upland soils due to intensified precipitation, severe and frequent flooding area due to deforestation, and coastal inundation undergoing sea level rise. These findings improve our capability in assessing and predicting the influence of anthropogenic perturbation on organic carbon mobilization, which have important implications in land use management and regulation of different environmental systems to sustain the future perturbation.

Chapter 5

CONCLUSIONS

5.1 Summary of Research

The research presented in this dissertation combined field measurements and laboratory investigations and was aimed to (1) accurately quantify the colloidal pool and assess its quantitative contribution to the mobilization of colloid-associated-organic carbon in different natural systems; (2) identify and understand major environmental conditions/pathways, especially reducing conditions, leading to dissolved organic matter (DOM) release and transport as affected by colloid mobilization in different natural systems. In Chapter 2, I investigated the complex interplay of colloid release, OM content and redox conditions via batch experiments to quantify and characterize soil colloid release after addition of DOM. The results show that the interactions of DOM and colloid behaved differently under different redox conditions. These findings suggest that simultaneous release of DOM_{in} under reducing conditions due to iron dissolution and its interaction with colloid can complicate and modify colloid mobilization and thus influence the mobility of colloid-associated-contaminants or –nutrients. In addition, the interactions and association between colloid and DOM demonstrated the role of colloids in carrying or retaining carbon, therefore, it is critical to further the investigation of colloid mobilization in order to achieve a better understanding of its successive impact on carbon cycles in natural reducing environments.

In chapter 3, I tested the reliability of using turbidimetric measurement to quantify colloid concentration in aquatic environmental samples and developed size-dependent turbidity-concentration correlations curves for three colloidal size fractions (< 1.0, 0.45 – 1.0, 0.1-0.45, and < 0.1 μm) based on measurements from a large number of soil samples. The results demonstrated that particle size is the dominant factor affecting the correlation between turbidity and colloid concentration while effects of particle composition and OM are largely negligible. The size-dependent concentration-turbidity correlations provide more accurate estimations when tested against gravimetric measurements using field samples compared to the combined curve of < 1.0 μm, which is more commonly used. The relatively insignificant particle composition effect indicates the practically "universal" applicability of the reported correlations. In addition, the correlations, for the first time, allow quantification of colloids in different size fractions in environmental samples, especially colloids that are < 0.45 μm, which have been traditionally considered as part of the dissolved phase and hence underestimated. The developed colloid quantification method will enhance our capability in quantifying colloidal pools in natural systems, especially the < 0.45 μm fraction and therefore provide more accurate assessment in the mobility of colloid-associated-constituent, such as nutrients, contaminants, and trace elements.

In Chapter 4, mobile colloids and colloid-associated-organic-carbon in 0.1-0.45, 0.45-0.7/1.0 and 0.1-0.7/1.0 μm were quantified and analyzed in samples collected from different natural systems, i.e. agricultural, forestry stream, freshwater wetland, and estuarine field sites. The results show that (1) colloid and COC, especially those < 0.45 μm, are substantial in natural systems regardless the difference in environmental conditions, and COC account for 8-19% of DOC < 0.45 μm; (2)

COC concentration proportionally increase with colloid concentration, and COC proportionally increase with colloid concentration in all size fractions; (3) wetland and agricultural fields were found to be hotspots of colloid and COC mobilization and release, compared to forestry and estuary sites. These results clearly show that the COC is a significant component in the global carbon pool, and thus its contribution should not be neglected and should be considered in models of carbon budget estimation. These findings fill the gap in quantification of < 0.45 μm colloids and provide the basis for possibly considering COC as a separate phase in carbon cycling and assessment of carbon budget in different natural environments, as COC is likely to behave differently from truly dissolved or particulate organic carbon in these systems. Additionally, colloids and COC formation and mobilization are extremely sensitive to the physicochemical changes of the environments as the alteration of climate and anthropogenic changes, indicating the contribution of COC to the global carbon pool could be more intensive in regions undergoing significant environmental changes, e.g. intermittent anoxia in upland soils due to intensified precipitation.

5.2 Future Research

Better understanding of colloid release and mobilization under varying redox conditions provide us with the capability of mechanistically explaining the release and transport behavior of colloid and colloid-associated-carbon in redox dynamic environments. Results in Chapter 2 demonstrated the dynamic processes and complex factors involved in controlling colloid and OM release and their fate. To extend this research, additional batch experiments may be conducted with extracted soil colloids under controlled solution chemistry, i.e. pH, IS and Eh, to test and validate the proposed mechanisms of organo-mineral interactions presented in Chapter 2. In well

controlled systems, the relative importance of electrostatic, steric repulsion and bridging effects on colloid dispersion might be evaluated by monitoring the shifts in zeta potential, electrophoretic mobility of colloids or simulating and comparing the thickness of the diffuse double layer and OM adsorption layer on colloids.

To further enhance the applicability and representativeness of size-dependent turbidity-concentration correlations, additional sample collection and analysis are necessary. Elemental compositions of colloids, such as minerology, determine the refractive index and shape of colloids, which are closely related to light scattering properties of colloids. Variations in elemental composition affect accuracy in prediction of concentration-turbidity correlations, but have not been adequately quantified. Further investigation on this may improve the accuracy in quantifying colloids.

To determine whether and how important to treat COC as a separate OC phase in addition to the particulate and dissolved phases, the mobility and biological reactivity of COC in laboratory and different natural systems should be quantified. Whether COC are mobile or immobile, labile or refractory largely determine the residence time and carbon turn-over rate during their transport through soil porous medium and aquatic water column. Although substantial amounts of COC were recognized in different representative natural systems in this study, the information of mobility and bioactivity of COC are still needed. This will provide us a more completed picture of carbon pool and inventory, and ultimately benefit the estimation of global carbon budget.

REFERENCES

1. Akbour, R.A. et al. 2002. Transport of kaolinite colloids through quartz sand: Influence of humic acid, ca2+, and trace metals. Journal of Colloid and Interface Science 253: 1-8. doi:10.1006/jcis.2002.8523.

2. Alva, A.K. et al. 1991. Relationship between ionic-strength and electrical-conductivity for soil solutions. Soil Science 152: 239-242. doi:10.1097/00010694-199110000-00001.

3. Amon, R.M.W. and R. Benner. 1996. Bacterial utilization of different size classes of dissolved organic matter. Limnology and Oceanography 41: 41-51.

4. Antelo, J. et al. 2007. Adsorption of a soil humic acid at the surface of goethite and its competitive interaction with phosphate. Geoderma 138: 12-19.

5. Baalousha, M. 2009. Aggregation and disaggregation of iron oxide nanoparticles: Influence of particle concentration, ph and natural organic matter. Science of the Total Environment 407: 2093-2101. doi:10.1016/j.scitotenv.2008.11.022.

6. Baalousha, M. et al. 2011. 3.05-natural colloids and manufactured nanoparticles in aquatic and terrestrial systems. In: W. Editor-in-Chief: Peter, editor Treatise on water science. Elsevier, Oxford. p. 89-129.

7. Baalousha, M. et al. 2008. Aggregation and surface properties of iron oxide nanoparticles: Influence of ph and natural organic matter. Environmental Toxicology and Chemistry 27: 1875-1882. doi:10.1897/07-559.1.

8. Bachmann, J. et al. 2008. Physical carbon-sequestration mechanisms under special consideration of soil wettability. Journal of Plant Nutrition and Soil Science-Zeitschrift Fur Pflanzenernahrung Und Bodenkunde 171: 14-26.

9. Baker, E.T. et al. 2001. Field and laboratory studies on the effect of particle size and composition on optical backscattering measurements in hydrothermal plumes. Deep-Sea Research Part I-Oceanographic Research Papers 48: 593-604. doi:10.1016/s0967-0637(00)00011-x.

10. Bauer, J.E. and T.S. Bianchi. 2011. Dissolved organic carbon cycling and transformation. Treatise on Estuarine and Coastal Science, Vol 5: Biogeochemistry: 7-67.

11. Bauer, J.E. et al. 2013. The changing carbon cycle of the coastal ocean. Nature 504: 61-70. doi:10.1038/nature12857.

12. Bauer, J.E. et al. 1996. Cross-flow filtration of dissolved and colloidal nitrogen and phosphorus in seawater: Results from an intercomparison study. Marine Chemistry 55: 33-52. doi:10.1016/s0304-4203(96)00047-3.

13. Benner, R. and R.M.W. Amon. 2015. The size-reactivity continuum of major bioelements in the ocean. Annual Review of Marine Science, Vol 7 7: 185-205. doi:10.1146/annurev-marine-010213-135126.

14. Bergamaschi, B.A. et al. 1997. The effect of grain size and surface area on organic matter, lignin and carbohydrate concentration, and molecular compositions in peru margin sediments. Geochimica et Cosmochimica Acta 61: 1247-1260. doi:10.1016/s0016-7037(96)00394-8.

15. Bolt, G.H. et al., editor. 1991. Interactions at the soil colloid-soil solution interface. Kluwer Academic Publishers Group, State University of Ghent, Belgium.

16. Bouyoucos, G.J. 1962. Hydrometer method improved for making particle size analyses of soils. Agronomy Journal 54: 464-&.

17. Bremner, J.M. 1996. Nitrogen-total. In: D. L. Sparks, A. L. Page, P. A. Helmke and R. H. Loeppert, editors, Methods of soil analysis part 3—chemical methods. Soil Science Society of America, American Society of Agronomy. p. 1085-1121.

18. Buettner, S.W. et al. 2014. Mobilization of colloidal carbon during iron reduction in basaltic soils. Geoderma 221: 139-145. doi:10.1016/j.geoderma.2014.01.012.

19. Buffle, J. and G.G. Leppard. 1995. Characterization of aquatic colloids and macromolecules. 1. Structure and behavior of colloidal material. Environmental Science & Technology 29: 2169-2175. doi:10.1021/es00009a004.

20. Buffle, J., Perret, D., and Newman, M. 1992. The use of filtration and ultrafiltration for size fractionation of aquatic particles, colloids and macromolecules. In: J. B. a. H. P. V. Leeuwen, editor Environmental particles. Lewis Publishers, Boca Raton. p. 554.

21. Bunn, R.A. et al. 2002. Mobilization of natural colloids from an iron oxide-coated sand aquifer: Effect of ph and ionic strength. Environmental Science & Technology 36: 314-322. doi:10.1021/es0109141.

22. Chen, C. et al. 2014. Properties of fe-organic matter associations via coprecipitation versus adsorption. Environmental Science & Technology 48: 13751-13759. doi:10.1021/es503669u.

23. Chen, K.L. and M. Elimelech. 2007. Influence of humic acid on the aggregation kinetics of fullerene (c-60) nanoparticles in monovalent and divalent electrolyte solutions. Journal of Colloid and Interface Science 309: 126-134. doi:10.1016/j.jcis.2007.01.074.

24. Chen, K.L. et al. 2006. Aggregation kinetics of alginate-coated hematite nanoparticles in monovalent and divalent electrolytes. Environmental Science and Technology 40: 1516-1523.

25. Chin, Y.P. et al. 1998. Abundance and properties of dissolved organic matter in pore waters of a freshwater wetland. Limnology and Oceanography 43: 1287-1296.

26. Christian, P. et al. 2008. Nanoparticles: Structure, properties, preparation and behaviour in environmental media. Ecotoxicology 17: 326-343. doi:10.1007/s10646-008-0213-1.

27. Chu, Y.J. et al. 2000. Virus transport through saturated sand columns as affected by different buffer solutions. Journal of Environmental Quality 29: 1103-1110.

28. Cornell, R.M. and U. Schwertmann. 2003a. The iron oxides structure, properties, reactions, occurrences, and uses. Wiley-VCH, Weinheim, Germany.

29. Cornell, R.M. and U. Schwertmann. 2003b. The iron oxides: Structure, properties, reactions, occurrences and uses.Wiley-vch.

30. Dai, M. et al. 1995. The significant role of colloids in the transport and transformation of organic-carbon and associated trace-metals (cd, cu and ni) in the rhone delta (france). Marine Chemistry 51: 159-175. doi:10.1016/0304-4203(95)00051-r.

31. Dalzell, B.J. et al. 2005. Flood pulse influences on terrestrial organic matter export from an agricultural watershed. Journal of Geophysical Research-Biogeosciences 110. doi:10.1029/2005jg000043.

32. De-Campos, A.B. et al. 2009. Short-term reducing conditions decrease soil aggregation. Soil Science Society of America Journal 73: 550-559. doi:10.2136/sssaj2007.0425.

33. de Jonge, L.W. et al. 2004a. Colloids and colloid-facilitated transport of contaminants in soils: An introduction. Vadose Zone Journal 3: 321-325.

34. de Jonge, L.W. et al. 2004b. Particle leaching and particle-facilitated transport of phosphorus at field scale. Vadose Zone Journal 3: 462-470.

35. Dhillon, G.S. and S. Inamdar. 2013. Extreme storms and changes in particulate and dissolved organic carbon in runoff: Entering uncharted waters? Geophysical Research Letters 40. doi:10.1002/grl.50306.

36. Dhillon, G.S. and S. Inamdar. 2014. Storm event patterns of particulate organic carbon (poc) for large storms and differences with dissolved organic carbon (doc). Biogeochemistry 118: 61-81. doi:10.1007/s10533-013-9905-6.

37. Dong, H. and I.M.C. Lo. 2013. Influence of calcium ions on the colloidal stability of surface-modified nano zero-valent iron in the absence or presence of humic acid. Water Research 47: 2489-2496. doi:10.1016/j.watres.2013.02.022.

38. Doucet, F.J. et al. 2007. Colloid–trace element interactions in aquatic systems. Environmental colloids and particles. John Wiley & Sons, Ltd. p. 95-157.

39. Ellerbrock, R.H. and M. Kaiser. 2005. Stability and composition of different soluble soil organic matter fractions - evidence from delta c-13 and ftir signatures. Geoderma 128: 28-37.

40. Eshel, G. et al. 2004. Critical evaluation of the use of laser diffraction for particle-size distribution analysis. Soil Science Society of America Journal 68: 736-743.

41. Everett, D.H. 1972. Manual of symbols and terminology for physicochemical quantities and units, appendix ii: Definitions, terminology and symbols in colloid and surface chemistry. Pure and Applied Chemistry. p. 577-638.

42. Feachem, R. et al. 1983. Sanitation and disease: Health aspects of excreta and wastewater management. John Wiley & Sons, New York, NY.

43. Feng, W. et al. 2014. Soil organic matter stability in organo-mineral complexes as a function of increasing c loading. Soil Biology & Biochemistry 69: 398-405. doi:10.1016/j.soilbio.2013.11.024.

44. Ferris, M.J. et al. 1996. Denaturing gradient gel electrophoresis profiles of 16s rrna-defined populations inhabiting a hot spring microbial mat community. Applied and Environmental Microbiology 62: 340-346.

45. Fiedler, S. and K. Kalbitz. 2003. Concentrations and properties of dissolved organic matter in forest soils as affected by the redox regime. Soil Science 168: 793-801. doi:10.1097/01.ss.0000100471.96182.03.

46. Filella, M. 2007. Colloidal properties of submicron particles in natural waters. Environmental colloids and particles. John Wiley & Sons, Ltd. p. 17-93.

47. Filella, M. et al. 2006. Variability of the colloidal molybdate reactive phosphorous concentrations in freshwaters. Water Research 40: 3185-3192. doi:10.1016/j.watres.2006.07.010.

48. Filella, M. et al. 1997. Analytical applications of photon correlation spectroscopy for size distribution measurements of natural colloidal suspensions: Capabilities and limitations. Colloids and Surfaces a-Physicochemical and Engineering Aspects 120: 27-46. doi:10.1016/s0927-7757(96)03677-1.

49. Findlay, A.D. et al. 1996. The aggregation of silica and haematite particles dispersed in natural water samples. Colloids and Surfaces A: Physicochemical and Engineering Aspects 118: 97-105.

50. FitzPatrick, E.A. 1993. Soil microscopy and micromorphology. J. Wiley, Chichester, NY.

51. Flury, M. et al. 2002. In situ mobilization of colloids and transport of cesium in hanford sediments. Environmental Science & Technology 36: 5335-5341. doi:10.1021/es025638k.

52. Foster, I. et al. 1992. The impact of particle size controls on stream turbidity measurement; some implications for suspended sediment yield estimation. Erosion and sediment transport monitoring programmes in river basins 210: 51-62.

53. Fuller, C.C. and J.A. Davis. 1987. Processes and kinetics of cd-2+ sorption by a calcareous aquifer sand. Geochimica et Cosmochimica Acta 51: 1491-1502. doi:10.1016/0016-7037(87)90331-0.

54. Furukawa, Y. et al. 2009. Aggregation of montmorillonite and organic matter in aqueous media containing artificial seawater. Geochemical Transactions 10.

55. Gimbert, L.J. et al. 2005. Comparison of centrifugation and filtration techniques for the size fractionation of colloidal material in soil suspensions using sedimentation field-flow fractionation. Environmental Science & Technology 39: 1731-1735. doi:10.1021/es049230u.

56. Gippel, C.J. 1995. Potential of turbidity monitoring for measuring the transport of suspended-solids in streams. Hydrological Processes 9: 83-97. doi:10.1002/hyp.3360090108.

57. Goldberg, E.D. et al. 1952. Microfiltration in oceanographic research .1. Marine sampling with the molecular filter. Journal of Marine Research 11: 194-204.

58. Green, S.A. and N.V. Blough. 1994. Optical-absorption and fluorescence properties of chromophoric dissolved organic-matter in natural-waters. Limnology and Oceanography 39: 1903-1916.

59. Greswell, R.B. et al. 2010. An inexpensive flow-through laser nephelometer for the detection of natural colloids and manufactured nanoparticles. Journal of Hydrology 388: 112-120. doi:10.1016/j.jhydrol.2010.04.033.

60. Griffin, B.A. and J.J. Jurinak. 1973. Estimation of activity coefficients from the electrical conductivity of natural aquatic systems and soil extracts. Soil Science 116: 26-30.

61. Grolimund, D. and M. Borkovec. 1999. Long term release kinetics of colloidal particles from natural porous media. Environmental Science & Technology 33: 4054-4060. doi:10.1021/es990194m.

62. Grybos, M. et al. 2009. Increasing ph drives organic matter solubilization from wetland soils under reducing conditions. Geoderma 154: 13-19.

63. Gschwend, P.M. and S.C. Wu. 1985. On the constancy of sediment water partition-coefficients of hydrophobic organic pollutants. Environmental Science & Technology 19: 90-96. doi:10.1021/es00131a011.

64. Gu, B.H. et al. 1994. Adsorption and desorption of natural organic-matter on iron-oxide - mechanisms and models. Environmental Science & Technology 28: 38-46. doi:10.1021/es00050a007.

65. Guo, L. and R.W. Macdonald. 2006. Source and transport of terrigenous organic matter in the upper yukon river: Evidence from isotope (delta c-13, delta c-14, and delta n-15) composition of dissolved, colloidal, and particulate phases. Global Biogeochemical Cycles 20. doi:10.1029/2005gb002593.

66. Guo, L. and P.H. Santschi. 2007. 4 ultrafiltration and its applications to sampling and characterisation of aquatic colloids. In: K. J. Wilkinson and J. R. Lead, editors, Environmental colloids and particles: Behaviour, separation and characterization. Wiley, West Sussex, England. p. 159-221.

67. Guo, L.D. et al. 1994. The distribution of colloidal and dissolved organic-carbon in the gulf-of-mexico. Marine Chemistry 45: 105-119. doi:10.1016/0304-4203(94)90095-7.

68. Guo, L.D. and P.H. Santschi. 1997. Isotopic and elemental characterization of colloidal organic matter from the chesapeake bay and galveston bay. Marine Chemistry 59: 1-15. doi:10.1016/s0304-4203(97)00072-8.

69. Guo, L.D. et al. 1995. Dynamics of dissolved organic carbon (doc) in oceanic environments. Limnology and Oceanography 40: 1392-1403.

70. Gustafsson, O. and P.M. Gschwend. 1997. Aquatic colloids: Concepts, definitions, and current challenges. Limnology and Oceanography 42: 519-528.

71. Hagedorn, F. et al. 2000. Effects of redox conditions and flow processes on the mobility of dissolved organic carbon and nitrogen in a forest soil. Journal of Environmental Quality 29: 288-297.

72. Haiss, W. et al. 2007. Determination of size and concentration of gold nanoparticles from uv-vis spectra. Analytical Chemistry 79: 4215-4221. doi:10.1021/ac0702084.

73. Hama, T. et al. 2004. Decrease in molecular weight of photosynthetic products of marine phytoplankton during early diagenesis. Limnology and Oceanography 49: 471-481.

74. Hart, B.T. et al. 1993. Characterization of colloidal and particulate matter transported by the magela creek system, northern australia. Hydrological Processes 7: 105-118. doi:10.1002/hyp.3360070111.

75. Haygarth, P.M. et al. 1997. Size distribution of colloidal molybdate reactive phosphorus in river waters and soil solution. Water Research 31: 439-448. doi:10.1016/s0043-1354(96)00270-9.

76. Helms, J.R. et al. 2008. Absorption spectral slopes and slope ratios as indicators of molecular weight, source, and photobleaching of chromophoric dissolved organic matter. Limnology and Oceanography 53: 955-969. doi:10.4319/lo.2008.53.3.0955.

77. Hendershot, W.H. and L.M. Lavkulich. 1983. Effect of sesquioxide coatings on surface-charge of standard mineral and soil samples. Soil Science Society of America Journal 47: 1252-1260.

78. Her, N. et al. 2003. Characterization of dom as a function of mw by fluorescence eem and hplc-sec using uva, doc, and fluorescence detection. Water Research 37: 4295-4303. doi:10.1016/s0043-1354(03)00317-8.

79. Herrera Ramos, A.C. and M.B. McBride. 1996. Goethite dispersibility in solutions of variable ionic strength and soluble organic matter content. Clays and Clay Minerals 44: 286-296.

80. Hoffmann, S.R. et al. 2007. Strong colloidal and dissolved organic ligands binding copper and zinc in rivers. Environmental Science & Technology 41: 6996-7002. doi:10.1021/es070958v.

81. Hu, J.-D. et al. 2010. Effect of dissolved organic matter on the stability of magnetite nanoparticles under different ph and ionic strength conditions. Science of the Total Environment 408: 3477-3489. doi:10.1016/j.scitotenv.2010.03.033.

82. Hunter, R.J. and L.R. White. 1987. Foundations of colloid science. Clarendon Press; Oxford University Press, Oxford, NY.

83. Inamdar, S. et al. 2011. Fluorescence characteristics and sources of dissolved organic matter for stream water during storm events in a forested mid-atlantic watershed. Journal of Geophysical Research-Biogeosciences 116. doi:10.1029/2011jg001735.

84. Ishida, T. et al. 1991. Estimation of complex refractive-index of soil particles and its dependence on soil chemical-properties. Remote Sensing of Environment 38: 173-182. doi:10.1016/0034-4257(91)90087-m.

85. Jacobsen, O.H. et al. 1997. Particle transport in macropores of undisturbed soil columns. Journal of Hydrology 196: 185-203. doi:10.1016/s0022-1694(96)03291-x.

86. Jin, Y. et al. 2000. Virus removal and transport in saturated and unsaturated sand columns. Journal of Contaminant Hydrology 43: 111-128. doi:10.1016/s0169-7722(00)00084-x.

87. Jin, Y. et al. 1997. Sorption of viruses during flow through saturated sand columns. Environmental Science & Technology 31: 548-555. doi:10.1021/es9604323.

88. Johnson, S.B. et al. 2005. Adsorption of organic matter at mineral/water interfaces. 6. Effect of inner-sphere versus outer-sphere adsorption on colloidal stability. Langmuir 21: 6356-6365.

89. Jones, M.N. and N.D. Bryan. 1998. Colloidal properties of humic substances. Advances in Colloid and Interface Science 78: 1-48. doi:10.1016/s0001-8686(98)00058-x.

90. Kaiser, M. and R.H. Ellerbrock. 2005. Functional characterization of soil organic matter fractions different in solubility originating from a long-term field experiment. Geoderma 127: 196-206.

91. Kalbitz, K. et al. 2000. Controls on the dynamics of dissolved organic matter in soils: A review. Soil Science 165: 277-304. doi:10.1097/00010694-200004000-00001.

92. Kan, J.J. et al. 2006. Temporal variation and detection limit of an estuarine bacterioplankton community analyzed by denaturing gradient gel electrophoresis (dgge). Aquatic Microbial Ecology 42: 7-18. doi:10.3354/ame042007.

93. Kang, P.-G. and M.J. Mitchell. 2013. Bioavailability and size-fraction of dissolved organic carbon, nitrogen, and sulfur at the arbutus lake watershed, adirondack mountains, ny. Biogeochemistry 115: 213-234. doi:10.1007/s10533-013-9829-1.

94. Kappler, A. et al. 2004. Electron shuttling via humic acids in microbial iron(iii) reduction in a freshwater sediment. FEMS Microbiology Ecology 47: 85-92. doi:10.1016/s0168-6496(03)00245-9.

95. Kappler, A. and K.L. Straub. 2005. Geomicrobiological cycling of iron. Molecular Geomicrobiology 59: 85-108. doi:10.2138/rmg.2005.59.5.

96. Karavanova, E.I. 2013. Dissolved organic matter: Fractional composition and sorbability by the soil solid phase (review of literature). Eurasian Soil Science 46: 833-844. doi:10.1134/s1064229313080048.

97. Kayler, Z.E. et al. 2011. Application of delta c-13 and delta n-15 isotopic signatures of organic matter fractions sequentially separated from adjacent arable and forest soils to identify carbon stabilization mechanisms. Biogeosciences 8: 2895-2906.

98. Kepkay, P.E. et al. 1997. Colloidal organic carbon and phytoplankton speciation during a coastal bloom. Journal of Plankton Research 19: 369-389. doi:10.1093/plankt/19.3.369.

99. Kepkay, P.E. et al. 1993. Low-molecular-weight and colloidal doc production during a phytoplankton bloom. Marine Ecology Progress Series 100: 233-244. doi:10.3354/meps100233.

100. Khilar, K.C. and H.S. Fogler. 1984. The existence of a critical salt concentration for particle release. Journal of Colloid and Interface Science 101: 214-224. doi:10.1016/0021-9797(84)90021-3.

101. Kia, S.F. et al. 1987. Effect of ph on colloidally induced fines migration. Journal of Colloid and Interface Science 118: 158-168. doi:10.1016/0021-9797(87)90444-9.

102. Kibet, L.C. et al. 2016. Persistence and surface transport of urea-nitrogen: A rainfall simulation study. Journal of Environmental Quality 45: 1062-1070. doi:10.2134/jeq2015.09.0495.

103. Kim, J.-I. and C. Walther. 2007. Laser-induced breakdown detection. Environmental colloids and particles. John Wiley & Sons, Ltd. p. 555-612.

104. Kjaergaard, C. et al. 2004. Properties of water-dispersible colloids from macropore deposits and bulk horizons of an agrudalf. Soil Science Society of America Journal 68: 1844-1852.

105. Kleber, M. et al. 2015. Chapter one - mineral–organic associations: Formation, properties, and relevance in soil environments. In: L. S. Donald, editor Advances in agronomy. Academic Press. p. 1-140.

106. Kleber, M. et al. 2007. A conceptual model of organo-mineral interactions in soils: Self-assembly of organic molecular fragments into zonal structures on mineral surfaces. Biogeochemistry 85: 9-24.

107. Kleinman, P.J.A. et al. 2007. Dynamics of phosphorus transfers from heavily manured coastal plain soils to drainage ditches. Journal of Soil and Water Conservation 62: 225-235.

108. Koynov, K. and H.J. Butt. 2012. Fluorescence correlation spectroscopy in colloid and interface science. Current Opinion in Colloid & Interface Science 17: 377-387. doi:10.1016/j.cocis.2012.09.003.

109. Kretzschmar, R. et al. 1999. Mobile subsurface colloids and their role in contaminant transport. Advances in Agronomy 66: 121-193.

110. Kretzschmar, R. et al. 1997. Effects of adsorbed humic acid on surface charge and flocculation of kaolinite. Soil Science Society of America Journal 61: 101-108.

111. Kretzschmar, R. et al. 1998. Influence of ph and humic acid on coagulation kinetics of kaolinite: A dynamic light scattering study. Journal of Colloid and Interface Science 202: 95-103. doi:10.1006/jcis.1998.5440.

112. Kretzschmar, R. et al. 1995. Influence of natural organic-matter on colloid transport through saprolite. Water Resources Research 31: 435-445.

113. Kretzschmar, R. and H. Sticher. 1997. Transport of humic-coated iron oxide colloids in a sandy soil: Influence of ca2+ and trace metals. Environmental Science and Technology 31: 3497-3504.

114. Krumbein, W.C. and F.J. Pettijohn. 1938. Manual of sedimentary petrography: I. Sampling, preparation for analysis, mechanical analysis and statistical analysis. D. Appleton Century Co., New York. NY.

115. Kuligowski, K. and T.G. Poulsen. 2009. Phosphorus leaching from soils amended with thermally gasified piggery waste ash. Waste Management 29: 2500-2508. doi:10.1016/j.wasman.2009.04.004.

116. Lafon, S. et al. 2006. Characterization of iron oxides in mineral dust aerosols: Implications for light absorption. Journal of Geophysical Research-Atmospheres 111. doi:10.1029/2005jd007016.

117. Lafuma, F. et al. 1991. Bridging of colloidal particles through adsorbed polymers. Journal of Colloid and Interface Science 143: 9-21.

118. Landers, M.N. and T.W. Sturm. 2013. Hysteresis in suspended sediment to turbidity relations due to changing particle size distributions. Water Resources Research 49: 5487-5500. doi:10.1002/wrcr.20394.

119. Lead, J.R. and K.J. Wilkinson. 2006. Aquatic colloids and nanoparticles: Current knowledge and future trends. Environmental Chemistry 3: 159-171. doi:10.1071/en06025.

120. Lead, J.R. and K.J. Wilkinson. 2007. Environmental colloids and particles: Current knowledge and future developments. Environmental colloids and particles. John Wiley & Sons, Ltd. p. 1-15.

121. Ledin, A. et al. 1995. Characterization of the submicrometer phase in surface waters - a review. Analyst 120: 603-608. doi:10.1039/an9952000603.

122. Levia, D.F. et al. 2010. Temporal variability of stemflow volume in a beech-yellow poplar forest in relation to tree species and size. Journal of Hydrology 380: 112-120. doi:10.1016/j.jhydrol.2009.10.028.

123. Lewis, J. 1996. Turbidity-controlled suspended sediment sampling for runoff-event load estimation. Water Resources Research 32: 2299-2310. doi:10.1029/96wr00991.

124. Lipson, D.A. et al. 2010. Reduction of iron (iii) and humic substances plays a major role in anaerobic respiration in an arctic peat soil. Journal of Geophysical Research-Biogeosciences 115. doi:10.1029/2009jg001147.

125. Liu, X. et al. 2011. Influence of ca2+ and suwannee river humic acid on aggregation of silicon nanoparticles in aqueous media. Water Research 45: 105-112. doi:10.1016/j.watres.2010.08.022.

126. Loeppert, R.H. and W.P. Inskeep. 1996. Iron. In: D. L. Sparks, A. L. Page, P. A. Helmke and R. H. Loeppert, editors, Methods of soil analysis part 3—chemical methods. Soil Science Society of America, American Society of Agronomy. p. 639-664.

127. Lorah, M.M. et al., 2012, Evaluating nutrient fate and redox controls in groundwater in riparian areas, USGS MD-DE-DC Water Science Center, Baltimore, MD, http://md.water.usgs.gov/posters/nutrientsRedox/, Nov. 30

128. Lovley, D.R. 1987. Organic-matter mineralization with the reduction of ferric iron - a review. Geomicrobiology Journal 5: 375-399.

129. Lovley, D.R. et al. 1996. Humic substances as electron acceptors for microbial respiration. Nature 382: 445-448. doi:10.1038/382445a0.

130. Lovley, D.R. and E.J.P. Phillips. 1986. Organic-matter mineralization with reduction of ferric iron in anaerobic sediments. Applied and Environmental Microbiology 51: 683-689.

131. Lu, S.-G. et al. 2013. Occurrence, structure and mineral phases of nanoparticles in an anthrosol. Pedosphere 23: 273-280.

132. Lyven, B. et al. 2003. Competition between iron- and carbon-based colloidal carriers for trace metals in a freshwater assessed using flow field-flow fractionation coupled to icpms. Geochimica et Cosmochimica Acta 67: 3791-3802. doi:10.1016/s0016-7037(03)00087-5.

133. Magaritz, M. et al. 1990. Distribution of metals in a polluted aquifer: A comparison of aquifer suspended material to fine sediments of the adjacent environment. Journal of Contaminant Hydrology 5: 333-347. doi:http://dx.doi.org/10.1016/0169-7722(90)90024-B.

134. Martin, J.M. et al. 1995. Significance of colloids in the biogeochemical cycling of organic-carbon and trace-metals in the venice lagoon (italy). Limnology and Oceanography 40: 119-131.

135. Mavrocordatos, D. et al. 2007. Strategies and advances in the characterisation of environmental colloids by electron microscopy. Environmental colloids and particles. John Wiley & Sons, Ltd. p. 345-404.

136. McCarthy, J.F. and L.D. McKay. 2004. Colloid transport in the subsurface: Past, present, and future challenges. Vadose Zone Journal 3: 326-337.

137. Mccarthy, J.F. and J.M. Zachara. 1989. Subsurface transport of contaminants - mobile colloids in the subsurface environment may alter the transport of contaminants. Environmental Science & Technology 23: 496-502.

138. McDowellboyer, L.M. 1992. Chemical mobilization of micron-sized particles in saturated porous-media under steady flow conditions. Environmental Science & Technology 26: 586-593. doi:10.1021/es00027a023.

139. Minella, J.P.G. et al. 2008. Estimating suspended sediment concentrations from turbidity measurements and the calibration problem. Hydrological Processes 22: 1819-1830. doi:10.1002/hyp.6763.

140. Molnar, I.L. et al. 2015. Predicting colloid transport through saturated porous media: A critical review. Water Resources Research 51: 6804-6845. doi:10.1002/2015wr017318.

141. Moran, S.B. and R.M. Moore. 1989. The distribution of colloidal aluminum and organic-carbon in coastal and open ocean waters off nova-scotia. Geochimica et Cosmochimica Acta 53: 2519-2527. doi:10.1016/0016-7037(89)90125-7.

142. Morrisson, A.R. et al. 1990. Application of high-performance size-exclusion liquid-chromatography to the study of copper speciation in waters extracted from sewage-sludge treated soils. Analyst 115: 1429-1433. doi:10.1039/an9901501429.

143. Mylon, S.E. et al. 2004. Influence of natural organic matter and ionic composition on the kinetics and structure of hematite colloid aggregation: Implications to iron depletion in estuaries. Langmuir 20: 9000-9006. doi:10.1021/la049153g.

144. Nebbioso, A. and A. Piccolo. 2013. Molecular characterization of dissolved organic matter (dom): A critical review. Analytical and Bioanalytical Chemistry 405: 109-124. doi:10.1007/s00216-012-6363-2.

145. Nelson, D.W. and L.E. Sommers. 1996. Total carbon, organic carbon, and organic matter. In: D. L. Sparks, A. L. Page, P. A. Helmke and R. H. Loeppert, editors, Methods of soil analysis part 3—chemical methods. Soil Science Society of America, American Society of Agronomy. p. 961-1010.

146. Newbold, J.D. et al. 1997. Organic matter dynamics in white clay creek, pennsylvania, USA. Journal of the North American Benthological Society 16: 46-50. doi:10.2307/1468231.

147. Ogawa, H. and N. Ogura. 1992. Comparison of 2 methods for measuring dissolved organic-carbon in sea-water. Nature 356: 696-698. doi:10.1038/356696a0.

148. Olivie-Lauquet, G. et al. 2001. Release of trace elements in wetlands: Role of seasonal variability. Water Research 35: 943-952. doi:10.1016/s0043-1354(00)00328-6.

149. Penn, R.L. et al. 2001. Iron oxide coatings on sand grains from the atlantic coastal plain: High-resolution transmission electron microscopy characterization. Geology 29: 843-846. doi:10.1130/0091-7613(2001)029<0843:iocosg>2.0.co;2.

150. Pfannkuche, J. and A. Schmidt. 2003. Determination of suspended particulate matter concentration from turbidity measurements: Particle size effects and calibration procedures. Hydrological Processes 17: 1951-1963. doi:10.1002/hyp.1220.

151. Philippe, A. and G.E. Schaumann. 2014. Interactions of dissolved organic matter with natural and engineered inorganic colloids: A review. Environmental Science & Technology 48: 8946-8962. doi:10.1021/es502342r.

152. Pokrovsky, O.S. et al. 2005. Fe-al-organic colloids control of trace elements in peat soil solutions: Results of ultrafiltration and dialysis. Aquatic Geochemistry 11: 241-278. doi:10.1007/s10498-004-4765-2.

153. Pokrovsky, O.S. and J. Schott. 2002. Iron colloids/organic matter associated transport of major and trace elements in small boreal rivers and their estuaries (nw russia). Chemical Geology 190: 141-179. doi:10.1016/s0009-2541(02)00115-8.

154. Pokrovsky, O.S. et al. 2006. Trace element fractionation and transport in boreal rivers and soil porewaters of permafrost-dominated basaltic terrain in central siberia. Geochimica et Cosmochimica Acta 70: 3239-3260. doi:10.1016/j.gca.2006.04.008.

155. Ponnamperuma, F.N. 1972. The chemistry of submerged soils. Advances in Agronomy 24: 29-96.

156. Pourret, O. et al. 2007. Organo-colloidal control on major- and trace-element partitioning in shallow groundwaters: Confronting ultrafiltration and modelling. Applied Geochemistry 22: 1568-1582. doi:10.1016/j.apgeochem.2007.03.022.

157. Qafoku, N.P. et al. 2000. Mineralogy and chemistry of some variable charge subsoils. Communications in Soil Science and Plant Analysis 31: 1051-1070. doi:10.1080/00103620009370497.

158. Rakshit, S. et al. 2009. Iron(iii) bioreduction in soil in the presence of added humic substances. Soil Science Society of America Journal 73: 65-71. doi:10.2136/sssaj2007.0418.

159. Ranville, J.F. et al. 2005. Particle-size and element distributions of soil colloids: Implications for colloid transport. Soil Science Society of America Journal 69: 1173-1184. doi:10.2136/sssaj2004.0081.

160. Regnier, P. et al. 2013. Anthropogenic perturbation of the carbon fluxes from land to ocean. Nature Geoscience 6: 597-607. doi:10.1038/ngeo1830.

161. Rick, A.R. and Y. Arai. 2011. Role of natural nanoparticles in phosphorus transport processes in ultisols. Soil Science Society of America Journal 75: 335-347. doi:10.2136/sssaj2010.0124nps.

162. Roden, E.E. and M.M. Urrutia. 2002. Influence of biogenic fe(ii) on bacterial crystalline fe(iii) oxide reduction. Geomicrobiology Journal 19: 209-251. doi:10.1080/01490450252864280.

163. Ronen, D. et al. 1987. Anthropogenic anoxification (eutrophication) of the water-table region of a deep phreatic aquifer. Water Resources Research 23: 1554-1560. doi:10.1029/WR023i008p01554.

164. Ronen, D. et al. 1992. Characterization of suspended particles collected in groundwater under natural gradient flow conditions. Water Resources Research 28: 1279-1291. doi:10.1029/91wr02978.

165. Ross, J.M. and R.M. Sherrell. 1999. The role of colloids in tracemetal transport and adsorption behavior in new jersey pinelands streams. Limnology and Oceanography 44: 1019-1034.

166. Rostad, C.E. et al. 1997. Organic carbon and nitrogen content associated with colloids and suspended particulates from the mississippi river and some of its tributaries. Environmental Science & Technology 31: 3218-3225. doi:10.1021/es970196b.

167. Royer, R.A. et al. 2002a. Enhancement of hematite bioreduction by natural organic matter. Environmental Science & Technology 36: 2897-2904. doi:10.1021/es015735y.

168. Royer, R.A. et al. 2002b. Enhancement of biological reduction of hematite by electron shuttling and fe(ii) complexation. Environmental Science & Technology 36: 1939-1946. doi:10.1021/es011139s.

169. Rugner, H. et al. 2013. Turbidity as a proxy for total suspended solids (tss) and particle facilitated pollutant transport in catchments. Environmental Earth Sciences 69: 373-380. doi:10.1007/s12665-013-2307-1.

170. Ryan, J.N. and M. Elimelech. 1996. Colloid mobilization and transport in groundwater. Colloids and Surfaces a-Physicochemical and Engineering Aspects 107: 1-56. doi:10.1016/0927-7757(95)03384-x.

171. Ryan, J.N. et al. 1999. Bacteriophage prd1 and silica colloid transport and recovery in an iron oxide-coated sand aquifer. Environmental Science & Technology 33: 63-73. doi:10.1021/es980350+.

172. Ryan, J.N. and P.M. Gschwend. 1990. Colloid mobilization in 2 atlantic coastal-plain aquifers - field studies. Water Resources Research 26: 307-322.

173. Ryan, J.N. and P.M. Gschwend. 1994a. Effect of solution chemistry on clay colloid release from an iron oxide-coated aquifer sand. Environmental Science & Technology 28: 1717-1726. doi:10.1021/es00058a025.

174. Ryan, J.N. and P.M. Gschwend. 1994b. Effects of ionic-strength and flow-rate on colloid release - relating kinetics to intersurface potential-energy. Journal of Colloid and Interface Science 164: 21-34. doi:10.1006/jcis.1994.1139.

175. Sakurai, K. et al. 1990. Changes in zero-point of charge (zpc), specific surface-area (ssa), and cation-exchange capacity (cec) of kaolinite and montmorillonite, and strongly weathered soils caused by fe and al coatings. Soil Science and Plant Nutrition 36: 73-81.

176. Schelde, K. et al. 2002. Diffusion-limited mobilization and transport of natural colloids in macroporous soil. Vadose Zone Journal 1: 125-136.

177. Schijf, J. and A.M. Zoll. 2011. When dissolved is not truly dissolved-the importance of colloids in studies of metal sorption on organic matter. Journal of Colloid and Interface Science 361: 137-147. doi:10.1016/j.jcis.2011.05.029.

178. Schwertmann, U. and R.M. Cornell. 2007. Frontmatter. Iron oxides in the laboratory. Wiley-VCH Verlag GmbH. p. i-xviii.

179. Sen, T.K. and K.C. Khilar. 2006. Review on subsurface colloids and colloid-associated contaminant transport in saturated porous media. Advances in Colloid and Interface Science 119: 71-96.

180. Sims, J.T. et al. 2000. Integrating soil phosphorus testing into environmentally based agricultural management practices. Journal of Environmental Quality 29: 60-71.

181. Six, J. et al. 2002. Stabilization mechanisms of soil organic matter: Implications for c-saturation of soils. Plant and Soil 241: 155-176. doi:10.1023/a:1016125726789.

182. Sloto, R.A. 1994. Geology, hydrology, and ground water quality of chester county, pennsylvania. Chester County Water Resources Authority.

183. Sondi, I. et al. 1997. Electrokinetic potentials of clay surfaces modified by polymers. Journal of Colloid and Interface Science 189: 66-73.

184. Stout, L.M. et al. 2016. Relationship of phytate, phytate-mineralizing bacteria, and beta-propeller phytase genes along a coastal tributary to the chesapeake bay. Soil Science Society of America Journal 80: 84-96. doi:10.2136/sssaj2015.04.0146.

185. Straub, K.L. et al. 2001. Iron metabolism in anoxic environments at near neutral ph. FEMS Microbiology Ecology 34: 181-186. doi:10.1111/j.1574-6941.2001.tb00768.x.

186. Stumm, W. 1993. Aquatic colloids as chemical reactants: Surface structure and reactivity. Colloids and Surfaces A: Physicochemical and Engineering Aspects 73: 1-18. doi:http://dx.doi.org/10.1016/0927-7757(93)80003-W.

187. Suarez, D.L. et al. 1984. Effect of ph on saturated hydraulic conductivity and soil dispersion. Soil Science Society of America Journal 48: 50-55.

188. Szilagyi, M. 1971. Reduction of fe3+ ion by humic acid preparations. Soil Science 111: 233-&. doi:10.1097/00010694-197104000-00005.

189. Thamdrup, B. 2000. Bacterial manganese and iron reduction in aquatic sediments. Advances in Microbial Ecology 16: 41-84.

190. Thompson, A. et al. 2006. Colloid mobilization during soil iron redox oscillations. Environmental Science & Technology 40: 5743-5749. doi:10.1021/es061203b.

191. Tiller, C.L. and C.R. Omelia. 1993. Natural organic-matter and colloidal stability - models and measurements. Colloids and Surfaces a-Physicochemical and Engineering Aspects 73: 89-102. doi:10.1016/0927-7757(93)80009-4.

192. Tipping, E. and D.C. Higgins. 1982. The effect of adsorbed humic substances on the colloid stability of haematite particles. Colloids and Surfaces 5: 85-92.

193. Tombacz, E. et al. 1999. Particle aggregation in complex aquatic systems. Colloids and Surfaces a-Physicochemical and Engineering Aspects 151: 233-244.

194. Upreti, K. et al. 2015. Factors controlling phosphorus mobilization in a coastal plain tributary to the chesapeake bay. Soil Science Society of America Journal 79: 826-837. doi:10.2136/sssaj2015.03.0117.

195. Urrutia, M.M. et al. 1999. Influence of aqueous and solid-phase fe(ii) complexants on microbial reduction of crystalline iron(iii) oxides. Environmental Science & Technology 33: 4022-4028. doi:10.1021/es990447b.

196. Vadas, P.A. et al. 2007. Hydrology and groundwater nutrient concentrations in a ditch-drained agroecosystem. Journal of Soil and Water Conservation 62: 178-188.

197. Vaidya, R.N. and H.S. Fogler. 1990. Formation damage due to colloidally induced fines migration. Colloids and Surfaces 50: 215-229. doi:10.1016/0166-6622(90)80265-6.

198. Van Bemmelen, J.M. 1890. Über die bestimmung des wassers, des humus, des schwefels, der in den colloïdalen silikaten gebundenen kieselsäure, des mangans u. S. W. Im ackerboden. Die Landwirthschaftlichen Versuchs-Stationen 37: 279-290.

199. Vepraskas, M.J. et al. 2001. Redox chemistry of hydric soils. Wetland soils: Genesis, hydrology, landscapes, and classification. Lewis Publishers, Boca Raton, FL. p. 85-106.

200. Vignati, D. and J. Dominik. 2003. The role of coarse colloids as a carrier phase for trace metals in riverine systems. Aquatic Sciences 65: 129-142. doi:10.1007/s00027-003-0640-2.

201. Vignati, D.A.L. et al. 2005. Estimation of the truly dissolved concentrations of cd, cu, ni, and zn in contrasting aquatic environments with a simple empirical model. Ecological Modelling 184: 125-139. doi:10.1016/j.ecolmodel.2004.11.010.

202. Vital, M. et al. 2010. Evaluating the growth potential of pathogenic bacteria in water. Applied and Environmental Microbiology 76: 6477-6484. doi:10.1128/aem.00794-10.

203. Vold, R.D. and M.J. Vold. 1983. Colloid and interface chemistry. Addison-Wesley, Reading, MA.

204. Walther, C. et al. 2006. Probing particle size distributions in natural surface waters from 15 nm to 2 mu m by a combination of libd and single-particle counting. Journal of Colloid and Interface Science 301: 532-537. doi:10.1016/j.jcis.2006.05.039.

205. Wang, D.J. et al. 2015a. Cotransport of hydroxyapatite nanoparticles and hematite colloids in saturated porous media: Mechanistic insights from mathematical modeling and phosphate oxygen isotope fractionation. Journal of Contaminant Hydrology 182: 194-209. doi:10.1016/j.jconhyd.2015.09.004.

206. Wang, D.J. et al. 2015b. Effect of size-selective retention on the cotransport of hydroxyapatite and goethite nanoparticles in saturated porous media. Environmental Science & Technology 49: 8461-8470. doi:10.1021/acs.est.5b01210.

207. Wang, X. et al. 2013. Variations in abundance and size distribution of carbohydrates in the lower mississippi river, pearl river and bay of st louis. Estuarine Coastal and Shelf Science 126: 61-69. doi:10.1016/j.ecss.2013.04.008.

208. Wass, P.D. and G.J.L. Leeks. 1999. Suspended sediment fluxes in the humber catchment, uk. Hydrological Processes 13: 935-953. doi:10.1002/(sici)1099-1085(199905)13:7<935::aid-hyp783>3.0.co;2-l.

209. Weber, K.A. et al. 2006. Microorganisms pumping iron: Anaerobic microbial iron oxidation and reduction. Nature Reviews Microbiology 4: 752-764. doi:10.1038/nrmicro1490.

210. Wells, M.L. and E.D. Goldberg. 1991. Occurrence of small colloids in sea-water. Nature 353: 342-344. doi:10.1038/353342a0.

211. Wells, M.L. and E.D. Goldberg. 1992. Marine submicron particles. Marine Chemistry 40: 5-18. doi:10.1016/0304-4203(92)90045-c.

212. Wells, M.L. and E.D. Goldberg. 1994. The distribution of colloids in the north-atlantic and southern oceans. Limnology and Oceanography 39: 286-302.

213. Wen, L.S. et al. 1997. Colloidal and particulate silver in river and estuarine waters of texas. Environmental Science & Technology 31: 723-731. doi:10.1021/es9603057.

214. Wilkinson, K.J. et al. 1998. Different roles of pedogenic fulvic acids and aquagenic biopolymers on colloid aggregation and stability in freshwaters. Limnology and Oceanography 42: 1714-1724.

215. Wilkinson, K.J. et al. 1997. Coagulation of colloidal material in surface waters: The role of natural organic matter. Journal of Contaminant Hydrology 26: 229-243.

216. Wolf, A. and D. Beegle. 1995. Recommended soil tests for macronutrients: Phosphorus, potassium, calcium, and magnesium. Recommended soil testing procedures for the northeastern United States. Northeast Regional Bull 493: 25-34.

217. Yan, J. et al. 2016. Soil colloid release affected by dissolved organic matter and redox conditions. Vadose Zone Journal 15: 10. doi:10.2136/vzj2015.02.0026.

218. Zhang, J.W. and J. Buffle. 1995. Kinetics of hematite aggregation by polyacrylic-acid - importance of charge neutralization. Journal of Colloid and Interface Science 174: 500-509. doi:10.1006/jcis.1995.1417.

Appendix A

LIST OF SYMBOLS AND ABBREVIATIONS

Abbreviations

CEC	Cation exchange capacity
COC	Colloidal organic carbon
COM	Colloidal organic matter
DGGE	Denaturing gradient gel electrophoresis
DOC	Dissolved organic carbon
DOC_{tr}	Truly dissolved organic carbon
DOC_{op}	Operationally defined dissolved organic carbon
DOM	Dissolved organic matter
DOM_{in}	Indigenous dissolved organic matter
DIP	Dissolved inorganic phosphorus
DOP	Dissolved organic phosphorus
CEC	Cation exchange capacity
FCS	Fluorescence correlation spectroscopy
FIFFF	Field flow filtration fractionation
Fluorescence-EEM	Fluorescence excitation emission matrix
HIX	Humification index
HMW	High molecular weight
ICP-MS	Inductively coupled plasma mass spectrometry

IS	Ionic strength
LIBD	Laser induced break down detection
LMW	Low molecular weight
NOM	Natural organic matter
OM	Organic matter
PCHO	Particulate carbohydrates
PCR	Polymerase chain reaction
PIP	Particulate inorganic phosphorus
POM	Particulate organic matter
POP	Particulate organic phosphorus
PVC	Polyvinyl chloride
PZC	Point of zero charge
SEM-EDs	Scanning electron microscopy with X-ray microanalysis
SOM	Soil organic matter
SSA	Specific surface area
TCHO	Total carbohydrates
TEM	Transmission electron microscopy
TFF	Tangential flow filtration
TOC	Total organic carbon
TP	Total phosphorus
XRD	X-ray diffraction

Appendix B

PRELIMNARY RESULTS OF COLLOIAL INORGANIC PHOSPORUS IN EAST CREEK

Colloidal inorganic phosphorus in different size fractions (< 10 kDa, 0.1, 0.45 and 1.0 μm) were measured on June 15th or 16th, 2015 for samples collected along the East Creek from a drainage ditch near an agricultural farm to the mouth of creek at the Chesapeake Bay as shown in Figure 4.4. The inorganic phosphorus concentration in each size fractions are presented as followed.

Table A.1 Colloidal inorganic phosphorus concentration in East Creek

	Inorganic phosphorus concentration in μmol/L			
Sampling sites	< 10 kDa	< 0.1 μm	< 0.45 μm	< 1.0 μm
A	0.14 ± 0.20	2.27 ± 0.22	3.20 ± 0.21	3.12 ± 0.43
B	3.62 ± 0.20	6.38 ± 0.28	6.92 ± 0.18	6.62 ± 0.22
C	1.38 ± 0.18	2.19 ± 0.19	5.49 ± 0.20	6.02 ± 0.20
D	0.61 ± 0.21	2.16 ± 0.20	5.74 ± 0.67	4.61 ± 0.21
E	1.92 ± 0.20	2.89 ± 0.18	4.91 ± 0.28	7.91 ± 0.24
F	0.87 ± 0.43	2.43 ± 0.58	3.72 ± 0.43	5.17 ± 0.45
G	2.14 ± 0.44	3.15 ± 0.43	4.41 ± 0.43	5.53 ± 0.46
H	5.13 ± 0.44	5.50 ± 0.44	5.93 ± 0.43	9.46 ± 0.42
I	4.43 ± 0.45	7.30 ± 0.46	7.66 ± 0.48	9.67 ± 0.44
J	10.57 ± 0.48	15.74 ± 0.47	18.20 ± 0.44	N/A†
J1	14.57 ± 0.45	20.42 ± 0.44	23.77 ± 0.45	25.29 ± 0.44
K	47.21 ± 0.47	55.97 ± 0.46	73.65 ± 0.42	84.94 ± 0.46
L	108.65 ± 0.48	107.57 ± 0.42	117.12 ± 0.43	120.95 ± 0.48

† N/A represents “not analyzed”

Appendix C

REPRINT PERMISSION LETTER

Permission are requested to reprint “Yan, J. et al. 2016. Soil colloid release affected by dissolved organic matter and redox conditions. Vadose Zone Journal 15: 10” from American Society of Agronomy Inc. The permission is shown as followed.

American Society of Agronomy Inc. LICENSE TERMS AND CONDITIONS

Dec 01, 2016

This is a License Agreement between Jeanne Brewster ("You") and American Society of Agronomy Inc. ("American Society of Agronomy Inc.") provided by Copyright Clearance Center ("CCC"). The license consists of your order details, the terms and conditions provided by American Society of Agronomy Inc., and the payment terms and conditions.

All payments must be made in full to CCC. For payment instructions, please see information listed at the bottom of this form.

License Number	4000371307363
License date	Dec 01, 2016
Licensed content publisher	American Society of Agronomy Inc.
Licensed content title	Vadose zone journal : VZJ
Licensed content date	Jan 1, 2002
Type of Use	Thesis/Dissertation
Requestor type	Author of requested content
Format	Electronic
Portion	chapter/article
Title or numeric reference of the portion(s)	full article
Title of the article or chapter the portion is from	Soil Colloid Release Affected by Dissolved Organic Matter and Redox Conditions
Editor of portion(s)	n/a
Author of portion(s)	Jing Yan
Volume of serial or monograph.	15
Issue, if republishing an article from a serial	3
Page range of the portion	
Publication date of portion	2016
Rights for	Main product
Duration of use	Life of current edition
Creation of copies for the disabled	no
With minor editing privileges	no
For distribution to	Worldwide
In the following language(s)	Original language of publication
With incidental promotional use	no

The lifetime unit quantity of new product	Up to 499
Made available in the following markets	education
The requesting person/organization is:	Jing Yan
Order reference number	
Author/Editor	Jing Yan
The standard identifier of New Work	n/a
The proposed price	n/a
Title of New Work	Quantification and Characterization of Mobile Colloids: Their Potential Role in Carbon Cycling under Varying Redox Conditions
Publisher of New Work	University of Delaware/Proquest
Expected publication date	Dec 2016
Estimated size (pages)	150
Total (may include CCC user fee)	0.00 USD
Terms and Conditions	